ADDIS ABABA UNIVERSITY
SCHOOL OF GRADUATE STUDIES
DEPARTMENT OF EARTH SCIENCES

GEOLOGY AND GEOCHEMISTRY

OF

GUNA VOLCANIC MASSIF
NORTH WESTERN ETHIOPIAN PLATEAU

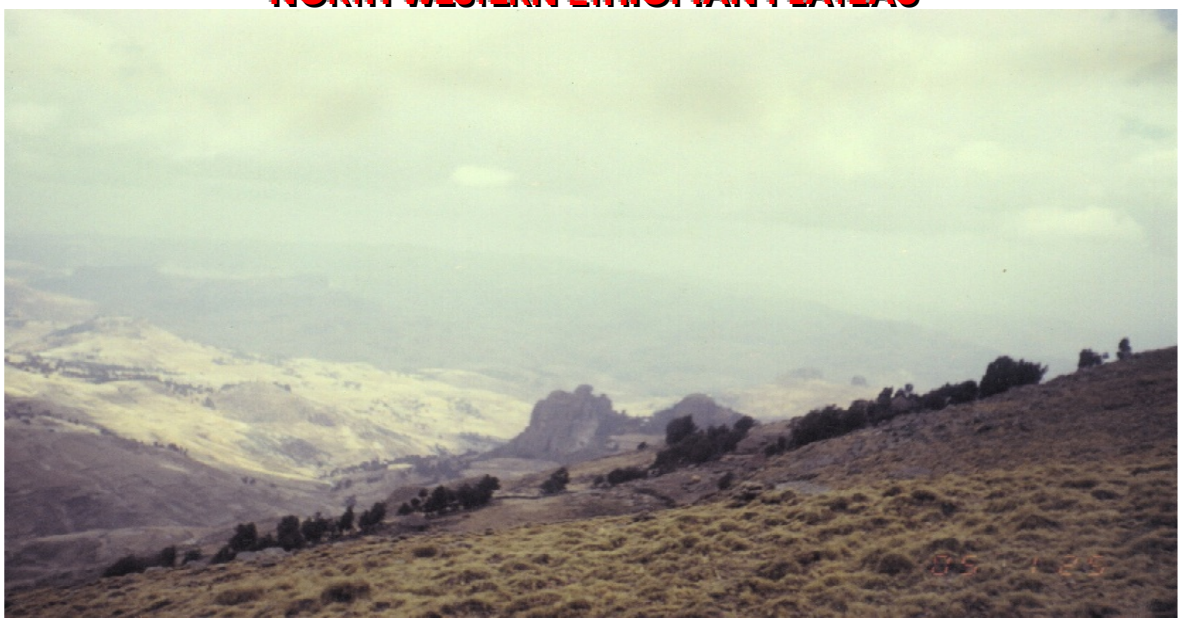

A THESIS SUBMITTED TO
THE SCHOOL OF GRADUATE STUDIES OF
ADDIS ABABA UNIVERSITY IN PARTIAL FULFILLMENT OF THE
DEGREE OF MASTER OF SCIENCE IN
MINERALOGY PETROLOGY & GEOCHEMISTRY

BY

ADISE MEKONNEN

July 2006

ADDIS ABABA UNIVERSITY
DEPARTMENT OF EARTH SCIENCES
SCHOOL OF GRADUATE STUDIES

Geology and Geochemistry of Guna Volcanic Massif Northwestern Ethiopian plateau

By

Adise Mekonnen
Faculty of Natural Science
Department of Earth Sciences

Approval by board of examiners

Dr. Dereje Ayalew _____
(Chairman)

Dr. Dereje Ayalew _____
(Advisor)

Dr. Tadiwos cherenet _____
(Examiner)

Dr. Meseret T/Mariam _____
(Examiner)

Declaration

This thesis is my original work and has not been presented for a degree in any other university, and that all sources of material used for the thesis have been duly acknowledged.

_____

Adise Mekonnen

Approved by_____

Dr. Dereje Ayalew (Advisor)

Date:_____

Addis Ababa University

ABSTRACT

Guna volcanic massif is found in Northwestern Ethiopia plateau. It has an average basal diameter of about 40 km and a height of 1553 m with elevation of 4135m at the peak. It covers an estimated area of about 760 m^2. A recent work of kieffer et al., 2004, provided an Ar/Ar age of 10.7 ma.

The general objective of this thesis research work is to study the geology and the petrogenetic processes responsible to produce the rock suites of the volcanic massif. The methodologies employed to achieve the objectives includes fieldwork for mapping and sampling, petrographic investigations, electro microprobe analysis on major phenocryst phases of phonolte lavas, major and trace element geochemical analysis by ICPMS method, analysis and interpretation of data using different computer soft wares.

Geologically the massif overlying the flood basalt mainly consists of rhyolite lava flow, pyroclastic flow deposit and phonolite lava flow from bottom to top.

The rhyolites occur as layered lava flows, glassy with columnar jointing and huge domes. In thin section they have vitrophyric, perlithic and porphyrithic textures with essential mineral composition of alkali fieldspars, plagioclase and quartz. The pyroclastic flow deposit includes ash, tuffs, ignimbrite and trachyte flows. The phonolite occurs as thick viscous lava flow. They show porphrithic and trachythic textures with phenocrysts of alkali feldspar, feldesphathoids (nepheline, leucite and nosean) and alkali pyroxenes.

The lavas are rich in silica and alkalis. Major element variation plots displays features agreeable with fractionation of major phenocryst phases, Fe-Ti oxides and apatites.

The chondrite normalized Rare earth element (REE) patterns shows enriched light rare earth element LREE, strong negative Eu anomaly and fairly flat heavy rare earth (HREE) pattern that indicates fractionation processes.

In the Primitive mantle normalized profiles (spider diagrams) Ba , Sr, Ti and P shows strong negative anomaly which verifies fractionation. In most samples, Nb shows a remarkable positive anomaly. The lavas have low Rb/Nb (0.31-1.31) and La/Nb (0.34-1.03) ratios high La/Lu ratios that increase from rhyolite through trachyte to phonolite.

The field observations, petrography, mineral chemistry and whole rock geo chemical data of this work indicates that Guna is not a basaltic shield volcano; instead it is a huge felsic centre mainly consisting of pyroclastic flow deposits, rhyolite, phonolite and trachyte lava flows. The lavas are co genetic and derived from mantle origin basaltic magma through low-pressure extensive fractional crystallization and limited crustal contamination.

ACKNOWLEDGEMENTS

I give thanks and glory to the Lord God Almighty in the Name of Jesus who strengthened me and made this work prosper.

I am very grateful to my advisor Dr. Dereje Ayalew for his constant supervision, reviewing the thesis and providing useful comments and encouragements I received. Similarly I am also very grateful to may second advisor Dr. Gezahegn Yirgu for his constant follow up and supervision in the filed, significant review of the thesis, helpful remarks and suggestions.

I am highly indebted to Dr. Tanya Furman, The Pennssylvannia State University (U.S.A) for providing the major and trace element analyses, and hosting me in Penn State for electron microprobe analysis. I would like to express my deepest appreciation for her kind assistance during my stay in United States.

I great fully acknowledge the Regional Geology and Geochemistry Department (RGGD) and the Economic Mineral Exploration and Evaluation Department of the Geological Survey of Ethiopia (GSE) for providing me field vehicle for my first and second fieldwork respectively.

I extend my gratitude to the Central Geological Laboratory of the Geological Survey of Ethiopia (GSE) for the preparation of thin sections, and allowing me to use all facilities for preparation of the thesis.

I wish to express my sincere appreciation to my friends in Central Geological Laboratory, Geo information center, Regional geology, Hydrogeology and Geothermal Departments of the Geological Survey of Ethiopia for there endless great help and encouragement to bring this work to its final form.

I am also indebted to my family, my beloved wife (Mimi Bekele) and sons (Eyoel and Benyam Adise) for their love and tolerance, many thanks are also for all other family and friends who constantly encouraged, helped and sustained me in prayer for the success of this work.

TABLE OF CONTENT

LIST OF FIGURES

Page

Page

LIST OF TABLES

Page

CHAPTER 1 INTRODUCTION

1.1. Location and accessibility

The study area Guna mountain massif is located in south Gonder Zone of Amhara National Regional State about 699 km north west of Addis Ababa. The massif covers an area about 760 km^2. It is bounded by 11° 24’ to 11°55’N latitude and 38°00’E to 38°20’E longitude and falls in the Ethiopian Mapping Agency topo sheet No. NC 37- 2. The nearest towns are Nefas Mewcha about 30 km to the east and Debre Tabor about 20 km to the west. Moreover the area is found along Woldiya – Woreta road (Chinese road).

The area can be reached either through Addis Ababa- Bahir Dar- Debre Tabor that is about 622km asphalt and 77 km gravel road or via Addis Ababa- Dese – Weldiya- Debre Tabor that is about 521km asphalt and 140 km gravel road. The road connections to other villages around the mountain, Gassay - Iste (western side), Kimir Dingay – Wegeda/Simada (eastern side) and Kimir dingay- Megendi (northern side) are dry weather roads motor able by four-wheel drive vehicles.

Figure 1.1 shows the geographic location and accessibility of the study area.

1.2. Physiography

Physiographycally Ethiopia is divided into three distinct units that are the product of major geological evolution of the region.

These are:

1. The Main Ethiopian Rift (MER) and the Afar depression, transect the territory into two and is bounded by steep escarpment and accompanying rift floor that characterized by a series of horst – graben systems. The lowest elevation at Afar depression is 125m below sea level

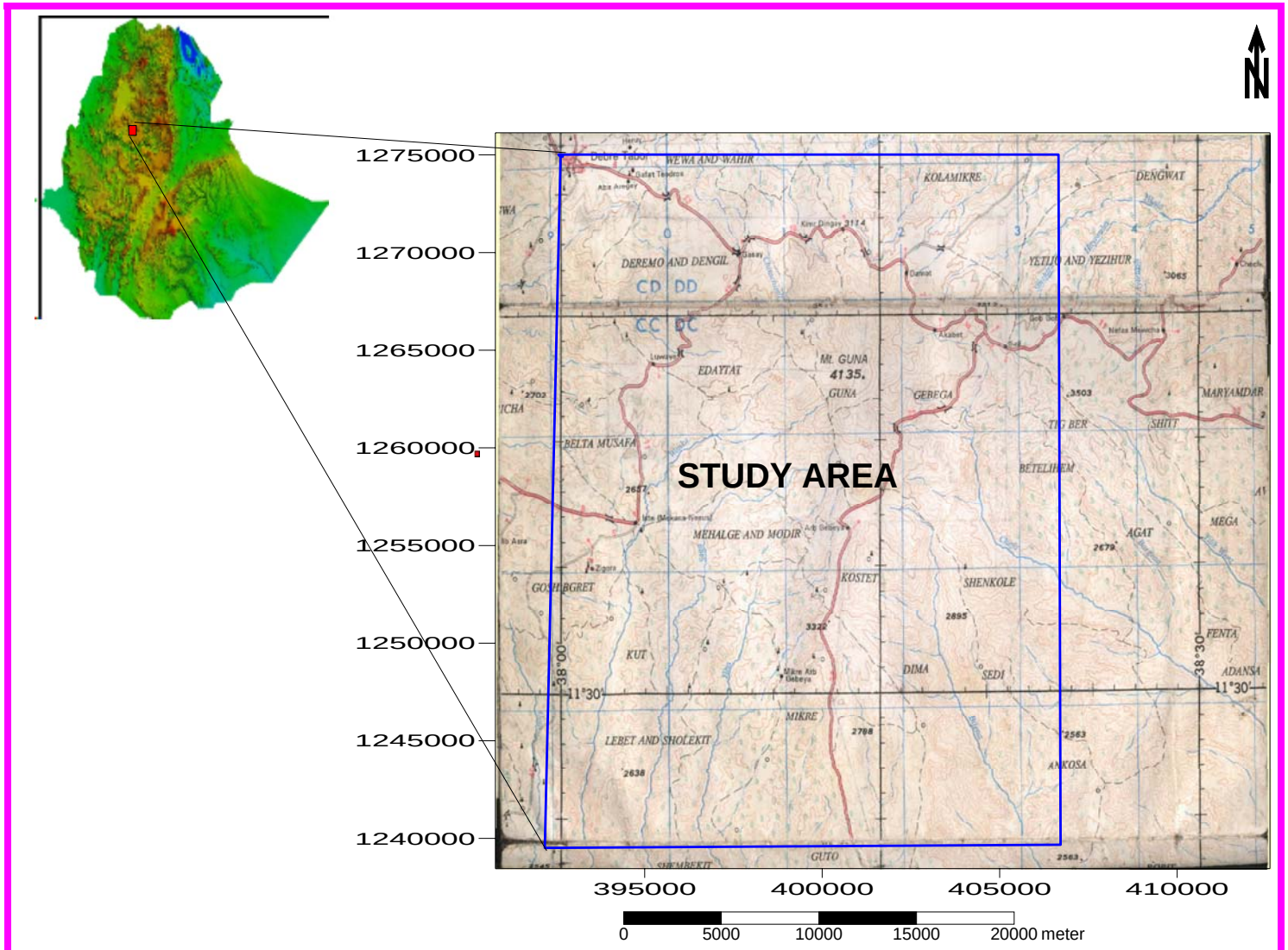

Figure 1.1 Location and Accessibility Map.

2. The Western (Ethiopian) plateau and adjacent lowlands, covers more than half of the country, and where the lowlands slope westward into the Sudanese plain.
3. The South – Eastern (Somali) plateau and eastern lowlands. The lowlands include flat plains starting from the Ogaden basin to the east and the Wabi – Shebelle and the Genale plains to the southeast.

Guna Mountain is found in the North – western (Ethiopian) plateau physiographic unit. The present landscape of Guna and its surroundings are the result of volcano tectonic events and subsequent denudation processes that mainly took place after the Mesozoic time (Mohr, 1963).

The mountain is bordered to the east by Beshilo river valley and to the southwest by Fogera plain. Guna Mountain is characterized by highly dissected country, showing steep ridges, intervening deep valleys and a relatively flat top. The elevation in the area varies from about 2,600m at the base to 4135m at the peak of the mountain.

Plugs and domes form numerous discontinuous prominent volcanic ridges with very sharp peaks. Several intermittent streams with dendritic to sub dendritic pattern drain from the mountain and flow into Abay and Tekeze river systems (see figure 3.18).

1.3. Population, climate and vegetation

According to the population census of 1994 conducted by the Ethiopian Central Statistical Office (C SA, 1995) the total rural population of South Gonder was 1,652, 030. Further the Guna massif adjoining woredas' rural population was 695,023 of which 41.2%, 36.7% and 22.1% are from Istie, Farta and Laygaynt woredas, respectively.

The population density of the study area is relatively high. Their livelihood is subsistence farming. In most rural area of Guna potato and barely are major crops cultivated and are staple food items. But communities living at the lower elevation part cultivate fava beans, field peas and wheat to some extent.

Guna Mountain is marked by cool temperate (to cool climate) that has a local name "Dega" and "Kur". Rainfall data for Guna massif is not available; the data from Debre Tabor and Nefas Mewcha meteorological stations show that the mean annual rainfall is 1068.45 mm. The lowest rainfall occurs during November, December, January and February and highest rainfall occurs during the months of June, July, August and

September. There is one really distinct dry season in which there is usually no or low rainfall. This extends from late December to February.

The average annual temperature for Debre Tabor is 15.6°C where as it is 13°C for Nefas Mewcha station. The Guna Mountain is characterized by scarce vegetation except the mountain grassland. High altitude Afro-Alpine flora covers the peak areas.

1.4. Review of previous geological work

The Guna volcanic massif has not been studied to any detail prior to this work. Earlier regional studies have included Guna in the framework of the shield volcanoes overlying the Tertiary Ethiopian Trap formation. Recent works have provided some information on the age and over all petrological features of the volcanic massif.

Some of the previous works on Trap formation and shield volcanoes are:

Mohr (1963) divided the Cenozoic volcanic rocks of Ethiopia in to Traps and Aden series. The term Trap series is still widely used to represent the whole pile of pre rift Tertiary flood basalt with minor intercalations of silicic extrusive particularly in the upper most units.

Kazmin, (1972) and (1979), Mohr, (1967), Zanettin et al., (1980), Merla et al., (1979), Berhe et al., (1987), Mohr and Zanettin (1988), Tefera et al., 1996 with some modifications generally classified the volcanism of the northern and central part of western Ethiopian plateau in to four formations as: The Ashangi formation, Aiba basalts, Alaji formation and Termaber Guassa and Termaber Megezeze formation.

In addition Merla et al., (1973), Zanettin and Justin – Vistin, (1974), Piccirillo et al., (1979) ,Zanettin, (1988), and Hart et al., (1989) contributed considerable in put to the study of the geology and geochemistry of volcanic rocks of Ethiopia.

Zanettin, 1993 mentioned the composition of the lavas in Mt. Guna (younger volcano) is exceptionally different from the other shields and include the silica under saturated rock types basanits nephelinites and phonolite.

Pik et al., 1998 under take detailed geochemical studies on the Oligocene flood basalt (Trap formation) of the North Western Ethiopian region, identified three distinct geochemical groups as the low Ti (LT), High Ti-1, (HT1) and high Ti -2 (HT_2) corresponding to three magma types.

Pik, et al., (1999) identified the mantle and crustal sources involved in the genesis of pre rift continental flood basalt of the northwestern Ethiopian plateau. They present their trace element and radiogenic isotopes (Sr, Nd, and Pd) data.

Dercq, et al., (2001) studied the petrologic and geochemical characteristics of the volcanic plugs in the North Ethiopian volcanic plateau and compared with those of the volcanic rocks in order to establish their relationship.

Recently Hofmann, et al., (1997) Coulie et al., (2001), Ukistins et al., (2002), Kieffer et al., (2004) provide absolute $^{40}Ar/^{39}Ar$ age determination on Oligocene-Miocene flood volcanics and Miocene -Pliocene volcanoes from the western Ethiopian plateau. Summarized in table 1.1.

Kieffer et al., (2004) studied the petrology, geochemistry, and isotopic compositions of the large shield volcanoes, compared their compositions with those of the flood volcanics and also traced the variations in eruption style and magma flux of lavas with ages ranging from 30 to ~10 Ma, or from the peak of flood volcanism to the on set of major rifting in the northern part of the volcanic plateau.

Table 1.1 Summery of age data on western Ethiopian Plateau

No.	Age	Location	Rock type	Source
1	10.6-3.2Ma	North Addia Ababa	Mio-Pliocene Volcano	Ukstine et al., (2002)
2	10.7Ma	Mt.Guna	Mio-Pliocene Volcano	Kiffer et al., (2004)
3	11.7-10.9Ma	Beetwen Addis Ababa and Dese	Mio-Pliocene Volcano	Ukstine et al., (2002)
4	19.8-14.9Ma	Beetwen Addis Ababa and Dese	Mio-Pliocene Volcano	Ukstine et al., (2002)
5	18.7Ma	Simien Mt.	Mio-Pliocene Volcano	Kiffer et al., (2004)
6	21.6Ma	Alem Ketema	Mio-Pliocene Volcano	Coulie, (2001)
7	22.3 Ma	Guguftu Mt.	Mio-Pliocene Volcano	Coulie, (2001)
8	22.4 Ma	Mt. Choke	Mio-Pliocene Volcano	Coulie, (2001)
9	25.3 Ma	Beetwen Addis Ababa and Dese	Flood Basalt	Ukstine et al., (2002)
10	26.9-29.4 Ma	Blue Nile river	Flood Basalt	Hofmann etal. ,(1997)
11	30.9-25.0 Ma	Near Dese	Flood Basalt	Hofmann etal. ,(1997)

12	30.2-28.2 Ma	WegelTena	Flood Basalt	Hofmann etal., (1997)
13	30.2-29.0 Ma	North of Dese	Flood Basalt	Coulie, (2001)
14	29.4-30.8 Ma	Limolimo	Flood Basalt	Hofmann etal., (1997)
15	29.5 Ma	Chinese Road	Flood Basalt	Hofmann etal., (1997)
16	30.4 Ma	Adigrat	Flood Basalt	Hofmann etal.. (1997)
17	30.4 Ma	Simen Mt.	Flood Basalt	Kiffer et al., (2004)
18	30.9 Ma	Bora	Flood Basalt	Kiffer et al., (2004)
19	31.0 Ma	Lalibela	Flood Basalt	Kiffer et al., (2004)

In the previous works the geology of Guna is not mapped to any detail. Its volcano logy, petrology and geochemistry are not well known. In addition to this the occurrence of under saturated volcanic rocks, which are rare in Ethiopian igneous province are poorly understood. These are the needs to study Guna.

1.5. Objectives of the present study

The general objective of this research work is

i. To study the geology of the Guna volcanic massif
ii. To recognize the mineralogical and petrographic features of the volcanic rocks and lavas in the area
iii. To undertake a geo chemical study of the lavas to understand the petrogenetic processes responsible to produce the rock suites of the area

In general these help to

- Fill the existing gap of information
- Promote the understanding of the geo chemical characteristics of these rocks in order to establish their genesis (source and history)
- Contribute some data set to the on going worldwide studies of continental volcanism.

1.6. Methodology

- Literature review

Relevant previous works on the geology, volcano logy, tectonic setting, petrology and geochemistry of the study area were reviewed from published or un published reports maps, journals, scientific publications, web sites, etc.

- Fieldwork

Sampling and mapping was performed from January 14 to February 02/2005 and from June24/2005 to July 03/2005 for a total of about 30 days.

The field traverses were primarily aimed for systematic sampling different flows and variety of rocks for petrographic and geochemical analysis. Rocks were described at the outcrops. Photographs were taken at representative structures and out crop features. During traverses an attempt was made to select complete sections having all lithologic units.

A total of 53 rock samples were collected during the fieldwork. The sample numbers have a prefix "GUN" standing for Guna. Most of the samples are collected from phonolite and rhyolite lava flows, few from pyroclastic flows, trachytic flows, and rhyolitie domes.

- Map preparations

The geological map of the area is produced based on ground traverses and aerial photo interpretation. A total of 64 aerial photos were used for interpretation of the lithologies and structures. Some of the aerial photographs taken by the Ethiopian mapping authority (EMA) were recent (1980) where as the others are of 1957. Along with the aerial photos 1:250,000 topographic maps of "Debre tabor Nc.37-2" map sheet and 6 sub sheets (1:50,000) were used as base maps. In addition land sat imagery were also utilized. The map is scanned, digitized & processed by different computer soft wares mainly ILWS 3.2 academic, Map Info, Correl drow, etc.

- Petrographic investigations

A total of 37 standard thin sections were prepared in the mineralogy and petrography laboratory of Geological Survey of Ethiopia (GSE). The thin sections were described using polarized petrographic microscope. With this 25 relatively fresh samples i.e. free of alteration or secondary minerals were selected for geochemical analysis. A detailed

petrographic study /thin section descriptions/ including mineral identification, modal proportion, textural descriptions, and rock naming were performed. Representative mineral assemblage and peculiar textures were photographed under the microscope. The samples selected for geochemical analysis were crushed and powdered at Central Geological laboratory of the Geological survey of Ethiopia. The 5-1mm crushing was dome by manganese steel jaw crusher and 200-mesh powdering was by a cobalt mixer mill.

- Geo chemical analysis

The powdered samples were analyzed for major, trace and rare earth elements by ICP MS (Inductively Coupled Plasma Mass Spectroscopy), and DCP MS (Direct Current Argon Plasma Mass Spectroscopy) methods at Pennsylvania state university (U.S.A).

- Electro microprobe analysis

10 uncovered thin sections from the phonolite lava were also shipped to Pennsylvania state university (USA) for electro microprobe analysis. The slides were polished by 0.3 & 0.05 μm Aluminum Oxide powder and 6, 3, 1, and ¼ μm diamond pastes, they were carbon coated by graphitic carbon coating and prepared for probing. The probing was performed by using Joel come bax 5x50 electron probe micro analyzer fitted with an energy dispersive system. For all element analysis an acceleration potential of 15 kev, a sample current of 20 nA, an electron beam diameters of 1μm and counting time of 20 seconds on peak position and 10 seconds on background position were used. Natural and synthetic minerals were employed as standards.

- Data analysis and interpretation

All the data collected from the various works conducted were organized analyzed and interpreted by using different computer soft wares such as Microsoft Excel, IGPET and Min pet.

1.7. Limitations / problems

In general, the challenging problems that have constrained the research work are

- In accessible deep gorges rugged mountainous nature of the topography.
- Very limited, resource for detailed fieldwork.
- Scarcity or absence of the field and analytical data (isotope data for all lavas, mineral chemistry data on rhyolite and trachyte lavas).
- Complex geological evolution of the felsic volcanism.

CHAPTER 2 REGIONAL GEOLOGIC SETTING

2.1. Introduction

At present, about 30% of Ethiopia has been mapped at the 1:250000 scale. The distribusition of lithologic varieties shows that the country is covered by about 18% proterozoic crystalline basement 25% Mesozoic sediment and 56% Cenozoic volcanic and sediments (Solomon Gerra 2000).

The three major geological terrains recognized in Ethiopia are

1. Proterozoic crystalline basement-

The Precambrian basement is consisting of various high-grade gneisses and schists, Meta –volcano Sedimentary rocks, and associated syn to post tectonic plutonic rocks; these crystalline basement rocks are poly deformed and metamorphosed rocks of pan African age related to both the Mozambique belt (MB) and the Arabian Nubian Shield (ANS) (Gichile, 1991, Davidson, 1983). The Precambrian basement of Ethiopia is divided in to three different litho tectonic units (Kazmin et al 1978,and 197 9).

i) The Lower Complex unit: -

Consisting of high-grade biotite –amphibole gneisses with minor qurtzo-feldsphatic gnessis, calc silicates and amphibolites, affected by faulting and folding.

ii) The Middle complex: -

Meta sediments in which the primary depositional structures are locally preserved generally represent this unit. It contains schists, marble, and meta-arkoses with patches of ophilites, amphibolites and other basic meta volcanites associated with graphitic schists phyllite and qurtzites. This unit is also affected by faulting and shearing.

iii) The Upper Complex:

This is the youngest and least deformed Precambrian rock assemblage, principally composed of detrital sediments and carbonates. In northern Ethiopia, this unit is associated with Meta volcanites varying from basalt through dacite to andesite. Andesite seems predominant in the area and is found associated with grey wackes.

2. Late –Paleozoic to Mesozoic marine and continental sedimentary rocks

The Paleozoic era in Ethiopia is marked by regional unconformity due to long period of peneplanation. Very few Paleozoic residual deposits (containing Precambrian basement debris and agglomerates) are observed on the peneplained surface in northern Ethiopia (Enticho sand stone). The permo- carboniferous glacial deposit of Ediga Arbi, which is about 160m thick, represents patches of Paleozoic deposits in northern Ethiopia.

The Mesozoic sequence in most part of Ethiopia consists of three major sedimentary units.

The basal sand stone (Adigrat Formation) is a deltaic near shore sand stone of late Permian-early Jurassic age and was deposited during the transgression.

The basal sand stone unit is overlain by mid –late Jurassic limestone, shale and gypsum of the Antalo formation. Early Cretaceous sand stone that marked the regression of the sea caps the Mesozoic sequence (Kazmin, 1972).

3. Cenozoic, basic and felsic volcanic and associated sedimentary rocks

The Cenozoic volcanic sequences rest either directly on Precambrian basement or on Mesozoic sedimentary sequences. The volcanic succession consists of a thick (up to 2500 m), distinctly bimodal, sequences of basalt and rhyolite, underlying low angle shield volcanoes (Tarmaber formation).

2.2. The Cenozoic Ethiopian Volcanic Province

Following the late Mesozoic-early Cenozoic regression of the sea to the east and southeast an epirogenic uplift of Afro-Arabia (East Africa, Arabia peninsula and the intervening regions now occupied by the Read Sea and Gulf of Aden) occurred on an immense scale (Cherenet, 1995). According to Mohr, (1963), the magnitude of the uplift was such that nowhere in the world out side the orogenic belts have basement rocks been uplifted to such an elevation (e.g. 3000m at Mt. Assimba, Tigray) as that associated with Afro Arbian swell. The cause and initiation of the major uplift is closely related to the first eruption of flood basalts, a mantle plume upraised the land mass which fissured

under tension and permitted the ascent of magma generated by high degree of decompression melting in the mantle to form the trap series.

Following this uplift tholeitic flood basalt volcanism was wide spread in the early Eocene-Oligocene to form the northwestern and southern plateaus.

The Ethiopia Large Igneous province (LIP) which is located near the triple junction of the Red sea, Gulf of Aden and East African Rifts is considered as a young example of continental flood basalt volcanism associated with continental break up. The CFB province was formed because of the impingement of the Afar mantle plume beneath the Ethiopian lithosphere. It covers an area of at least $6x10^5$ km^2 and has an estimated volume of volcanic rocks greater than $3.5x10^5$ km^3 (Mohr ,1983). The succession locally exceeds 2000m in thickness.

Most of the flood basalts were extruded over a short time period (possibly 1 - 2 ma) 30ma (Hofmann, 1997 and Hofmann et al, 1997) and significantly predates the main extensional phases (Menzies et al., 1992). However, there are evidences for older (as old as 45 ma) less extended flood magmatism further south in Ethiopia (Ebinger et al., 1993, George, 1997) and probably belong to separate phase of volcanism. Subsequent volcanism, from 22ma to present occurs as large central vent volcanoes on the plateau or is associated with extension and is localized in the rift axis.

The MER that is an important segment of the continental East African Rift dies out or bifurcates further south in to the lake Turkana and lake Stifane rifts and the Reirba proto rift south of lake Chamo. According to Kazmn et al., (1980), initial sagging of the MER started about 15Ma and was followed by major episodes of rifting at 10, 5, 4, and 1.8 to1.6 Ma. Each stage of rifting and down faulting was accompanied by a bimodal (felsic mafic) volcanism in the rift and formation of basaltic and trachytic shield volcanoes on the rift shoulder and margins.

The general consensus is that down faulting of the Afar depression started at a much earlier age and that rifting was accompanied by a voluminous flood basalt volcanism. Following the initiation of subsidence of the Afar depression and the MER, subsequent volcanism was restricted at first to the evolving rifts and then to the axial zones which later become a focus of quaternary and recent volcanic activity.

2.3. Volcanics of North Western Ethiopian plateau

The plateau volcanics is cut by the rift faulting and are distributed asymmetrically about the Afar and Main Ethiopian Rift. That lying to the west of the rift system is designated the Western Ethiopian plateau (WEP), while the other to the east is named the South Eastern Ethiopian plateau (SEP). The WEP comprises the northern, central, and southwestern sectors, whereas SEP includes the eastern, southeastern and southern most part of the Ethiopian flood volcanic province.

In the northwestern Ethiopian plateau, the volcanic succession is emplaced on the sub horizontal Mesozoic transgressive and regressive sedimentary strata. This volcanic plateau does not fit the popular image of a continental flood basalt province in that it is not a thick monotonous, rapidly erupted pile of un deformed flat lying tholeitic basalts. In stead it is made up of several distinct volcanic centers with different magmatic character and with a large range of ages (Kieffer et al., 2004).

The major volcanic units of the Western Ethiopian Plateau (WEP) include

- The Oligocene flood volcanics (Trap series) i.e. (Oligocene –Miocene basalts and rhyolites)
- Miocene- Pliocene shield volcanoes
- Volcanic plugs and domes
- Quaternary volcanics

(See Figure 2.1)

2.3.1. The Oligocene flood volcanics (Trap series)

In the WEP the flood volcanic succession includes basaltic lava flows, basaltic tuffs, as well as a considerable volume of rhyolitic, trachytic and phonolitic products (Mohr and Zenettin, 1988). Intermediate lavas are lacking and the volcanism is of a distinctly bimodal basalt rhyolite type (Chazot and Bertand, 1993) a feature common to most continental flood basalt provinces (e.g Karoo and Parana). In their mineralogical composition most of the flood basalt are aphyric to sparsely phyric and contain phenocrysts of plagioclase and clino pyroxene with or with out olivine. They have tholeitic to transitional chemical composition (Pik, et al., 1998, Mohr ,1983).

Recently determined ^{40} Ar/ ^{39} Ar dating has yielded 30ma ± few Ka for most of the trap series in northern Ethiopia (Hoffmann et al., 1997, Coulie et al., 2003, Kieffer et al., 2004). Hoffmann et al investigated three sections i.e. (Lima Limo, Wegel Tena and Central sections), they reported 30.2 to 28.2 Ma for basalts from the Wegel Tena section (200 km north of Addis Ababa), 30.8 to 29.4 plateau age for basalts from Lima Limo section (450 km north of Addis Ababa), 29.2 to 29.6 Ma for basalts from the central section (100 km further north along Woreta – Woldia or Chinese road) and 30.4 Ma at the base of the Adigrat section, the lowermost lava flow overlaying the Jurassic sediments, 29.4 to 26.9 M.a for basalts from the Blue Nile Valley (Blue Nile Basalt).

Pik et al (1998) sub divided the flood basalts of the North Western Ethiopian region into three, types the Low Ti (LT), High Ti-1, HT_1) and high Ti -2 (HT_2) on the basis of their geochemistry. The low Ti (LT) basalts are transitional to tholeritic and characterized by low $Ti0_2$, P_2O_5, Fe_2O_3 and Nb/La and high SiO_2. The high Ti_2 (HT_2) are sub alkaline basalts which display high Tio_2, P_2O_5, Fe_2O_3 and Nb/La and low SiO_2.The high Ti-1 (HT_1) basalts exhibit intermediate characteristics between the LT and HT_2 groups. The high TiO_2 series are found in the southeastern sector of the plateau, and a low TiO_2 type found in the Northwestern sector.

Despite the predominance of basalts, the flood volcanics (Trap series) contains significant volumes of felsic volcanic rocks usually in the upper parts of the sequence (Ayalew and Yirgu, 2003). The felsic volcanic rocks are mainly friable tuffs, rhyolites and ignimbrites, inter layered with the flood basalt particularly in the upper parts of the sequence (Ayalew et al., 1999, Mohr & Zanettin, 1988, Pik, et al., 1998).

The Oligocene ignimbrites are exposed over large part of the northern and southern Ethiopian plateaus. They cover an area of about $7x10^4 km^2$ and have an estimated volume of at least $6x10^4 km^3$ that represent 20% of that of the trap basalts (Ayalew et al., 2002). The ignimbrites generally lie directly on the flood basalt sequences, but also occur inter bedded with the upper parts of the basalt succession. Their over all thickness is highly variable and locally reaches 700m. Individual flow units vary in thickness from < 3 m to 15 m.

Three regionally and geo chemically distinct plateau rhyolite units have been recognized by (Ayalew et al., 2002).

(1) Lima Limo rhyolites (0.25% < TiO_2 < 0.45%) outcropping in the northwestern sector of the northern plateau inter bedded with low TiO_2 flood basalt.

(2) Wegel Tena rhyolites 10.45% < TiO_2 < 1%) occurring in the eastern sector of the Afar rift margin overlying high TiO_2 basalt.

(3) Jima rhyolites (0.45% < TiO_2 < 0.72%) exposed in the southern Ethiopian plateau capping high TiO_2 flood basalt.

The Miocene rhyolites are situated in the Molale – Debre Birhan area close to the rift margin and overlie Miocene low Ti- flood basalts. Ignimbrite eruptions resumed in the Miocene during two episodes dated at 15.4 ±0.2 Ma and 8.0± 0.2Ma for the Debre Berhan area Central plateau.

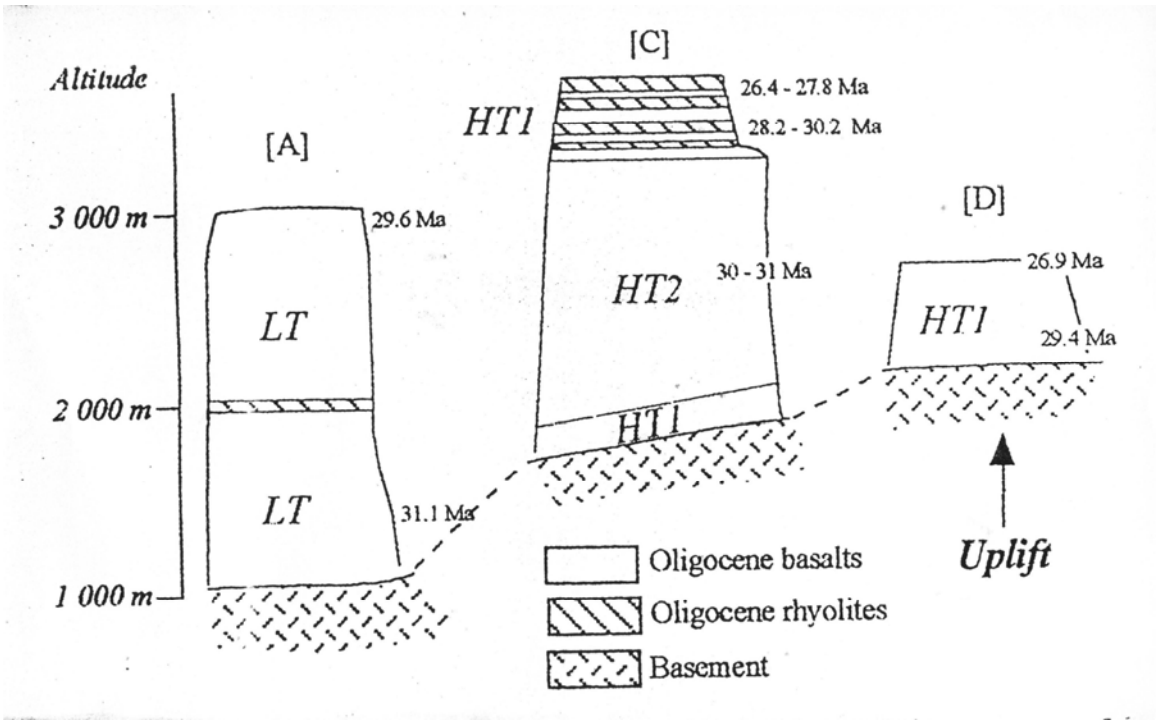

Figure 2.1: schematic logs after (Pik etal, 1999). A, C, and D are for the northwestern, eastern and southern part of the plateau respectively. LT, HT1, HT2 are three petrologically and geochemically distinct groups identified among the northwestern Ethiopian plateau basalt (pik et al.1998). Ages are from Hofmannn, (1997)

2. 3.2. The Miocene- Pliocene shield volcanoes (Termaber formation)

The flood volcanism was succeeded by emplacement of large shield volcanoes and by continental rifting (Mohr, 1983, Hoffmann et al., 1997). A number of large shield volcanoes developed on the surface of the volcanic plateau overlying the thick sequence of flood basalt.

These volcanoes are conspicuous features of the Ethiopian plateau and distinguish it from other well known, but less well preserved flood basalt provinces such as the Deccan and Karoo. According to Kieffer et al., (2004) currently about 20 % of the surface of the plateau is covered by shields, the summits of the shields are about 1.5km above the flood basalt. They also calculated that the volume of the shields was about 20% of that of the flood basalts that is about $4x10^4km^3$.

Simen, Mt Choke, Guguftu (Mt Uorra) and Mt Guna are the main shield volcanoes on the northern Ethiopian plateau. The Simen shield volcano with age of 30.4 Ma has 4533 m height (the highest point in Ethiopia) this peak rise almost 2000 m above the top of the flood basalt. Mt. choke has a basal diameter of over 1000 Km and rises to 4052m, some 1200m above the flood volcanic. Guguftu shield has 3859m peak at the summit of Mt Uorra. The age of both Choke and Guguftu is 22 Ma years.

Like the flood volcanics the shield volcanoes are bimodal and contain sequences of alternating basalts, rhyolitic and trachytic lava flows, tuffs, and ignimbrites, particularly near their summits.

The lava flows of the shield volcanoes are thinner and less continuous than the underlying flood basalts. They also are more porphyritic, containing abundant and often large phenocrysts of plagioclase and olivine. The Simen shield is tholeitic and surmounts tholeitic flood basalts while Choke and Guguftu are alkaline and overlies alkaline flood basalts (Kieffer et al., 2004).

Mt. Guna which is the focus of this study has an Ar - Ar age of 10.7 of Ma (Kieffer et al., 2004). It has 4135m heights, about 1500m above the flood basalts. The average estimated basal diameter is about 40 Km.

2.3.3. Volcanic plugs and domes

A conspicuous feature of the volcanic landscape in the northern Ethiopia volcanic plateau is the presence of numerous volcanic plugs. These structures are relicts of central conduits of volcanoes exposed by erosion of less resistant volcanic formations. They have felsic compositions and have been linked to the felsic volcanic rocks of the Ethiopian plateau. They have silica saturated, alkali rich trachytic composition. Their compositions are distinct from those of felsic rocks within trap sequences that are rhyolitic. The plugs are not the feeders to the trap volcanism but instead may be related to overlying shield volcanoes (Dercq et al., 2001). The plugs are compositionally distinct from the majority of felsic volcanic rocks of the plateau, which have rhyolitic compositions, and from more recent felsic volcanoes. Instead they resemble the trachytic sills and flows that are intercalated with pyroclastic rhyolites (tuffs and ignimbrites) in the upper units of shield volcanoes (Termaber formation).

Figure 2.2:Trachytic plug near Amed Ber

2.3.4. Quaternary volcanics

Quaternary alkali basalts (Tana lava) occur related to local rift structures north south trending extensional faults, (Chorowicz et al., (1998). Volcanic cones and flows of scoraceous basalts are well preserved in the Lake Tana graben. These basalts are considered Pleistocene in age. The volcanic rocks of the lake Tana area are usually described as olivine alkaline basalts (Merla et al., 1979), which may have a thickness up to 1300m (Mohr, 1971). In the recently compiled geological map of Ethiopia, (Tefera et al., 1996) described the rocks as plateau basalts, consisting of quaternary alkaline basalts and trachytes.

The region south of Lake Tana (figure 2.1) exposes Quaternary volcanic rocks composed of vesicular alkali basalt and cinder cones, indicating the volatile rich nature of the host magma**.** The host lavas are basanitic in composition and are dated 0.39± 0.03 Ma (Hofmann, 1997). The basanites occur as massive, vesicular and fragmented rocks. They are aphyric to sparsely porphyritic containing phenocrysts of in order of decreasing abundance olivine, plagioclase, clinopyroxene and occasionally nepheline set in a fine-grained matrix composed of the same phase as the phenocryst assemblage (Abate et al., 1998).

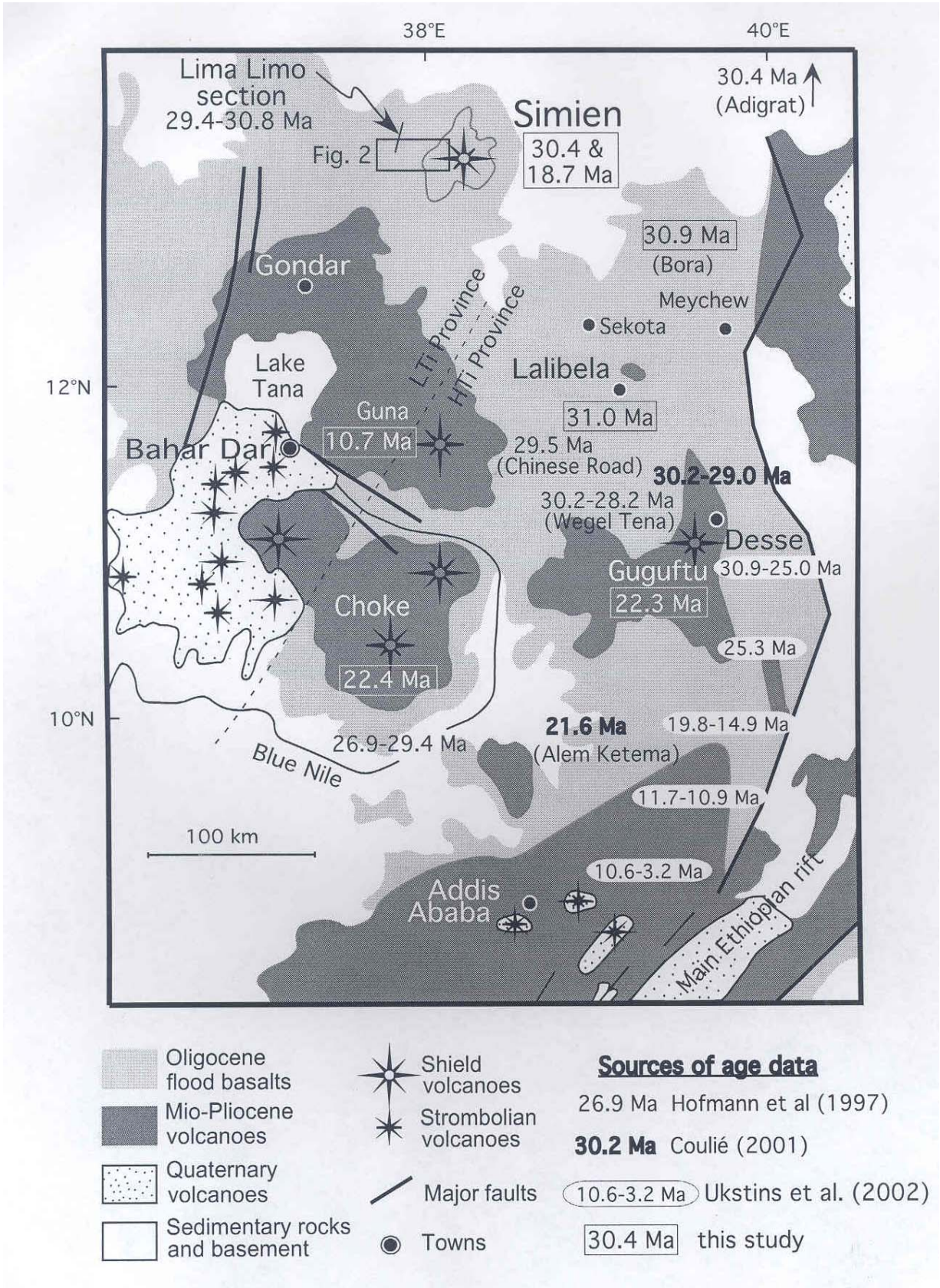

Figure 2.3: Regional geological sketch map of the WEP (After Kieffer et al., (2004)

CHAPTER 3 GEOLOGY OF GUNA VOLCANIC MASSIF

3. 1 Introduction

Guna Mountain is one of the huge volcanic centres on northwestern Ethiopian plateau. It is found between Seimen and Choke Miocene- Pliocene shield volcanoes, east of Lake Tana. The volcanic massif has a maximum basal diameter of about 50 km in N-S and 30 km in E-W directions, it covers an estimated area of about 760 km^2 The altitude varies from about 2600 m at the base to 4135 m at the peak. Kiffer et al., (2004) provided an $^{40}Ar/^{39}Ar$ age of 10.7 on a sample taken from the coordinate $11^0 47' 19'' N$, $38^0 16' 13'' E$ near the village Damat Fasiledes.

Active erosion forms short and V-shaped gullies and deep cut canyons. The volcano stands on a relatively flat topography with a height of 1553m above the surrounding area. It comprises different felsic flows over lying on regionally dominant flood basalts. The distribution of these rock units is shown in the geological map of Guna (Figure 3.15). For reasons that the petrographic description of the rocks is given in chapter 4 Petrography and mineral chemistry only field description of the units is summarized here.

3.2. Volcanic successions

The stratigraphy of Guna is shown in figure 3.1, including trap basalt, rhyolite lava flow, pyroclastic flow deposit, trachyte lava flow and phonolite lava flows (from bottom to top).

Elevation	Lithologic symbol	Rock unit	Description
3500	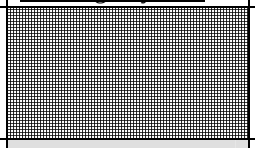	Phonolite	Dark gray to greenish gray, porphyriyhic with phenocrysts of alkali feldspars and feldsphatoids, with greasy luster, platy parting and sonorous ring when struck by hammer.
3000		Pyroclastics	The voluminous product of the volcanic center including ash, tuffs, ignimbrite and trachytic flows.
2650	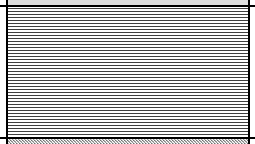	Rhyolite	Lower most guna product including layered lava flow, glassy and columnar jointed lavas and huge domes.
	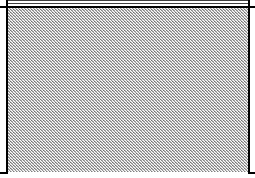	Flood basalt	Black to dark gray colored, aphyric to poorly porpheritic. With micro phenocrysts of plagioclase and pyroxene.

Figure 3.1: Stratigraphic section of Guna massif

3.2.1. Flood basalt

The flood basalts form the base on which Guna volcano overlies. It is widely exposed around the mountain forming a flat -lying topography continuing up to an elevation of around 2650mt.

At the southern end of the massif south of Simada village an exposure of river cut a layered sequence of flows have been observed. Here the sequence consists three thin (<20m) flows. The overall thickness of flood basalt succession in this area is estimated to be about 650m considering the contact between the flood basalts and the Mesozoic sediments in Abbay river gorge around 2000m.

Generally, the basalt flows are black to dark grey in colour, massive, fine-grained, aphyric to poorly porphyritic. Plagioclase and clinopyroxens are present as phenocrysts. Sometimes they are slightly to moderately weathered.

Flows are sampled around Simada / Wegeda village (Gun-10, Gun-11 and Gun-12) on southwestern side of the mountain and near Iste (Mekane Iyesus) village (Gun-18) on the southeastern side of the mountain.

Figure 3.2: view of the contact area between the trap basalt (forming the flat lying topography) and the lower most Guna product (rhyolithic lava flows)

3.2.2. Rhyolitic lava flows

Rhyolitic lava flows are the lowermost and earliest products of Guna volcano. They un conformably overly the flood basalts. The contact between the flood basalts and rhyolitic lava flows is marked by red clay (paleosol) and weathered basalt. The rhyolites are the second most abundant flows of the volcano mapped between elevations 2650m and 3000m. It covers about 150 sq km generally forming flows, domes, plugs and peculiar ridges in the area. It is extensively exposed in the south central part of the massif while no out crop is observed in the north. Minor pyroceastic flow beds are seen to associate the rhyolitic lava flows.

In the field observation three types of rhyolitic lava were distinguished: -

- Layered rhyolite flow
- Glassy and columnar jointed lavas
- Domes and plugs

Figure 3.3: Exposure of layered (lower part) and glassy columnar jointed (upper part) rhyolithic lava flow north of Simada village along the road to Arb Gebaya

Layered rhyolite flow: - Exposure of this type of flow is observed and sampled north of Simada village along the road to Arb Gebya at elevation about 2650m. Here the thickness of this lava is estimated about 30m.

This is brownish grey to light grey colored, compacted aphyric to phyric, with composition of alkali feldspar, quartz and volcanic glass.

It forms horizontal flow banding with beds up to 5 cm thickness on the lower part. It has about 15-20m thicknesses. Samples Gun –14 and Gun- 39. Some are slightly weathered.

Figure 3.4: Closure view of layered rhyolitic lava flow, north of Simada village

***Glassy and columnar jointed rhyolite flow*: -**This is dark greenish to black colored, glassy and porphyritic with phenocrysts of alkali feldspar and some plagioclase. It occurs overlying the horizontally layered rhyolitic flows but some times intercalates with it. It commonly forms a hexagonal columnar jointing that is a cooling structure, in a lava flow. It is observed between Zenjero Gedel and Simada Village (Samples Gun–15 and Gun-13). Here it has an estimated thickness of about 50m.

In the western side of the massif along the road to Iste village thin flow about 10m thick of this glassy rhyolite are present resting on top of the trap basalts at elevation about 2657m (sample No. Gun-20). In many outcrops the unit is observed to be weathered.

Figure 3.5: Exposure of glassy and columnar jointed rhyolithic lava flow north of Simada village

***Rhyolithic domes and plugs:* -** Number of rhyolitic plugs, necks and domes are prominent features in the Guna area. The largest rhyolitic dome observed is at Iste Densa north of Iste Mekene Iyesus village intruding through the trap basalt. It has about 250m heights and a diameter of about 500m. Generally the rock is light grey coloured and very fine grained (Sample Na. GUN –19). Other smaller plugs are with a maximum diameter of about 250 m and with height about 120m.

Figure 3.6: Rhyolithic dome at Iste densa (north of Iste Mekaneysus)

3.2.3.Pyroclastic flow deposits

These are products of explosive volcanic activity from Guna felsic center. They consist of lapilli, crystals and rock fragments of varying size and composition. In the southern part of the area, the pyroclastics flows are seen to overly the rhyolite unit, while in the northern part they rest directly on the flood basalts. This unit with its different varieties is extensively exposed covering large area of the mountain. This major product of Guna covers about 500sq km, which is about 65% of the total Guna volcanic products. It occurs in between the two lava successions separating the underlying rhyolite and the overlying phonolite units.

This thick sequence (about 500m) includes

- Massive white ash
- Bedded and laminated ash flow
- Welded Tuff /Ignimbrite and
- Trachytic lava flows

➢ Massive ash flow deposits

This is light grey to white colured, fine-grained and unwelded pyroclastic ash deposit. It is poorly sorted, massive and composed of >50% ash size fragments. This occurs extensively around the central and northern part of the volcano with a thickness of about 200m. In hand specimens, it contains abundant angular and altered fragments of pumice, some crystals of quartz, feldspars and rock fragments. The lithic fragments are mainly of basalt and rhyolite having a maximum diameter of 3-4cm.

Figure 3.7: Massive pyroclastic ash flow deposit at north of Gassay village

- **Bedded (laminated) ash flow deposit**

This type of pyroclastic material occurs in many parts of the massif. Along the Gassy-Arb Gebya road an exposure of 15-20m thick unit of bedded pyroclastic flow deposit is observed resting on massive white ash. With detail observation, it contains tiny pumice fragments and up to 20% lithic fragments. The size of the fragments is ranging from tiny sand size up to about 5-6 cm diameter. The pumice fragments are spherical, altered and measuring 2-3 cm radius. Alternating lithic rich parts shows the layering. Compositionally the fragments are mainly of phonolitihic and rhyolithic. They are angular in shape.

Figure 3.8: Bedded pyroclastic flow deposit

Along the road to Arb Gebeya near the village of Wollela Bahire the ash flow is a light grey coloured composed of pumice, fine lithic fragments and some crystals. It is laminated and cross-laminated. The individual lamella has a thickness of up to 2cm and the bedding 5cm up to15cm

Figure 3.9: Bedded and laminated ash flow deposit near the village of Wollela Baher

A laminated /beded/ ash flow deposit is also observed along the road Gassay to Iste near the village of Luwaye; the bedding is from 2cm up to 15cm thick the pyoclastic material is composed of angular fragments of rhyolite, basalt and pumice, which have a size of up to 2cm radius.

- **Welded tuff /Ignimbritie/**

This is moderately to strongly welded tuff (ignimbritic) flow deposits. It occurs as a distinct cliff-forming unit. The strongly welded ignimbrite is exposed and sampled south of Luwaye village (sample No. GUN-23 and GUN -22) and north of Gassay (GUN 53). It has a light grey to darker greenish grey colour with characteristic tiny fiamme. Crystals of quartz and plagioclase, and rock fragments are the main components. It is observed resting on massive ash deposit that overlay the felsic (rhyolitic lava). Alternating sequences of ash and ignimbrite is also observed, the white ash in this sequence contains large rounded clasts of pumice a size of up to 20cm. The thickness of the welded ignimbrite is estimated to be 3-10m. The moderately welded one is about 50m thick.

Figure 3.10: Exposure of cliff forming ignimbrite (top) and alternating with the ash (middle) south of Luwaye village

- **Trachyte lava flows**

This unit is exposed in the southern part of the area around Zenjero Gedel and in the central part of the volcano commonly forming domes and huge cliff with columnar jointing structure. Figure 3.10 shows the cliff formed by the rock unit at Zenjero Gedel whose height is estimated to be 120 m in this section; it shows well developed columnar jointing. The trachytes are light grey in colour, aphanatic to poorly porphyritic in texture with phenocrysts of quartz, plagioclase and alkali feldspars (sample No. GUN-40, Gun-42 and GUN-29).

Figure 3.11: Trachyte lava flows, forming a cliff at Zenjero Gedel (south of Arb Gebeya)

3.2.4.phonolite lavas

This lava occurrence as a thick viscous lava flow capping the pyroclastc deposits and rhyolitic lava flows. It has a well-developed columnar jointing structure. It overlies the pyroclastic ash at elevations above 3,200 - 3,500m up to the summit area. It occurs with variable thickness 50- 700m forming huge cliffs. The aerial extent is relatively smaller restricted around the centre of the volcano. It covers an estimated area of about 120 $km^{2.}$

The phonolite unit has a greenish grey- to-grey colour, greasy lustre or appearance. It has very compact dense texture, poorly to highly porphyritic with phenocrysts of alkali feldspar and feldspatoids (nepheline).

They have a fissile character and give a sonorous ring when struck by a hammer. A well-developed thin slate like sheets characterizes them, and that the rocks break in to platy parting.

Figure 3.12: Exposure of phonolite lava flow and the contact with pyroclastic ash flow deposit

Figure 3.13: Exposure of cliff forming and columnar jointed phonlites lava flow near Moksh kidane Miheret

- **Phonolite plugs and domes**

Phonolite lava also occurs as plugs and domes. The plugs have a basal diameter of about 250 m and a height of about 100m. The exposures have similar character with the flows as described above. This occurrence is represented by sample No. GUN 35.

Figure 3.14: Phonolite plug

3.3. Structural features

Guna volcanic massif is highly affected by fault expressed by intense V-shaped gullies and rugged surface. The faults are volcano-tectonics and which are short and dense at the center and long but relatively sparse at the margins. As shown on the structural map Figure 3.17 the faults have different trend. However, the principal ones are NW-SE, NE-SW, and E-W trending. The later type appears to be curved and large at the southern margin. In this part of the volcano such faults are seen to block the rhyolite out crops northwards. The NW –SE and E –W trending normal faults are commonly well developed. Generally, they have radial orientations, some times crossing each other. At the central part, the faults are straight whereas they appear to be curved at the margins.

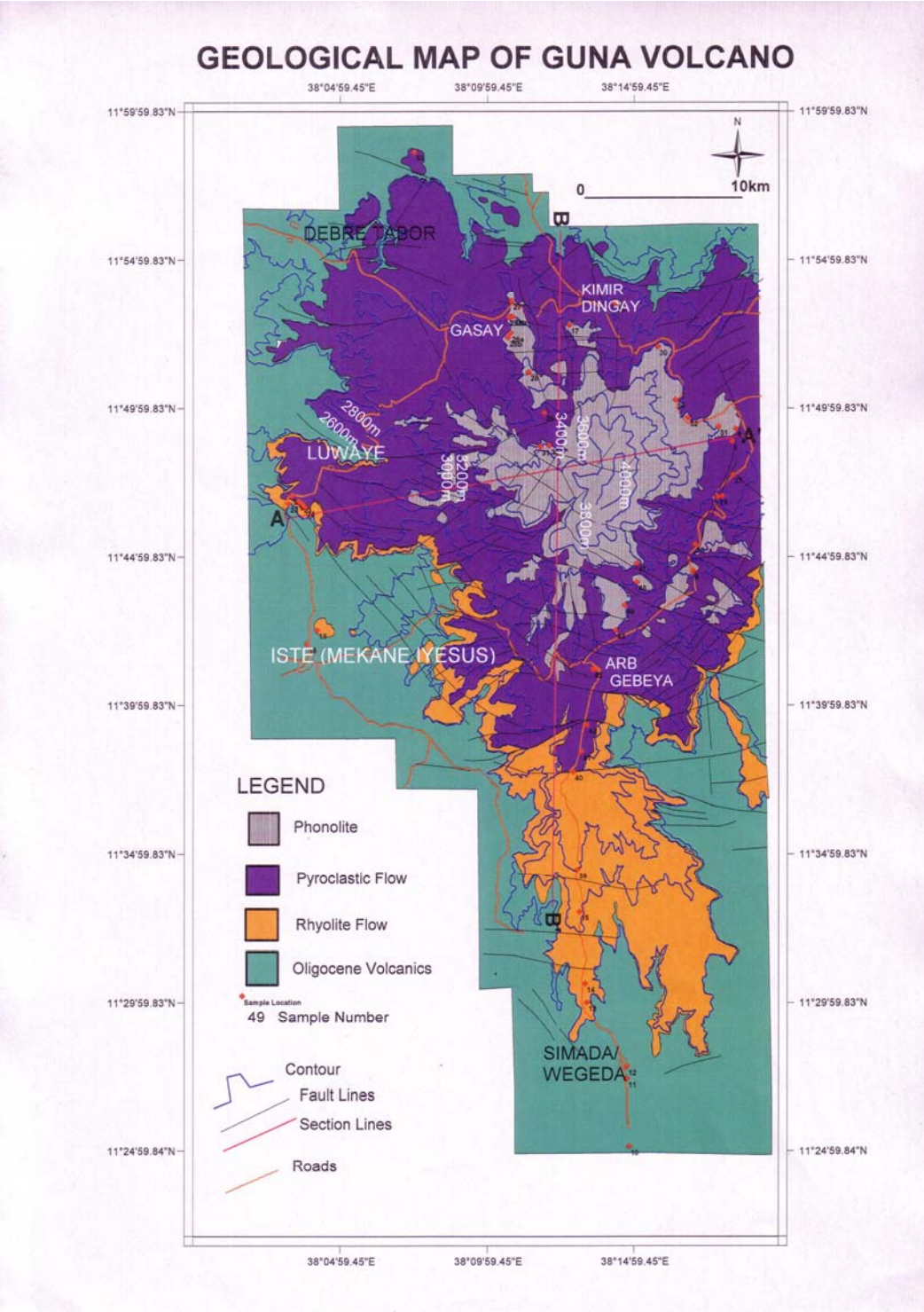

Figure 3.15: Geological Map of Guna

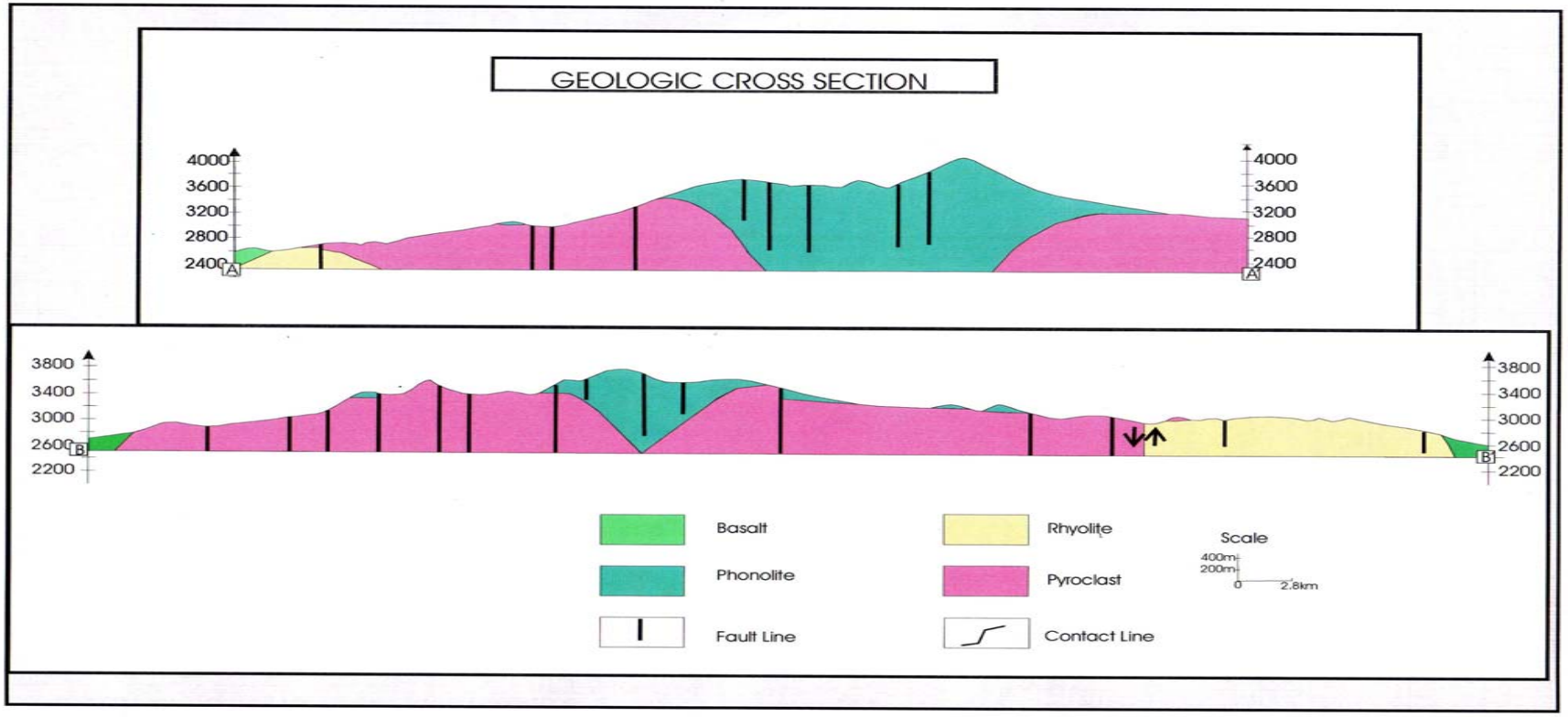
GEOLOGIC CROSS SECTION
4000
3600
3200
2800
2400
A
A'
3800
3400
3000
2600
2200
B
B'
Basalt
Phonolite
Fault Line
Rhyolite
Pyroclast
Contact Line
Scale
400m
200m
0
2.8km

Figure 3.16

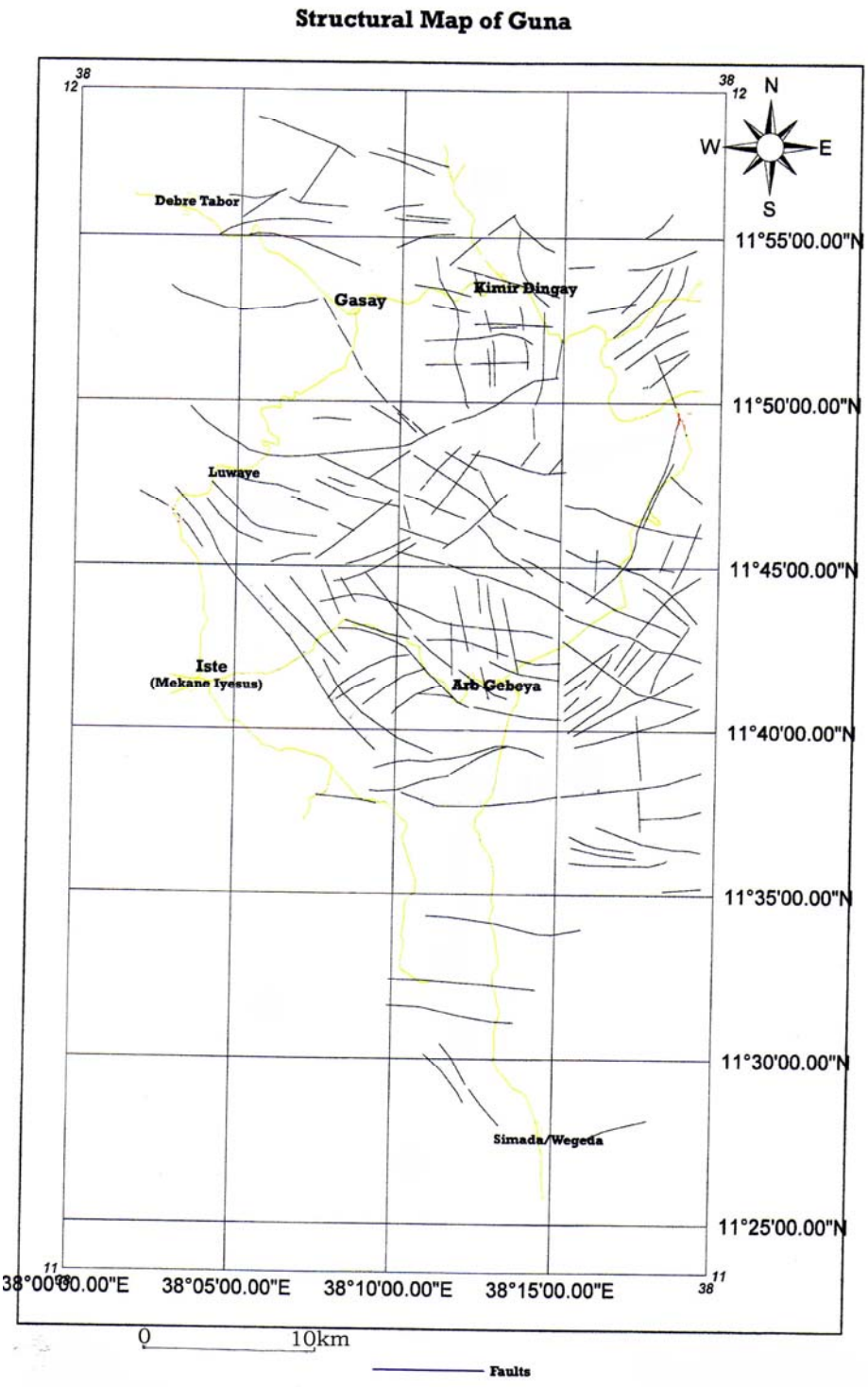

Figure 3.17: Structural Map of Guna

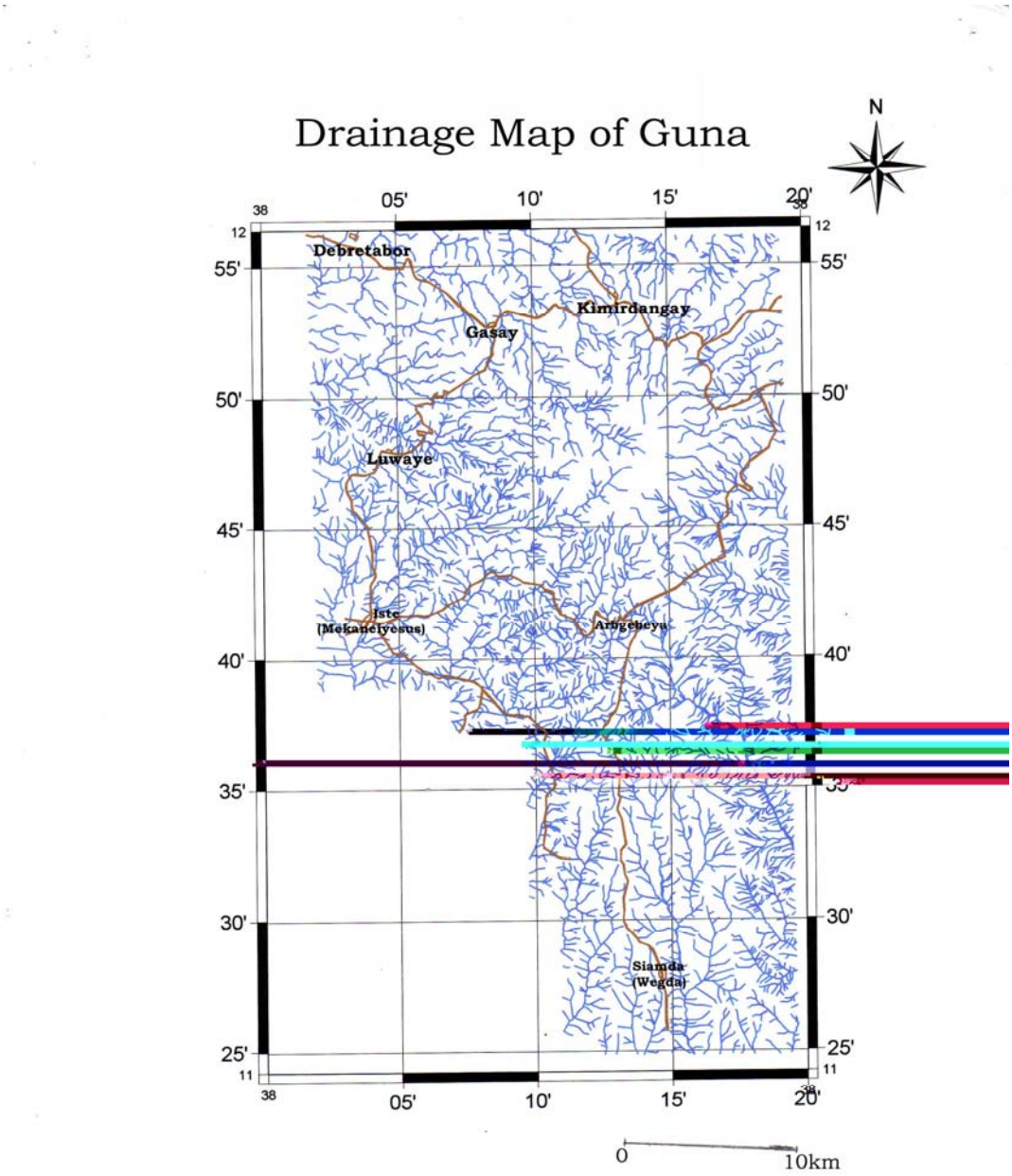

Figure 3.18: Drainage Map of Guna

CHAPTER 4. PETROGRAPHY AND MINERAL CHEMISTRY

4.1.Petrography

Petrographic investigations of 37 thin sections were performed and accordingly the rocks are classified as phonolite, rhyolite, trachyte and ignimbrite (tuffs). The total alkali versus silica classification plot after Le Bas et al (1986), Figure 5.1 also illustrates the samples fall in the filled of rhyolites, trachytes, and phonolites. The phonolite samples are all nepheline normative. Petrographic descriptions of textures and modal mineralogical composition of representative samples are summarized in table 4.1.

The complete petrographic descriptions of thin sections are presented in appendix A. petrographic characteristics of major lithologic units from the study area are briefly described below.

4.1.1. Flood basalts

Three samples GUN-11, GUN-12 and GUN-18 are from the upper part of the flood basalt succession. They show phorphyrithic, inter granular and trachythic /flow texture/. It is composed of 5-10% phenocryst 90-95% ground mass. The phenocryst assemblage consists of 4-7% lath euhedral plagioclase, 1-3% pyroxene (augite), ~1% olivine. The ground mass is also composed of lath shaped Plagioclase, pyroxene (augite), opaque and volcanic glass.

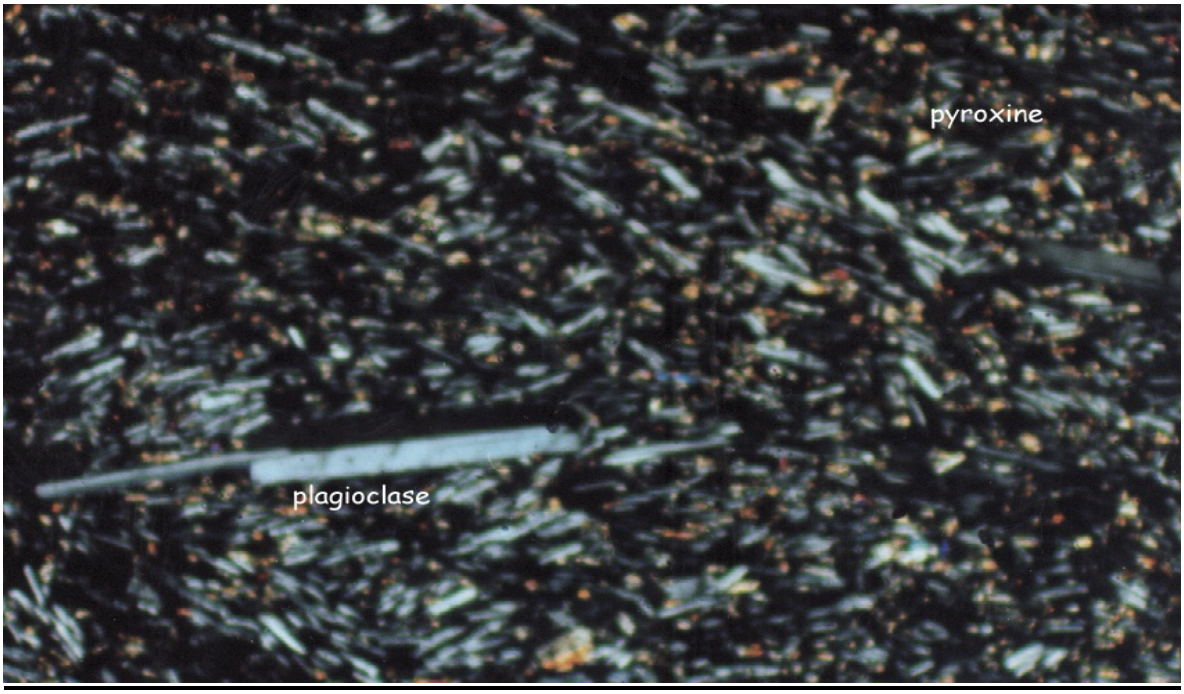

Figure 4.1: Microphenocryst of plagioclase on a fluidal (trachytic) groundmass in GUN-5 (5X XPL)

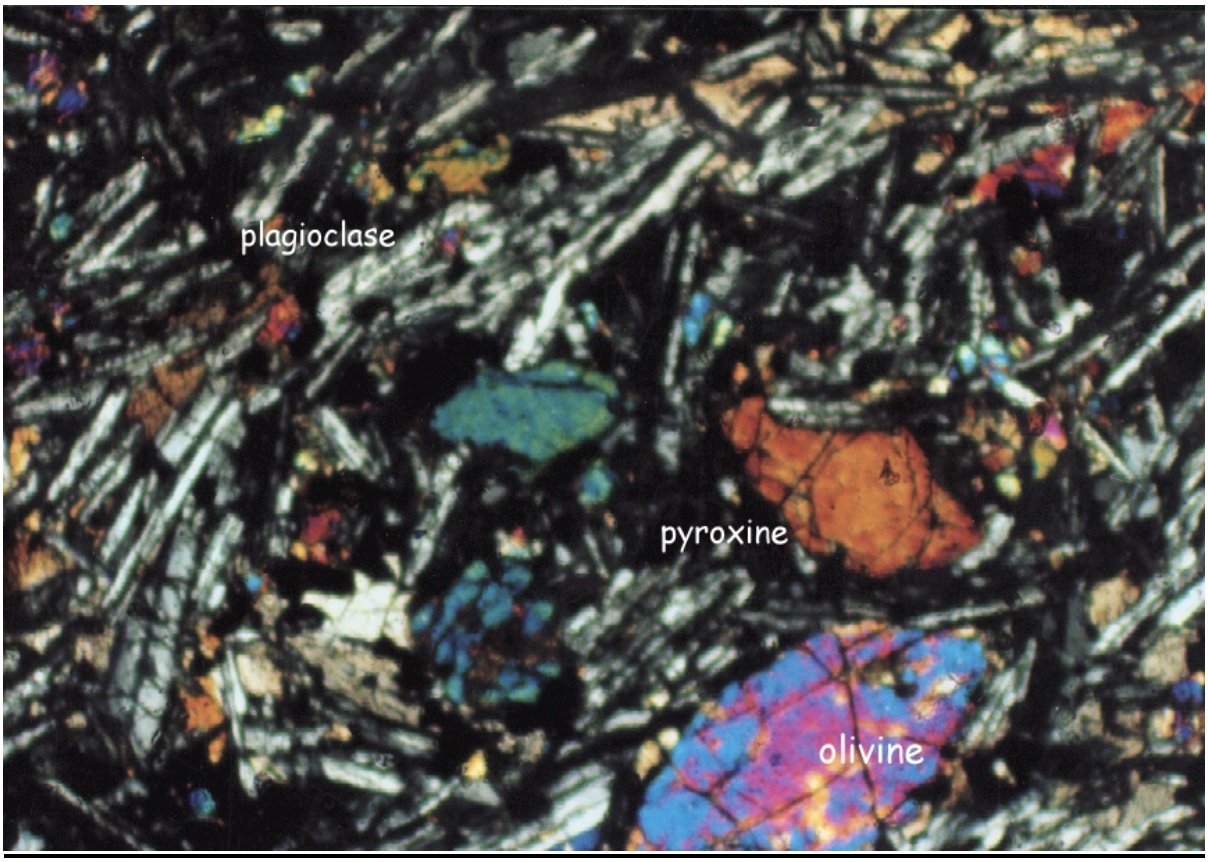

Figure 4.2: Phenocryst of pyroxene and olivine in GUN-18 (5X XPL)

4.1.2.Rhyolites

The rhyolite lavas are hypo crystaline with vitrophyric, porphyritic and perlitic (glassy) texture. Phenocrysts are alkali feldspar (sanidine), plagioclase and quartz. The ground mass is mainly volcanic glass.

GUN-20 is made of 20% phenocrysts and 80% glassy groundmass with perlitic texture and classified as perlite. GUN-14 and GUN -38 are vitrophyric with flow banding texture; they have 13-22% phenocrysts with in glassy and microcrystaline ground mass.

GUN-19 represents a large lava dome; is porphyritic with 12% phenocryst of sanidine quartz, plagioclase, opaque and apatite set in a groundmass of microlithic lath sanidine, volcanic glass, quartz and opaque.

GUN- 13 and GUN -15 are from the columnar jointed glassy lava; they are hypo cryatalline and vitrophyric. They have 15% phenocyst on 85 % volcanic glass ground mass. The phenocrysts are 7% sanidine, 3-5% plagioclase, 2-3% clino pyroxene and 1-2% opaque (Fe –oxide)

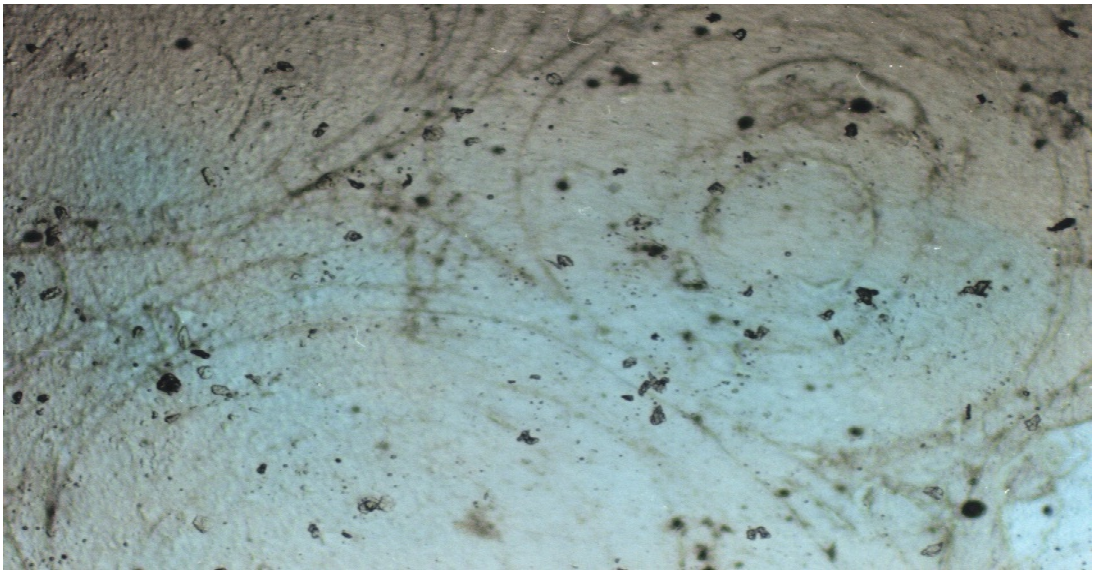

Figure 4.3: Perlithic cracks in a glassy groundmass at, 5X magnification and XPL in GUN-20

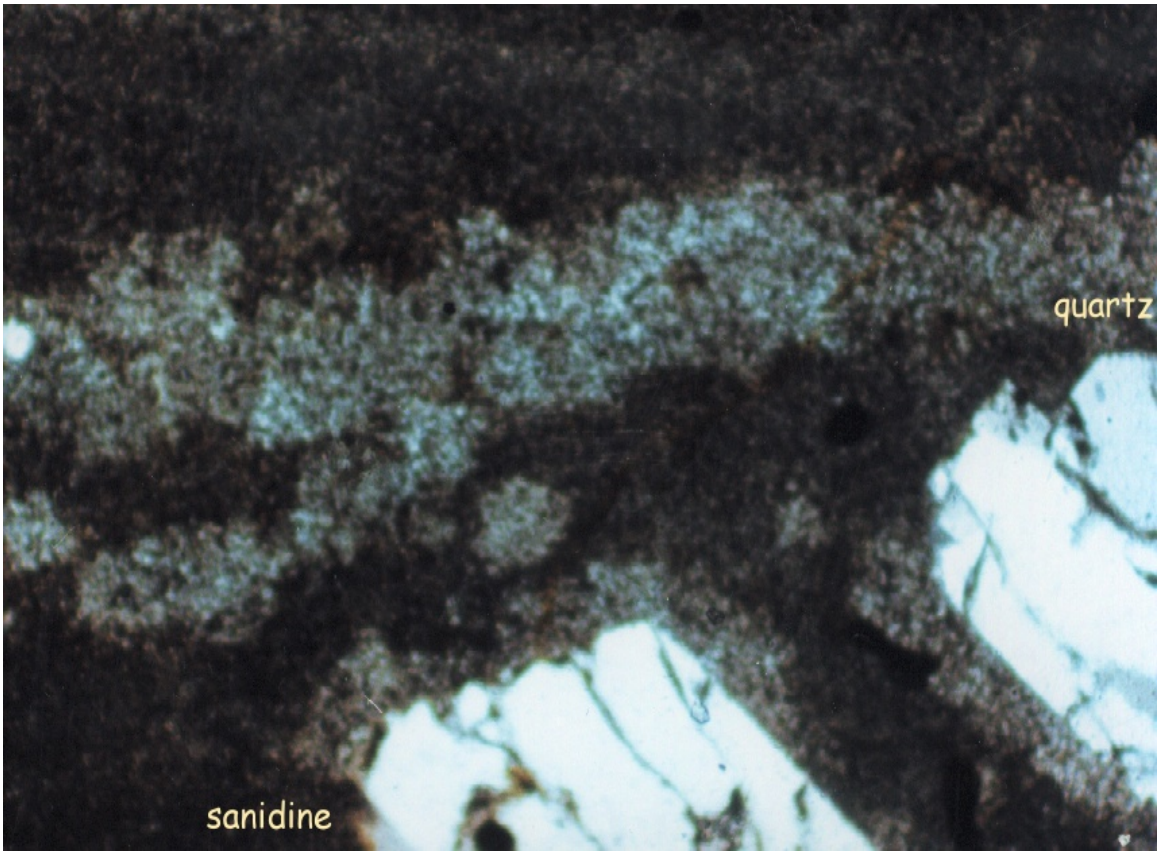

Figure 4.4: phenocryst of sanidine and quartz in a flow banded groundmass at, 5X magnification and PPL in GUN-14

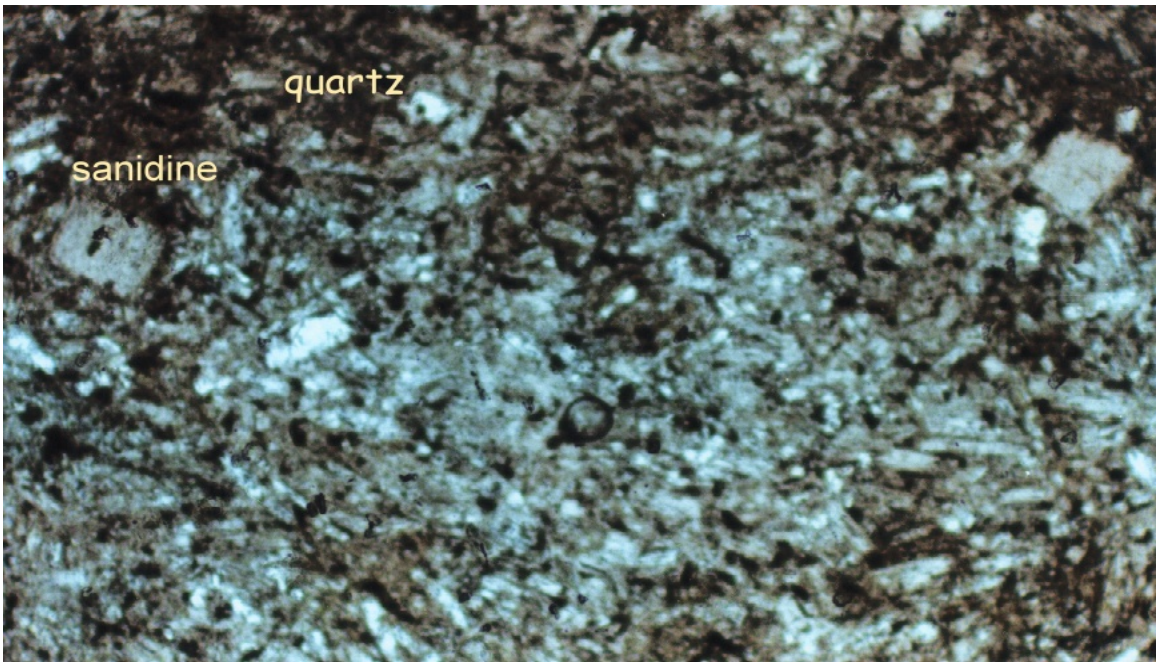

Figure 4.5: Micro phenocrysts of sanidine and quartz in a groundmass at, 5X magnification and PPL in GUN-19 (rhyolithic dome)

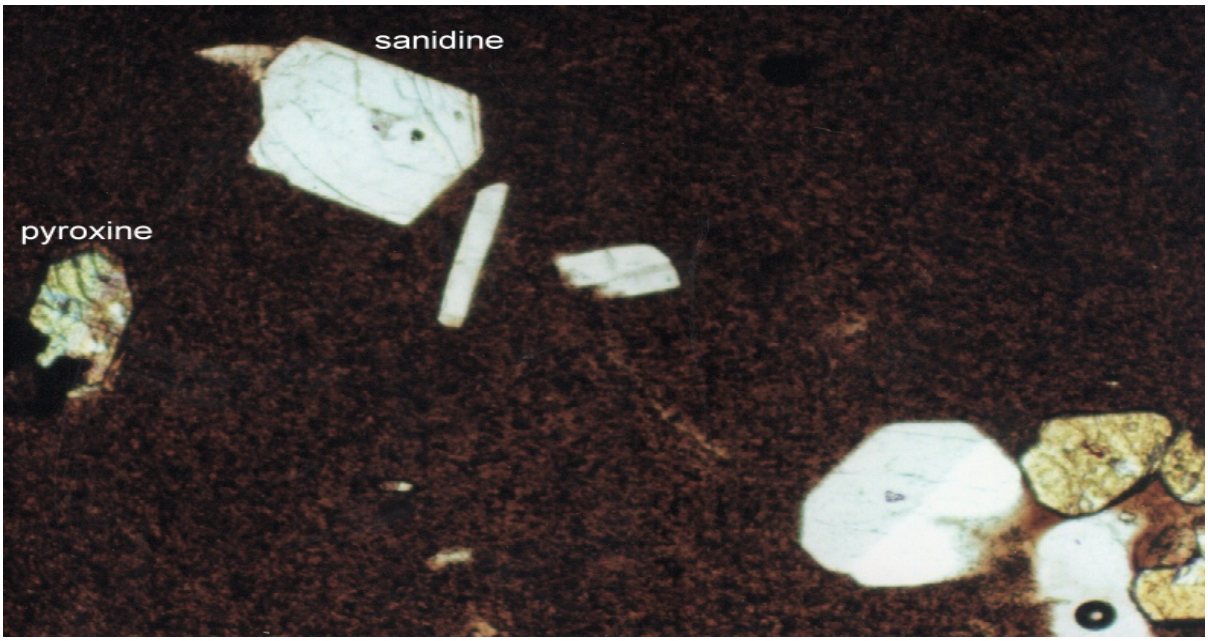

Figure 4.6: Phenocryst of Sanidine and Pyroxene in a glassy groundmass at, 5X magnification and PPL in GUN-13

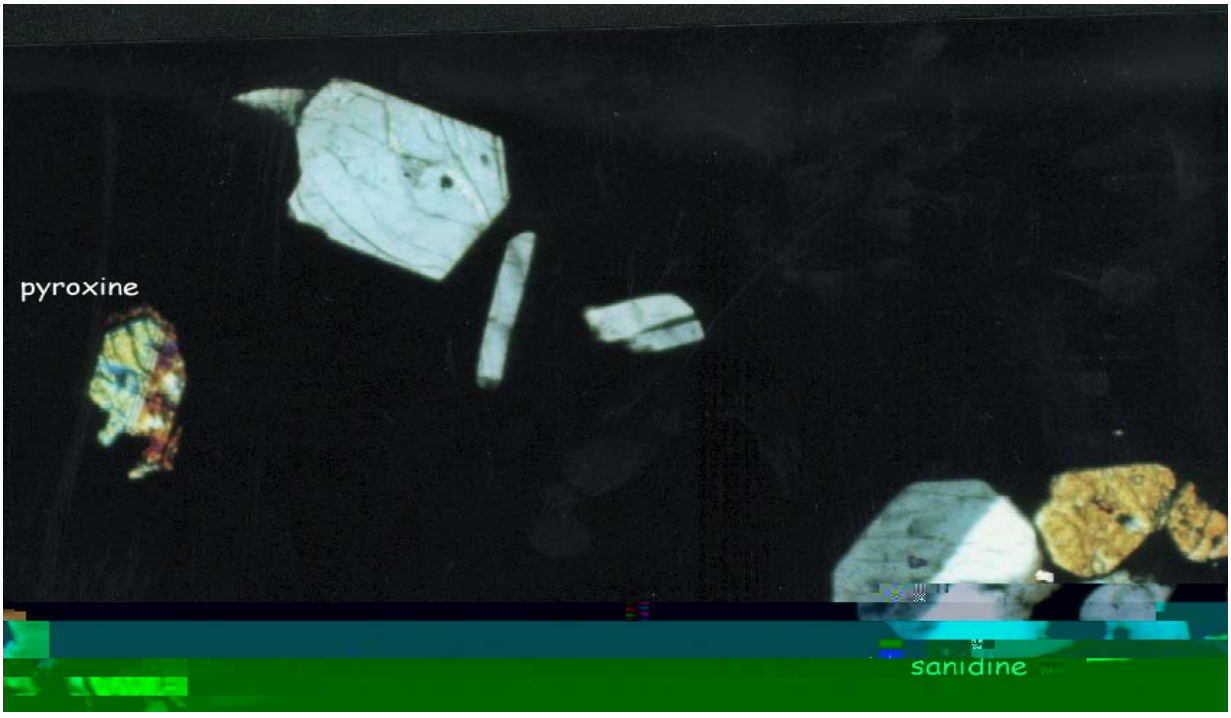

Figure 4.7: Phenocryst of Sanidine, Plagioclase and Pyroxene in a glassy groundmass at, 5X magnification and XPL in GUN-13

4.1.3. Trachytes

These are porphyritic textured with 15% phenocrysts and 85 % groundmass. The phenocryst phase is made of 9-10% large euhedral and tabular crystals of alkali feldspar (sanidine), 3-4% hornblende, 2-1% plagioclase, upto1% opaque and <1% pyroxene. They are set in a finely crystalline groundmass composed of alkali feldspar (sanidine), clino-pyroxene, hornblende and biotite. The groundmass has sub parallel orientation of microlitic sanidine (trachytic texture)

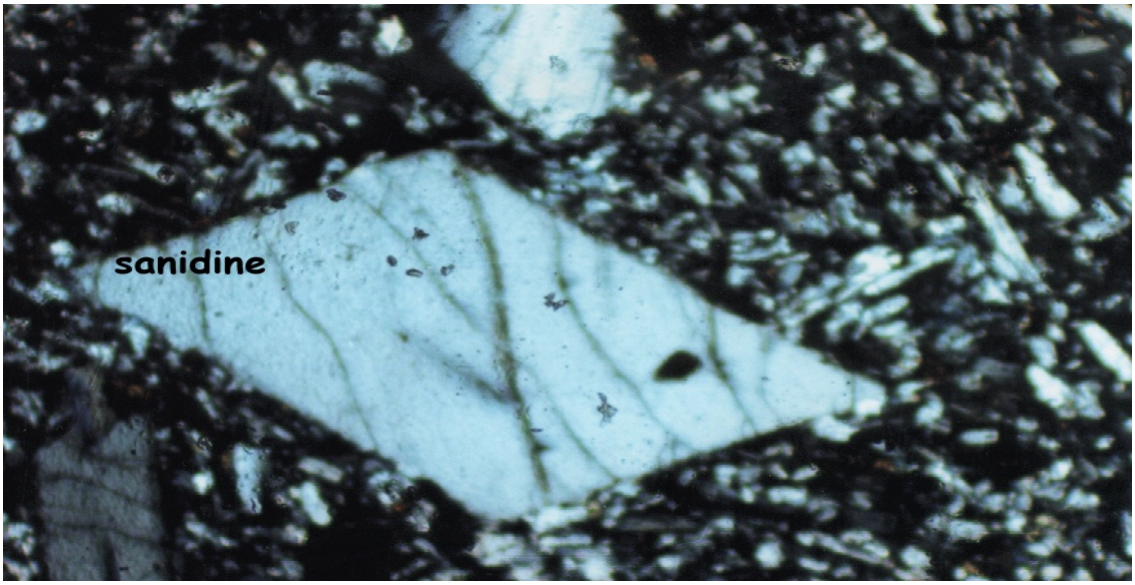

Figure 4.8 Phenocryst of sanadine at, 5X magnification and XPL in GUN-40

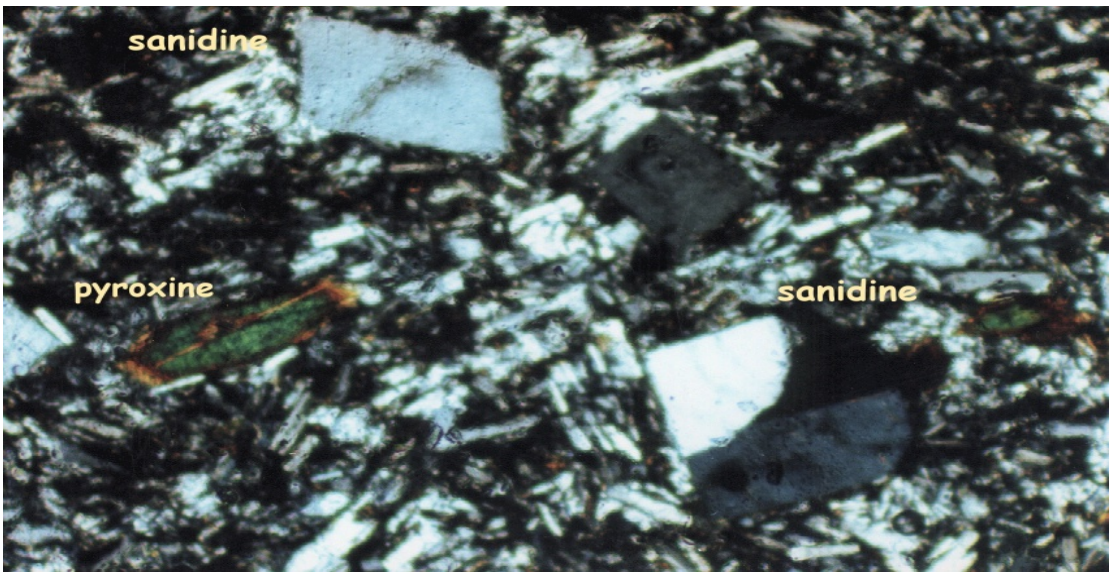

Figure 4.9 Phenocryst of sanadine and clino pyroxene in GUN-42 (5X and XPL)

4.1.4. Ignimbrites

Two samples GUN-23 and GUN- 22 from the pyroclastic flow deposite are classified as welded tuff / ignimbrite. On the total alkali versus silica classification plot after Le Bas et al (1986), Fig 5.1 GUN-23 falls in the filled of trachytes. They have vitrophyric texture with up to 25 % crystals, 25% rock fragments and about 50% volcanic glass. Crystals are euhedral to subhedral alkali-feldspar, quartz and plagioclase. The rock fragments are consists of andsite and rhyolite. They also contain flattened glass shards. Two samples GUN -8b and GUN -21 are unwelded tuff. They have 25-35% crystals, 25-50% rock fragments and 50-15% glassy components

Figure 4.10 Crystals (sanadine and quartz), and rock fragment at, 5X magnification and PPL in GUN-22

4.1.5. Phonolites

The Phonolites are holocrystaline. Their texture is porphyritic and trachytic. Porphyrithic phonolites have 13-40% phenocrysts. One sample GUN-17, with microporphritic texture has 5% microphenocrysts. Three samples GUN -5,GUN- 48 and GUN- 49 are trachytic textured and have <1% phenocrysts. The phenocryst assemblage consists of alkali feldspar (mainly sanadine), nepheline, nosean, lucite, clinopyroxene (aegirene augite) and sphene. The accessories are apatite, opaque (Fe-Oxide) and sphene. The groundmass is made up of mineral grains that are found as phenocrysts. Volcanic glass is not common. Secondary minerals are sercite, calcite, limonite, and zeolites.

Petrographic features of the major minerals are described as follows

- **Alkali Feldspars**

The common feldspar is sanidine generally in two generations as phenocrysts and groundmass. Its abundance as phenocysts is 6-20% in most samples. The phenocrysts are usually 3-5mm in length. They are euhedral to subhedral and show lath tabular or prismatic habit. Carlsbad twining is common. Sometimes the borders of the crystals are corroded or altered. Alteration to calcite and sericite is common.

In the ground mass sanadine is tiny usually lath shaped and shows trachytic texture. It is commonly free from inclusions and zonal growth.

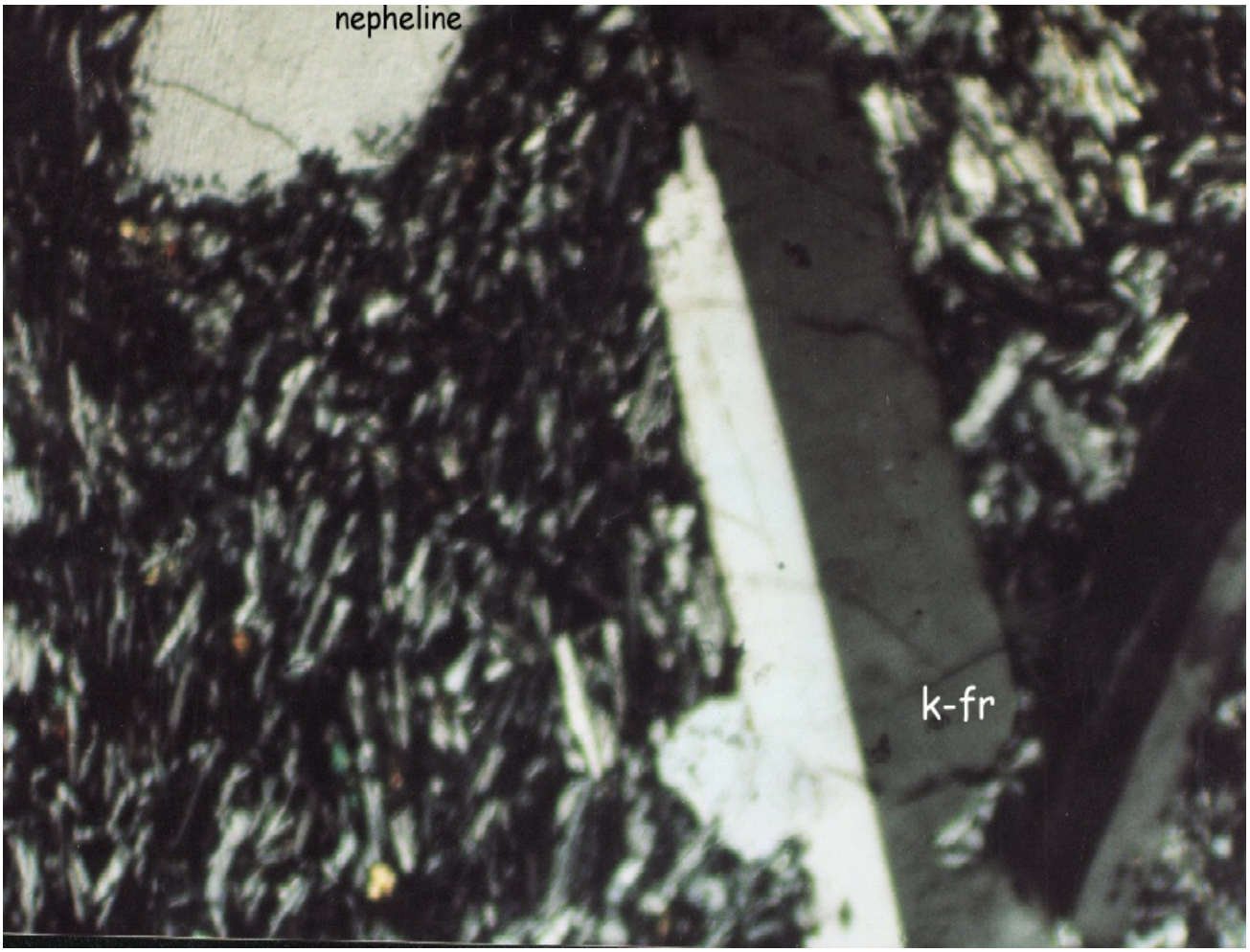

Figure 4.11: Phenocryst of K-feldspar (sanidine) and nepheline in a trachytic ground mass dominantly made up of sanidine in GUN-47 (5X magnification & XPL)

- **Nepheline**

Owing to the characteristic prismatic habit that forms rectangular and hexagonal cross setions, nepheline is usually recognized with ease under the microscope. Usually it is water clear and free from inclusions. It is found as phenocrysts and in the matrix where it builds tiny euhedral crystals yielding hexagonal or rectangular sections. Its abundance as phenocryst ranges 3-10% and its size about 0.75-1.75mm.

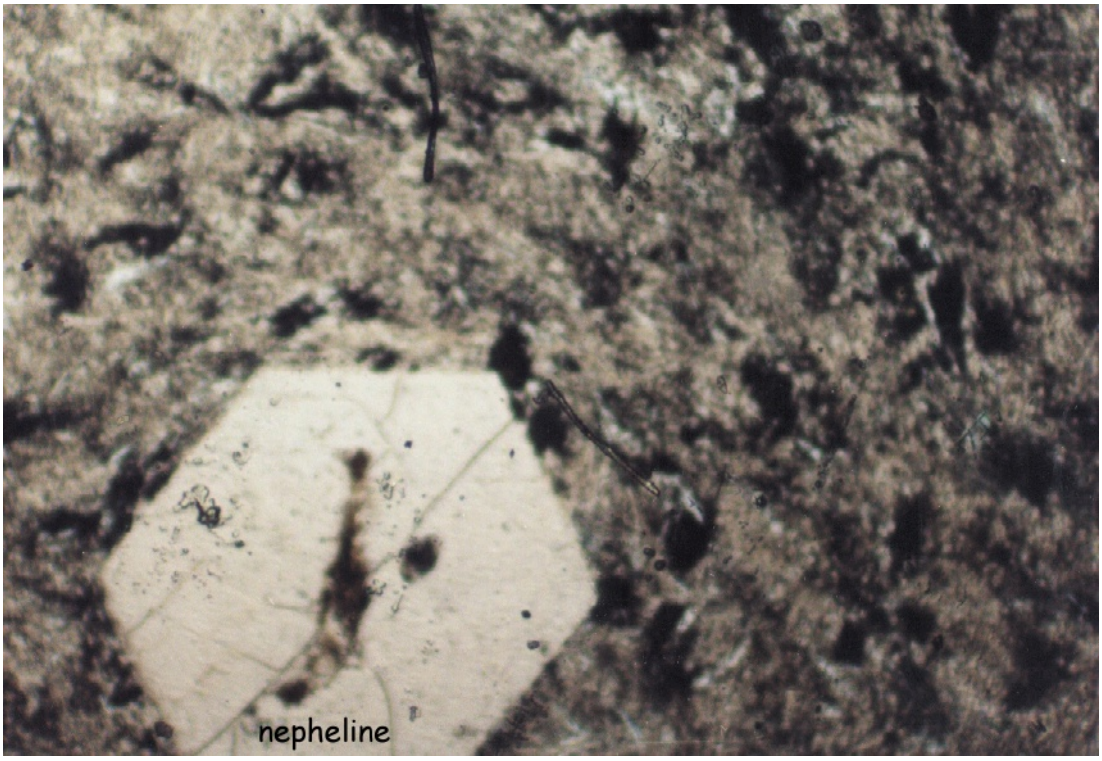

Figure 4.12: Phenocryst of nepheline at, 5X magnification and PPL in GUN-26b

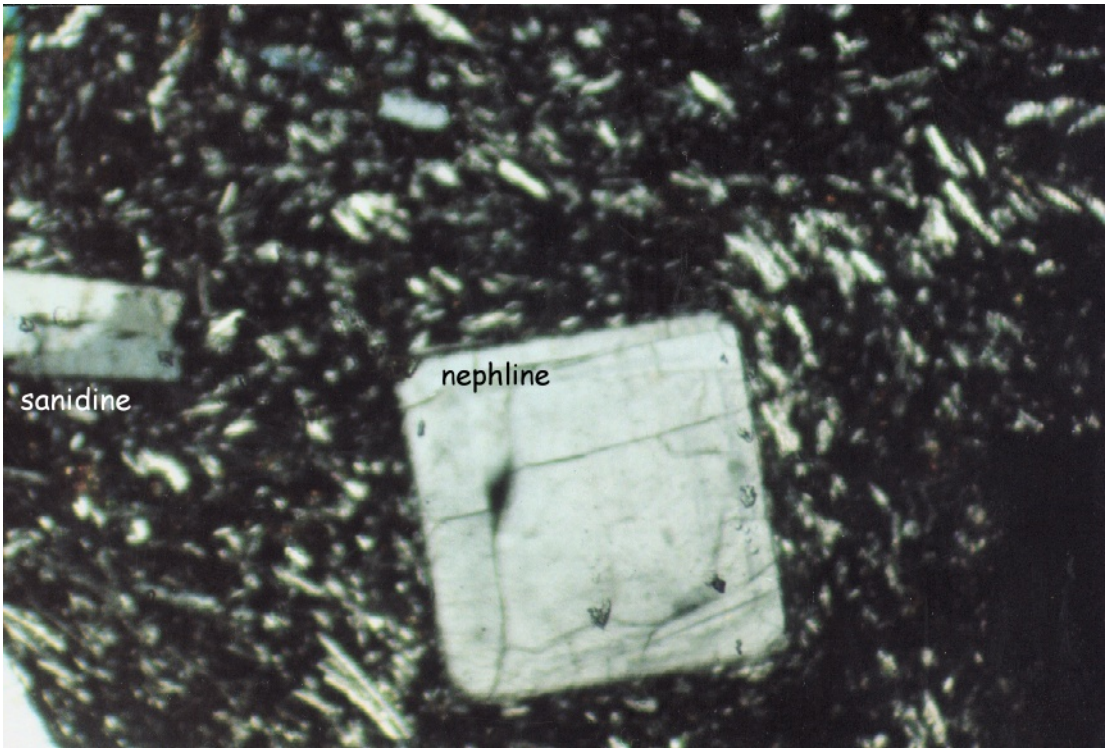

Figure 4.13: Phenocryst of nepheline in a trachytic groundmass at, 5X magnification and XPL in GUN-44

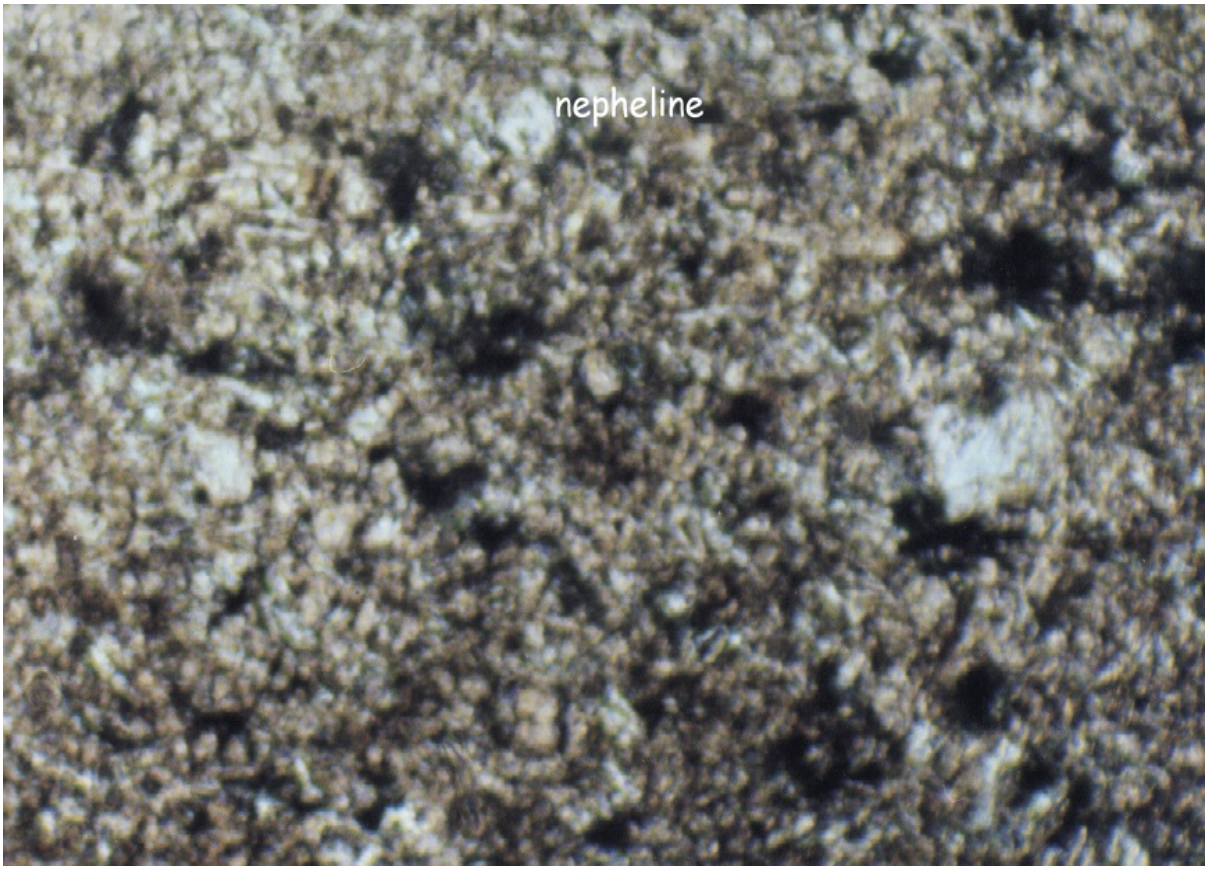

Figure 4.14: Crystals of nepheline in groundmass at, 10X magnification and PPL in GUN-48

- **Nosean**

This mineral occurs accompanying nepheline, with dodecahedron outlines. They are colorless, or gray blue under plane polarized light (PPL). In many cases, they show corroded outlines and embayment, and almost invariably are filled with microscopic dust like inclusions. In such cases the inclusions of dust may appear arranged along two series of lines at right angles to each other. In most of the samples, it appears as phenocrysts. Size of phenocrysts is about 0.75-2.75mm in length and its abundance range about 2-7%.

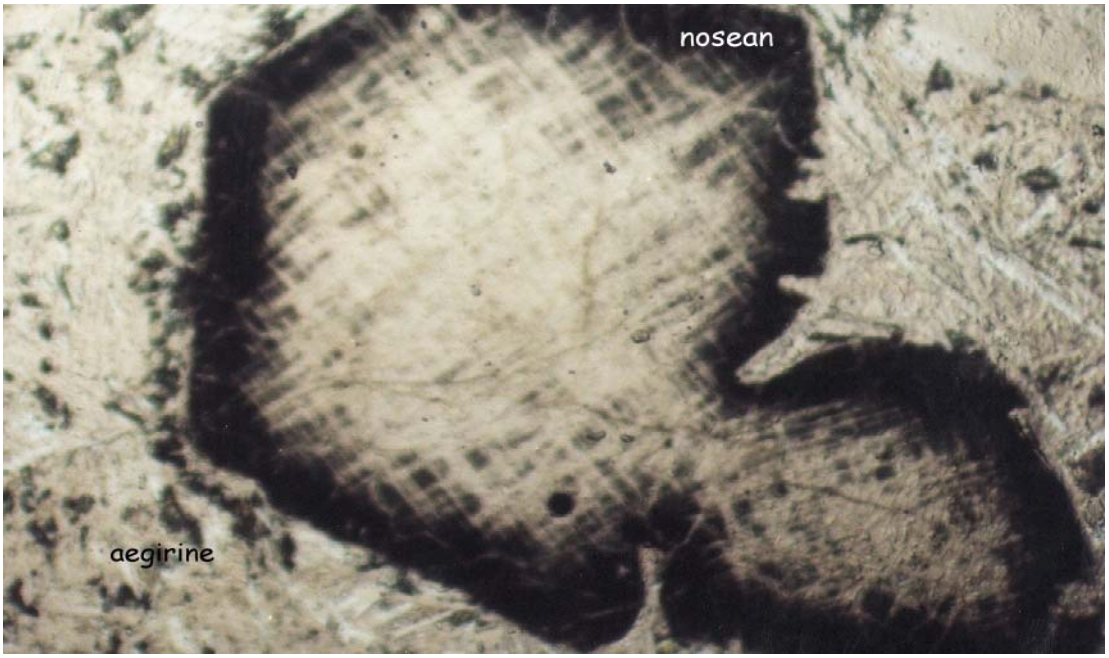

Figure 4.15: Phenocryst of nosean at, 5X magnification and PPL in GUN-36

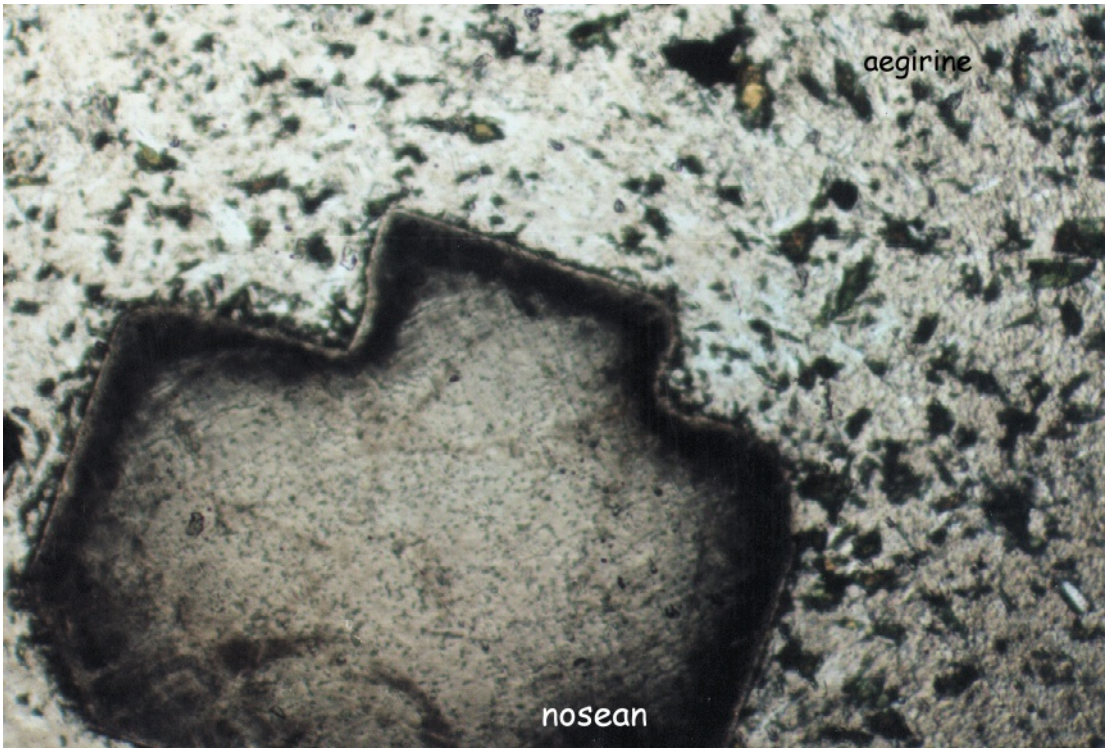

Figure 4.16: Phenocryst of nosean at, 5X magnification and PPL in GUN-35

➢ Leucite

It is found both as phenocrysts and in the groundmass. The phenocryst abundance is about 2-10%. The grain size is about 0.50-2.00mm. Phenocrysts are in octagonal or rounded outlines. When they are larger, they are twinned with a grating texture, so that they closely resemble microcline.

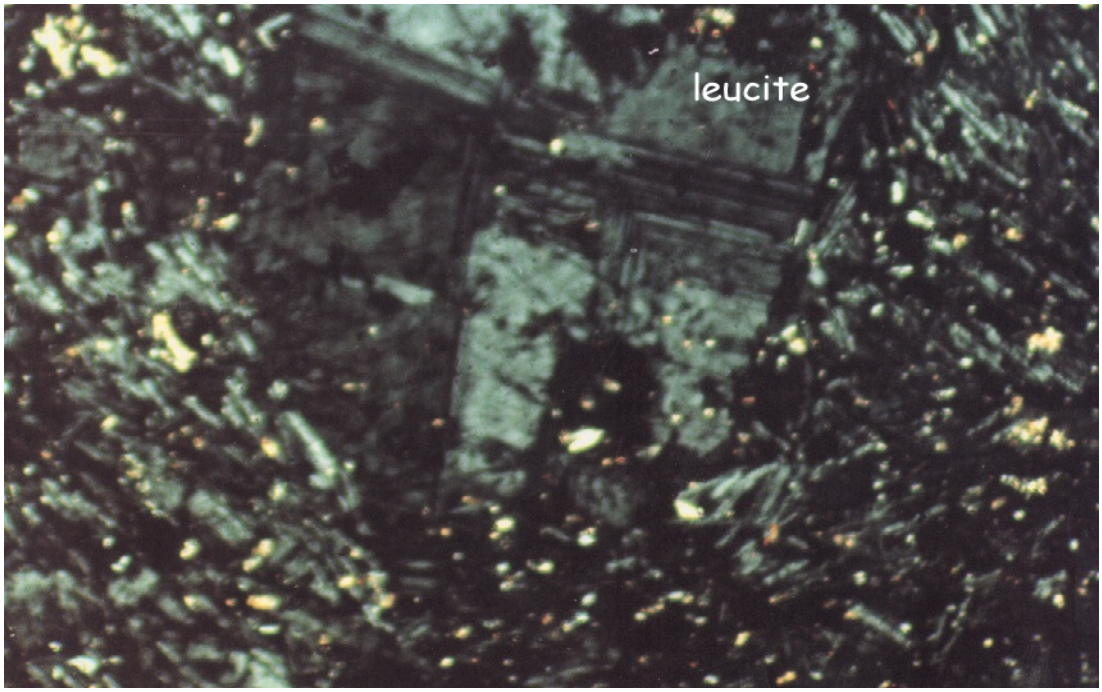

Figure 4.17: Phenocryst of leucite over a trachytic groundmass at, 5X magnification and XPL in GUN-32

➢ Pyroxene

The most common mafic mineral in the phonolites is clinopyroxene (aegirine and aegirine augite) predominate. The pyroxene usually occurs in two generations as phenocrysts and groundmass. The phenocryst abundance range 1-3% and its size is about 0.75-1.50 mm. As phenocrysts the form is euhedral - prismatic (lath shaped sections). In the ground mass the pyroxene is usually in needle or shreds with out terminal faces and some times in aggregates.

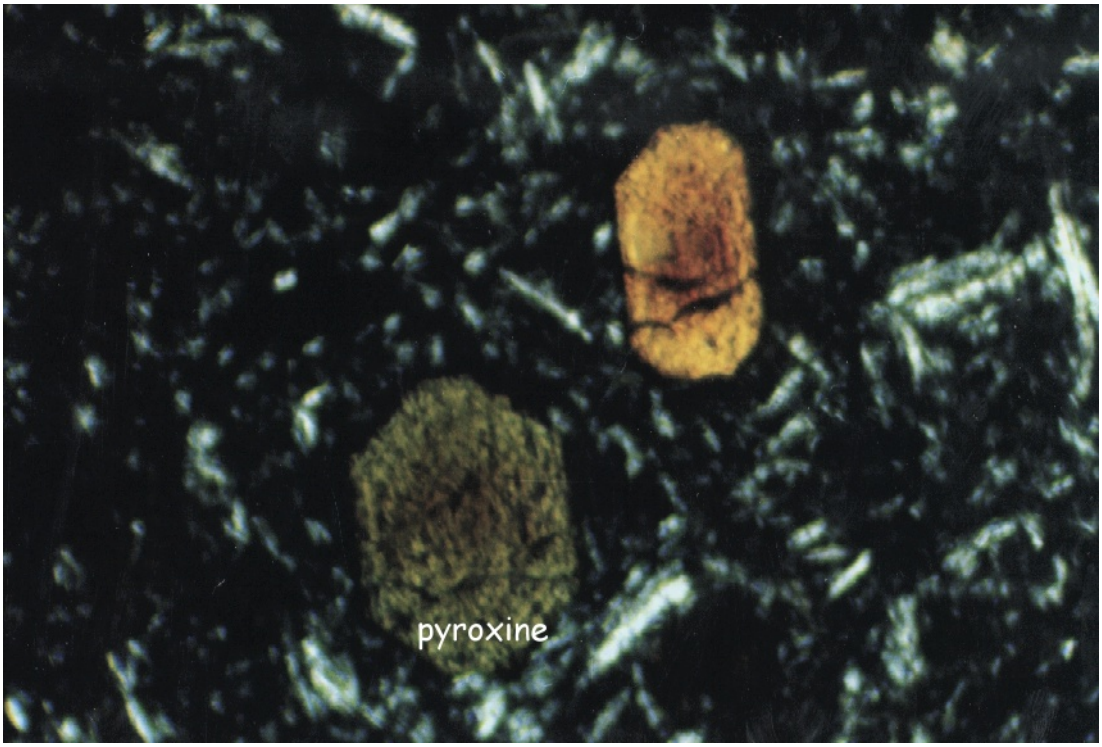

Figure 4.18: Phenocryst of pyroxene at, 10X magnification and XPL in GUN-26A

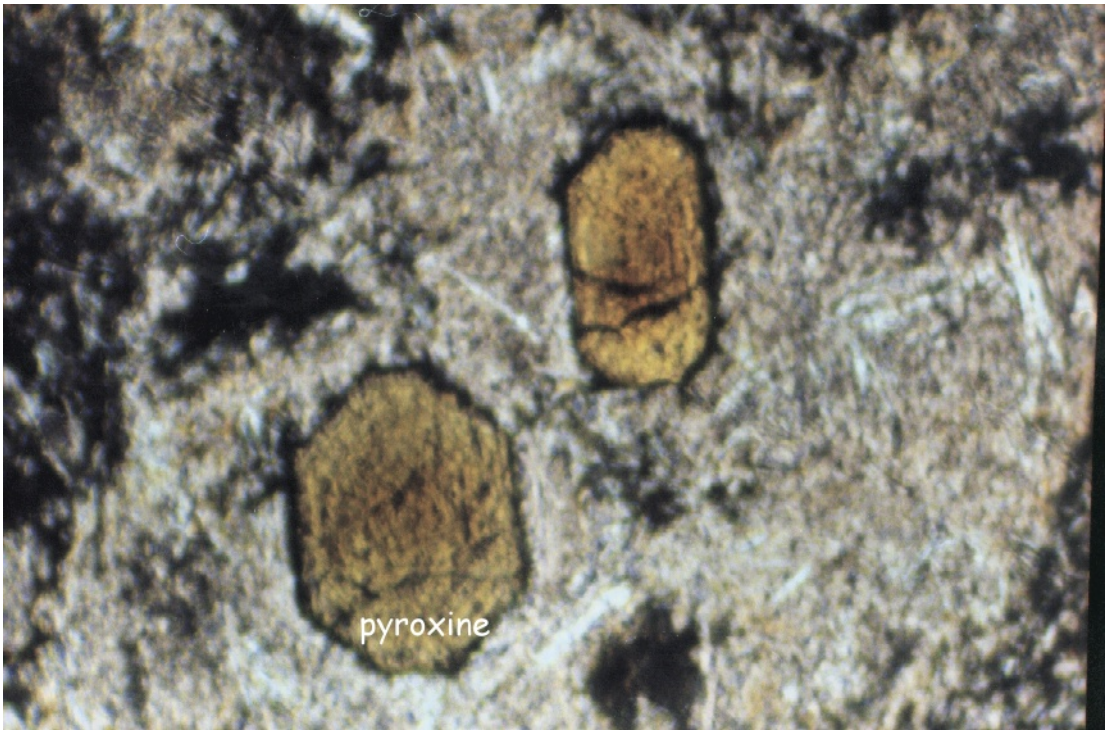

Figure 4.19: Phenocryst of Pyroxene at, 10X magnification and PPL in GUN-26A

- **Sphene**

It commonly occurs as accsessary in the groundmass but in few samples, it occurs as phenocryst and microphenocryst in its euhedral texture forming 1-3% proportion.

It commonly forms a diamond –shaped crystals of very high relief. Its size is about 0.5-0.85mm

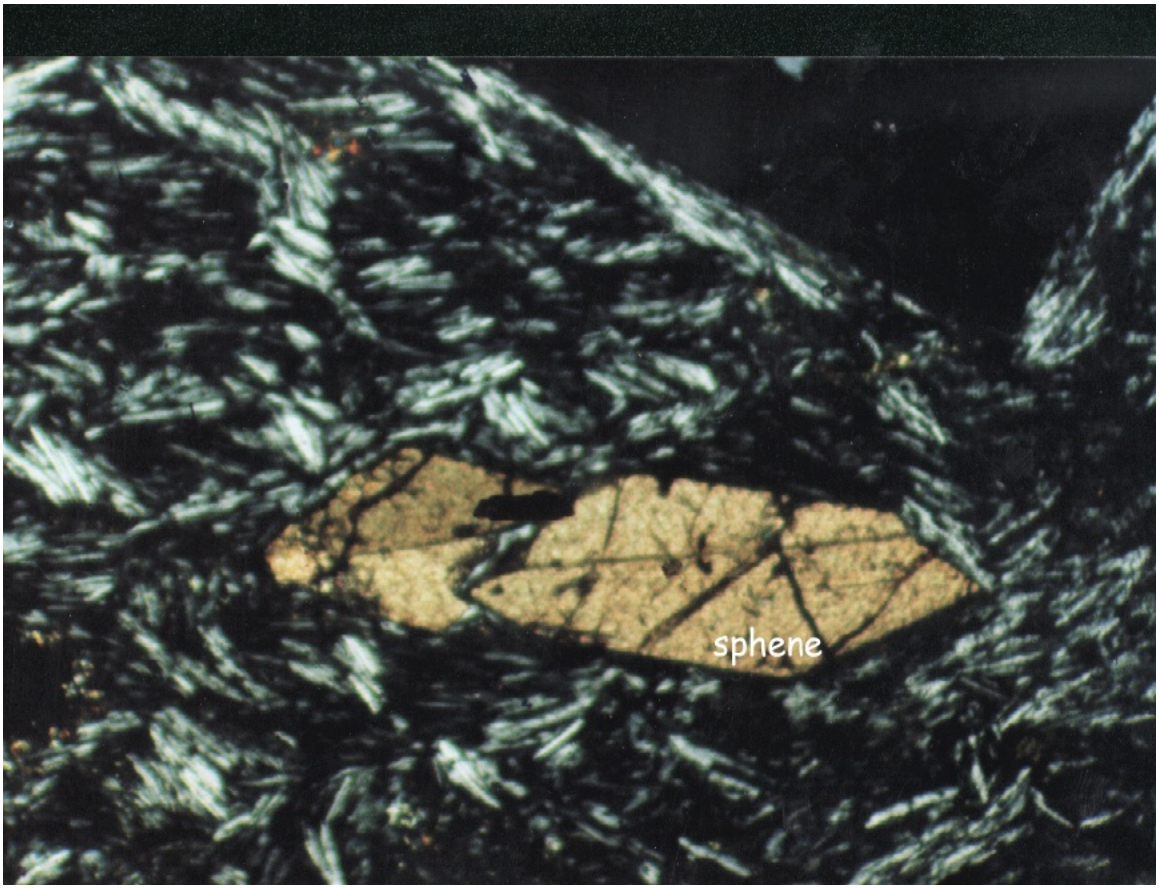

Figure 4.20: Phenocryst of sphene at, 5X magnification and XPL in GUN-45

Table 4.1. Summery of petrographic features for representative rock samples

No.	Rock Type	Texture	Modal composition
1	Phonolites	Porphyritic and glomeroporphyrhitic with trachythic ground mass.	13-40% phenocryst assemblage consists of 6-20% euhedral-subhedral, lath shaped and 3-5 mm length alkali feldspar (sanidine), 3-10% and 0.75-1.75 mm nepheline, 2-7 % and 0.75-2.75 mm nosean, 2-10% and 0.50-2.00 mm lucite, 1-3% and 0.75-1.50 mm clinopyroxene, 1-4% and 0.5-0.75 mm opaque (Fe- oxide) and 1-3% and 0.5-0.85 mm sphene. The groundmass has a trachytic (flow) texture, made of sanadine, clinopyroxene, nepheline, nosean, opaque and accessories of sphene and apatite. Secondary minerals are calcite and zeolite.
2	Ignimbrites	Hypo crystalline and vitrophyric	Composed of 20-35% crystals, about 25% rock fragments and about 50% volcanic glass. Crystals are euhedral to subhedral alkali feldspar (sanidine), quartz and plagioclase. The rock fragments are consists of andesite, basalt and rhyolite. With TAS chemical classification these are classified as trachyte.
3	Trachytes	Porphyritic and Trachythic	15-30% phenocryst phase made of 9-10% alkali feldspar mainly sanidine , 3-4% hornblende, 1-2% plagioclase, 1% opaque (Fe-oxide) and <1% pyroxene. The ground mass is composed of alkali feldspar, hornblende, pyroxene, biotite, opaque and minor volcanic glass.
4	Rhyolites	Hypocrystalline, Vitrophyric, porphyrithic ,perlithic and flow banding texture	12-22% phenocryst composed of 4-20% sanidine, 6-10% plagioclase, 2-3% quartz, 2-4% opaque and2-3% pyroxene. The ground mass is composed of sanidine, plagioclase, quartz, pyroxene, opaque and volcanic glass. Accessories are apatite and calcite. The volcanic glass is devitrified to calcite and biotite.
5	Basalts	porphyrithic, inter granular and trachythic /flow / texture	It is composed of 5-10% phenocryst and 90-95% ground mass. The phenocryst assemblage consists of 4-7% lath euhedral plagioclase, 1-3 pyroxene (augite) and, ~1% olivine The ground mass is also composed of lath shaped plagioclase, pyroxene (augite), opaque and volcanic glass.

4.2.Mineral chemistry

Electron microprobe analyses of phenocryst phases were performed on representative samples from the phonolite lava flows. In all cases an attempt was made to analyze core of phenocrysts with out inclusions and cracks. All analyses were made on carbon coated polished thin sections at the Pennsylvania State University (USA) using Come bax 5x50 electron microprobe. Major oxide chemical compositions of nepheline, feldspar & pyroxene phenocrysts were determined. Mineral formulae and calculations for detailed classifications of the minerals have been obtained utilizing different soft ware packages.

4.2.1Pyroxenes

Anhedral - euhedral Pyroxenes were analyzed & their representative compositions are listed in table 4.2. Pyroxene compositional variation in terms of enstatite (En), forestarite (Fo), wolastonite (Wo), and components is illustrated in Fig. 4.21. As indicated the figure pyroxenes in the phonolite are mainly augite in compositions.

Table 4.2 Chemical data of Pyroxenes

Sample Na.	Gun_ 28				GUN- 25b		GUN- 35	GUN- 9	GUN- 45		GUN - 26b	Gun_4 7			
N°Anal.	1	2	3	4	1	2	1	1	1	2	1	1	2	3	4
SiO2	52.41	52.70	53.00	52.17	52.56	52.38	50.32	51.83	52.17	50.71	51.21	51.82	53.06	52.40	52.72
Al2O3	2.52	1.63	1.61	2.09	1.36	1.42	3.27	1.36	2.09	3.11	1.97	2.06	1.23	2.04	2.11
TiO2	0.92	0.99	0.78	1.14	0.56	0.59	1.31	0.59	1.14	1.20	0.94	1.41	0.50	1.06	0.98
FeO	7.80	7.99	8.48	8.05	11.17	11.17	8.50	9.89	8.05	7.87	12.06	8.19	9.85	8.32	8.16
MgO	13.42	12.61	11.99	12.40	10.08	10.03	11.51	11.19	12.40	12.85	9.07	12.18	10.73	12.16	12.78
CaO	20.84	21.56	21.74	21.67	21.00	21.29	22.00	21.15	21.67	20.73	20.55	21.28	21.31	21.21	21.78
Na2O	1.10	1.20	1.26	1.17	1.60	1.57	1.16	1.45	1.17	0.99	2.04	1.29	1.51	1.21	1.09
K2O	0.00	0.02	0.00	0.00	0.00	0.00	0.00	0.00	0.00	0.00	0.01	0.03	0.00	0.02	0.00
TOTAL	99.02	98.70	98.87	98.69	98.33	98.43	98.06	97.45	98.69	97.47	97.86	98.26	98.85	98.40	99.62
Number of Cations on the bases of 6 oxygens															
Si	1.96	1.98	2.00	1.97	2.01	2.00	1.91	1.99	1.97	1.93	1.97	1.96	2.02	1.98	1.97
Al IV	0.04	0.02	0.00	0.03	0.00	0.00	0.09	0.01	0.03	0.07	0.03	0.04	0.00	0.02	0.03
AL VI	0.07	0.06	0.07	0.06	0.06	0.06	0.06	0.05	0.06	0.07	0.06	0.05	0.06	0.07	0.06
Ti	0.03	0.03	0.02	0.03	0.02	0.02	0.04	0.02	0.03	0.03	0.03	0.04	0.01	0.03	0.03
Fe3+	0.00	0.00	0.00	0.00	0.00	0.01	0.04	0.04	0.00	0.01	0.06	0.00	0.00	0.00	0.00
Mg	0.75	0.71	0.67	0.70	0.58	0.57	0.65	0.64	0.70	0.73	0.52	0.69	0.61	0.69	0.71
Fet	0.24	0.25	0.27	0.25	0.35	0.34	0.23	0.28	0.25	0.24	0.33	0.26	0.31	0.26	0.25
Fe2+	0.16	0.21	0.24	0.21	0.34	0.33	0.21	0.26	0.21	0.16	0.33	0.22	0.31	0.21	0.20
Ca	0.83	0.87	0.88	0.87	0.86	0.87	0.90	0.87	0.87	0.85	0.85	0.86	0.87	0.86	0.87
Na	0.08	0.09	0.09	0.09	0.12	0.12	0.09	0.11	0.09	0.07	0.15	0.09	0.11	0.09	0.08
K	0.00	0.00	0.00	0.00	0.00	0.00	0.00	0.00	0.00	0.00	0.00	0.00	0.00	0.00	0.00
T+M1+M2	4.00	4.00	4.00	4.00	4.00	4.00	4.00	4.00	4.00	4.00	4.00	4.00	4.00	4.00	4.00
Pyroxene composition															
%En	40.95	38.70	37.04	38.17	32.07	31.73	35.87	35.02	38.17	39.94	29.63	37.99	33.99	37.92	38.71
%Fs	13.34	13.75	14.70	13.90	19.92	19.83	14.85	17.37	13.90	13.73	22.11	14.33	17.50	14.56	13.87
%Wo	45.71	47.56	48.26	47.93	48.01	48.43	49.27	47.61	47.93	46.33	48.26	47.68	48.51	47.53	47.43
xFe	0.75	0.74	0.72	0.73	0.62	0.63	0.75	0.71	0.73	0.75	0.64	0.73	0.66	0.72	0.74

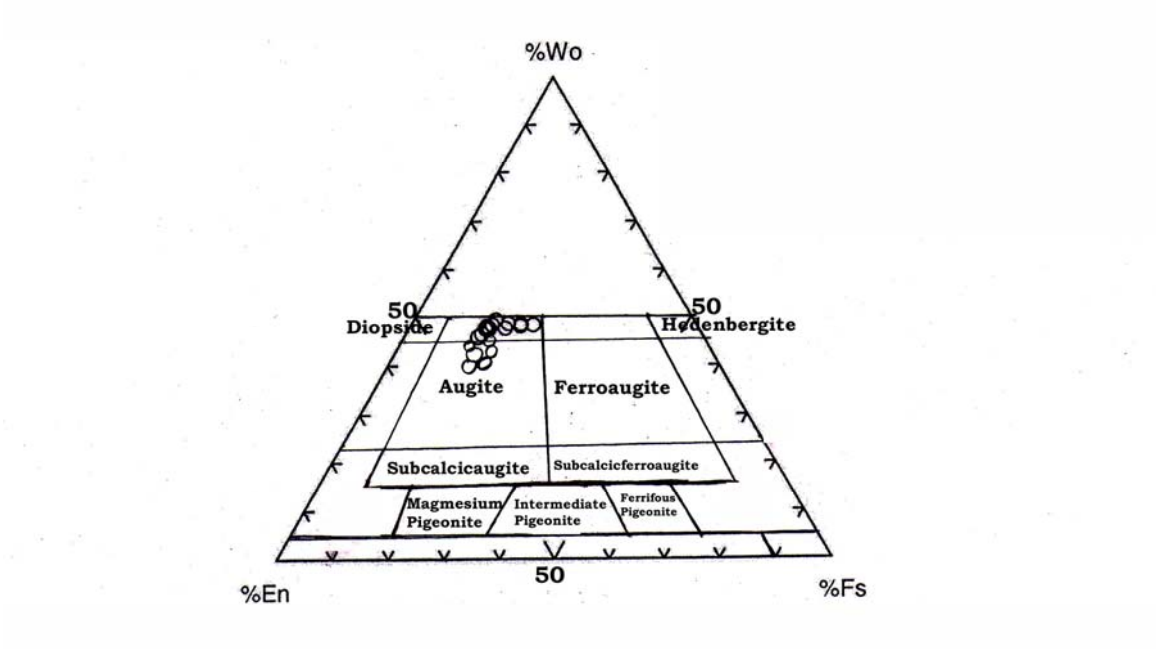

Figure 4-21 Diagrams showing compositional variation of pyroxenes in phonolites of guna

4.2.2.Feldspars

Representative feldspar analyses are presented in Table 4.3.

Table4.3. Chemical data of Feldspars

sample Na.	Gun_ 28					GUN-35		GUN-5		GUN-25b						GUN-45	GUN-9	
Anlysis	1	2	3	4	5	1	2	1	2	1	2	3	4	5	6	1	1	2
SiO2	67.20	67.20	67.41	67.40	67.64	67.47	65.85	67.75	68.44	66.90	67.76	67.38	67.72	67.01	67.72	66.61	67.22	67.33
Al2O3	19.47	19.34	19.58	19.64	19.18	18.88	19.60	19.11	19.58	19.21	19.55	18.83	19.18	19.63	19.38	19.23	19.66	19.59
TiO2	0.06	0.06	0.03	0.09	0.00	0.12	0.12	0.02	0.09	0.06	0.02	0.00	0.03	0.00	0.03	0.04	0.11	0.01
FeO	0.19	0.40	0.29	0.25	0.28	0.56	0.81	0.67	0.62	0.27	0.11	0.21	0.31	0.25	0.19	0.58	0.32	0.30
MgO	0.03	0.01	0.02	0.02	0.01	0.01	0.04	0.06	0.00	0.00	0.00	0.00	0.00	0.02	0.00	0.02	0.01	0.01
CaO	0.36	0.25	0.52	0.63	0.32	0.06	0.13	0.27	0.24	0.08	0.26	0.23	0.07	0.19	0.31	0.36	0.39	0.24
Na2O	5.91	6.09	6.32	6.33	6.54	5.20	5.70	6.59	7.55	5.11	5.90	6.06	5.16	5.56	5.84	5.89	6.22	6.25
K2O	7.13	7.28	6.83	6.87	6.86	8.75	8.65	6.44	5.76	8.65	7.61	7.75	8.57	7.96	7.64	7.41	6.98	7.09
TOTAL	100.36	100.64	100.98	101.23	100.82	101.05	100.89	100.89	102.29	100.27	101.20	100.45	101.05	100.61	101.12	100.13	100.90	100.82
Number of cations on the bases of 8 oxygen																		
Si	2.99	2.99	2.98	2.98	3.00	3.00	2.95	3.00	2.99	3.00	2.99	3.01	3.01	2.98	3.00	2.98	2.98	2.99
Al	1.02	1.01	1.02	1.02	1.00	0.99	1.04	1.00	1.01	1.01	1.02	0.99	1.00	1.03	1.01	1.02	1.03	1.02
Fe	0.01	0.01	0.01	0.01	0.01	0.02	0.03	0.02	0.02	0.01	0.00	0.01	0.01	0.01	0.01	0.02	0.01	0.01
Ca	0.02	0.01	0.02	0.03	0.02	0.00	0.01	0.01	0.01	0.00	0.01	0.01	0.00	0.01	0.01	0.02	0.02	0.01
Na	0.51	0.53	0.54	0.54	0.56	0.45	0.50	0.57	0.64	0.44	0.51	0.52	0.44	0.48	0.50	0.51	0.53	0.54
K	0.40	0.41	0.39	0.39	0.39	0.50	0.49	0.36	0.32	0.49	0.43	0.44	0.49	0.45	0.43	0.42	0.39	0.40
TOTAL	4.95	4.97	4.97	4.97	4.98	4.96	5.01	4.96	4.99	4.96	4.96	4.98	4.95	4.97	4.96	4.97	4.96	4.97
Plagioclase composition																		
An(%)	1.83	1.26	2.59	3.12	1.59	0.31	0.65	1.35	1.16	0.41	1.28	1.12	0.37	0.94	1.57	1.80	1.97	1.20
Ab(%)	54.74	55.27	56.93	56.52	58.24	47.31	49.69	60.06	65.81	47.09	53.42	53.70	47.61	51.05	52.88	53.75	56.42	56.57
Or(%)	43.43	43.47	40.49	40.36	40.17	52.38	49.66	38.59	33.03	52.49	45.30	45.18	52.02	48.02	45.55	44.45	41.61	42.24

4.2.3.Feldspathoids

Representative feldspathoids analyses are given in table 4.4 below.

Table 4.4. feldspathoids analyses

Sample Na.	GUN28	GUN 5		GUN 25b					GUN 26b				
N° of ana.l	1	1	2	1	2	3	4	5	1	2	3	4	5
SiO2	50.785	48.476	49.127	46.23	47.514	46.42	46.797	46.8	46.211	45.91	46.66	46.37	46.93
TiO2	0.125	0.08	0.088	0	0.008	0	0.032	0.032	0.022	0.04	0	0.017	0.035
Al2O3	29.611	30.667	29.713	32.56	32.343	32.65	32.477	32.39	31.873	30.22	32.15	33	32.68
FeO	1.036	1.777	1.791	0.576	0.737	0.684	0.642	0.654	0.683	0.63	0.67	0.603	0.594
MgO	0.272	0.08	0.192	0.012	0	0.012	0.012	0.032	0.002	0.035	0.005	0.027	0.043
CaO	0.295	0.01	0.298	0.034	0.018	0.046	0.035	0.031	0.036	0.024	0.031	0.008	0.031
Na2O	15.442	16.66	16.25	16.237	16.267	16.47	16.414	16.6	16.308	16.573	16.65	16.71	16.3
K2O	2.269	3.25	2.937	3.575	3.575	3.41	3.367	3.558	3.308	3.038	3.625	3.673	3.494
Total	99.835	101	100.4	99.224	100.462	99.69	99.776	100.1	98.443	96.47	99.79	100.4	100.1
				Number of cations on the bases of 32 oxygens									
Si	1.690458	1.6136	1.6353	1.5388379	1.58158	1.545	1.5577	1.558	1.538205	1.5282	1.553	1.543	1.562
Ti	0.003129	0.002	0.0022	0	0.0002	0	0.0008	8E-04	0.000551	0.001	0	4E-04	9E-04
Al	0.871242	0.9023	0.8742	0.9580107	0.95163	0.961	0.9556	0.953	0.937797	0.8892	0.946	0.971	0.962
Fe3+	0.021629	0.0371	0.0374	0.0120256	0.01539	0.014	0.0134	0.014	0.01426	0.0132	0.014	0.013	0.012
Mg	0.006749	0.002	0.0048	0.0002977	0	3E-04	0.0003	8E-04	4.96E-05	0.0009	1E-04	7E-04	0.001
Ca	0.00526	0.0002	0.0053	0.0006063	0.00032	8E-04	0.0006	6E-04	0.000642	0.0004	6E-04	1E-04	6E-04
Na	0.249149	0.2688	0.2622	0.2619761	0.26246	0.266	0.2648	0.268	0.263122	0.2674	0.269	0.27	0.263
K	0.024088	0.0345	0.0312	0.0379528	0.03795	0.036	0.0357	0.038	0.035118	0.0323	0.038	0.039	0.037
Ne	69.9155	75.05	74.32	74.08443	73.181	74.8	74.43	75.4	75.0652	78.38	75.9	75.6	73.6
Ks	7.4193	09.66	9.5	10.80592	10.62	10.3	10.12	10.7	10.098	9.51	10.9	10.9	10.5
Q	22.6652	15.29	16.18	15.10965	16.199	14.9	15.44	13.9	14.8368	12.11	13.1	13.5	15.9

Compositional variations of feldspar analysis plotted in the, Anorthite (An), Albite (Ab) Orthoclase (Or) ternary diagram (Fig 4.22) indicates that the feldspars in phonolites of Guna rocks are dominantly sanidine.

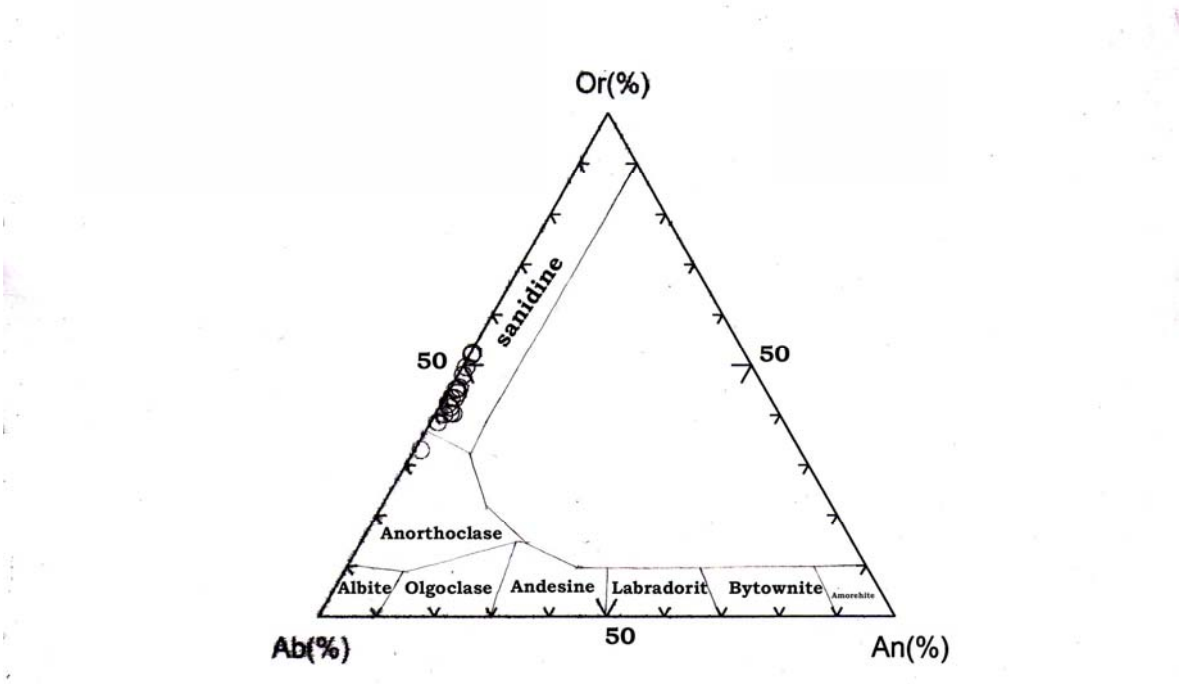

Figure 4.22 Diagrams showing compositional variation of pyroxenes in phonolites of guna

Feldspathoids compositions are plotted in the system quartz (Q) – nepheline (Ne) – Kalsilite (KS) in Fig 4.23 that indicates the feldspathoids are mainly nepheline.

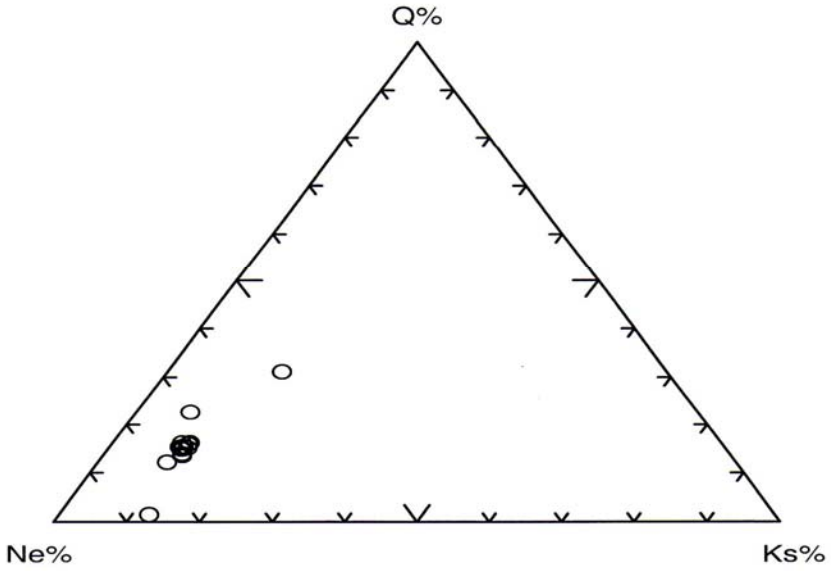

Figure 4.23 Diagrams showing compositional variation of pyroxenes in phonolites of guna

CHAPTER 6 DISCUSSION

Guna Volcanic massif is a 10.7 ma (Kiffer et al., 2004) huge felsic center overlying the flood basalt on northwestern Ethiopian plateau. It consists of rhyolithic lava flow, pyroclastic flow deposit, trachytic lava flow and phonolithic lava.

In Ethiopian igneous province during Miocene –Pliocene there was uplift, rifting and building of basaltic shields with associated rhyolites and phonolites. About 10ma is marked by one of the major episodes of rifting (Kazmin et al., 1980).

The presence of rift – related volcanics on the plateaus can be explained by the possibility that the Afar plume material may have been channeled to adjacent favorable fracture systems allowing 'fissure type' volcanic eruption to take place away from hotspot. Several models have been proposed to explain the origin of silicic magma these includes

1. Fractional crystallization of mantle derived basaltic magma commonly in combination with crustal contamination
2. Partial Melting of the continental crust (anatexis)
3. Partial re melting of under plated basic igneous rocks or their differentiates in the crust

The origin of huge volumes of silicic extrusive rocks (usually ignimbrites in the Afar and the main Ethiopian rift (MER) is attributed to fractional crystallization of basaltic magmas with limited crustal contamination. Notably, two-stage model has been proposed for the genesis of the Asela – Ziway pantellerites in the Main Ethiopian Rift (Tura et al., 1999). It involves small degrees of partial melting of a basaltic under plate to produce the least differentiated silicic magmas, which in turn undergo moderate degrees of fractional crystallization to generate the most evolved silicic rocks.

The new geochemical and petrographic results from the present work will be more profitably examined for evidence of fractional crystallization model.

The fractionating mineral assemblage is normally indicated by the phenocrysts present (Rollison, 1993). Petrographic investigations indicate that the major phenocryst phases in the lavas are feldspars (sanidine), feldsphatoids (nepheline, leucite, and nosean), clino pyroxene and Fe-Ti oxides. The mineral chemistry plots indicate the feldspars fall in the field of sanidine. The nepheline analysis plotted on quartz, nepheline and kalsilite end member triangle are classified as nepheline. The pyroxenes are classified as augite.

Major elements chemistry displays features agreeable with fractionation of phenocryst minerals assemblage that is also supported by trace element variation plots.

The chondorite normalized rare earth element pattern (Figure 5.6 A-C) displays enriched light rare earth (LREE), almost flat heavy rare earth (HREE) elements pattern and strong negative Eu anomaly that indicates significant fractionation. In compatible element abundances generally increase with fractionation. For example, the La abundances for rhyolite is 56.35-89.97 ppm, for trachyte is 77.36 -144.56 ppm and for Phonolites is 97.25-191.23 ppm,

In the primitive mantle normalized incompatible trace element profiles (Figure 5.7 - Figure 5.9) the sharp falls in Sr, Ba, Ti, and P verifies fractionation of feldspar, plagioclase, apatite and titano - magnetite. Strong depletions in Sr, Ba, and Ti in the more felsic rocks obviously produced by fractional crystallization of some combination of plagioclases alkali feldspar, apatite, Fe-Ti oxides, and titanaugite (Barker, 1996 and reference, there in)

The lavas also have high concentration of Nb content i.e. 175.55- 396.17 ppm for phonolites, 90.51-273.09 ppm for trachyte and 54.70-117.07 for rhyolites. Similarly the Th contents are also high which is 11.34-27.41 for phonolite, 12.56-25.37 for trachyte and 8.12-16.49 for rhyolite. Nb also shows a positive anomaly on primitive mantle normalized in compatible trace element profiles.

It is well known that crustal rocks and partial melts derived from them are characterized by very high Rb/Nb and La/Nb ratios (Pearce et al). In the table 6.1 below trace element ratio characteristics of Guna lavas are compared with rhyolite formed by partial melting of the crust (1-3) and the Wegel Tena rhyolite (4), which is mantle derived and that show a limited crustal contamination.

Table 6.1 Comparisons of trace ratios in different lavas

Na.	Lavas	Rb/Nb	La/Nb
1	Malusni, peru rhyolite	1. 22-45	0.8-1.7
2	Loch saridain UK rhyolite	2. 7-9	2.6-2.7
3	Yellow stone rhyolite	3. 2-5	0.8-2.3
4	Wegel Tena rhyolite	0.8-1.3	0.8-1.2
5. A	Guna Rhyolite	0.93-1.31	0.76-1.03
5. B	Guna Trachyte	0.40-0.57	0.37-0.84
5. C	Guna Phonolite	0.31-0.89	0.34-0.70

Data source are from Ayalew D. and Yirgu G. (2003) and references their in

The comparison shows that the Guna incompatible trace element ratios are different from those of typical crustal melts and similar with the Wegel Tena rhyolite, implying that they did not originate by partial melting of the crust. Instead, the geochemical features are consistent with their derivation from mantle derived basaltic magma by low-pressure fractionation. The Presence of leucite testifies to the low-pressures origin of lavas, as leucite is only stable at pressures of < 2 k bar (about 6 km depth) (Hall and references their in).

CHAPTER 7 CONCLUSION AND RECOMENDATIONS

7.1. Conclusion

Based on the field observations, petrography, mineral chemistry and whole rock geochemical (major and trace element) studies of this work it is concluded that

Guna is not a basaltic shield volcano; instead it is a huge felsic center mainly consisting of pyroclastic flow deposits, rhyolite, phonolite and trachyte flows.

The available petrographic and geochemical data shows that the silicic volcanic products of Guna are co genetic and derived from mantle origin basaltic magma through low-pressure extensive fractional crystallization and limited crustal contamination.

7.2. Recommendations

Further isotope geochemistry works, age determinations and additional whole rock and mineral chemistry analysis are recommended to adequately understand the magma source characteristics, petrological and geo chemical processes involved to produce the rock suites of Guna.

CHAPTER 5 WHOLE ROCK GEOCHEMISTRY

Lavas and pyroclastic materials from Guna volcanic centre reveal distinctive geochemical characters where intermediate and acid lavas are overwhelmingly dominant. These volcanic suites encompass rhyolites, trachyte and phonolites. Analytical data for major, trace and rare earth elements including LOI and CIPW norms is presented in Table 5.1. Several variation diagrams for major element oxides (Harker diagrams), trace elements versus silica, trace versus trace and trace ratios has been constructed. Chondrite normalized rare earth elements (REE) abundance patterns and primitive mantle normalized incompatible trace elements patterns (spider diagrams) are also plotted for representative samples.

5.1. Analytical method

25 fresh samples from different flows were selected for geochemical analysis after petrographic studies. The samples are two from the flood basalt (GUN 11 and GUN-12), one from pyroclastic (ignimbrite, GUN – 23), and others from rhyolite, trachyte and phonolite lavas.

The samples were crushed and powdered at Central Geological Laboratory of Geological Survey of Ethiopia. Manganese steel jaw crusher is used for 5-1 mm crushing. 200-mesh powdering was done by a cobalt mixer mill.

The powdered samples were analyzed for major elements oxide SiO_2, TiO_2, Al_2O_3, FeO(tot), MgO, MnO, CaO, Na_2O, K_2O, P_2O_5, LOI, trace and rare earth elements by ICP MS (Inductively Coupled Plasma Mass Spectroscopy), methods at Pennsylvania State University (U.S.A).

Sample preparation

Samples were dried at 105^0C in an electric oven and stored in desiccators. Sub samples of 200mg. were placed inside Teflon vessels and treated with 3 ml HF, 4ml Aquaregia (HNO_3- HCl 1:3) and 1 ml $HclO_4$. The microwave-heating program consists of a three-stage power and time settings as-30percentage power 10min.-45% power 20 min.-30% power 5 min.

After digestion, the vessels were cooled at room temperature in a water bath and uncapped. The solution was transferred into 100 ml PFA evaporating dishes and takes to dryness on a hot plate at 150^0C. Then 1 ml HNo_3 plus water and gently heated for 15 minutes. This clear solution was rinsed into 100ml volumetric flask and diluted to volume after the adding of 100 ppb of rhodium and rhenium as internal standards.

Instrumentation

Microwave oven was a Milestone MLS system, which has a 100% power output of 1200 Watts.

Spectrometer was a Perkin-Elmer SCIEXELAN model 5000 IC-MS

Instrumental operating conditions

Plasma Rf power----1100KW, plasma gas flow------15.0 L/min, Auxiliary gas flow---1.40 L/min, Nebulizer gas flow---0.85 L/min, Sample uptake flow---0.80 ml/min, Dwell time---50sec, Sweeps----3, replicate-----3, Point across peak------1

Limits of Quantitation

The limit of quantitation (LOQs) for the elements detected with ICP-MS were calculated for ten times the standard deviation (S) of the reagent blank, for 11 replicate determinations, divided by sensitivity as 5 μg/L concentration level, and multiplied by 500, that is, the diluted factor.

Precision

The precision of the analysis is based on two independent sources of error, the uncertainty in the sample preparation procedure and instrumental precision. The precision of the analysis was evaluated by decomposing 11 replicate of a sample. For each set solutions analyzed, the average (X), standard deviation (S) and relative standard deviation (RSD) were calculated. To test instrumental fluctuations, one solution was run 11 times.

The precision of the sample decomposition procedure was then calculated according to the following formula:

$S\ sp = (S\ tot^{2} - S\ ins^{2})^{1/2}$

Were Ssp = precision of the sample preparation

Stot = precision of the analysis

Sins = instrumental precision

Accuracy

The well-established reference standard materials Granite GSR-1 and Basalt GSR-3 were employed throughout the work to provide data quality assurance. Concentrations measured in each of the standard rocks were compared with available certificate values. **Er = ObV – CeV/CeV x 100 Were Er = Error %**

ObV = Obtained Value CeV = Certified Value

Table 5.1 Representative Geochemical data (Major Elements oxides in Wt%,Trace Elements in PPM)

Rock type	phonolite															
Sample	GUN5	GUN9	GUN17	Gun25b	GUN26b	GUN27	GUN28	GUN31	GUN35	GUN36	GUN44	GUN45	GUN47	GUN49	GUN50	GUN46
wt%																
SiO_2	59.55	60.63	61.66	57.40	57.23	57.16	61.28	57.57	56.81	59.40	56.74	59.67	59.57	60.09	60.50	60.58
TiO_2	0.66	0.62	0.64	0.44	0.47	0.45	0.75	0.90	0.60	0.71	0.35	0.66	0.73	0.47	0.73	0.92
$Al2O_3$	19.04	19.52	19.54	21.57	21.38	21.45	19.32	19.42	20.93	19.55	21.45	20.08	19.59	19.94	19.99	19.74
Fe_2O_3tot	3.84	3.09	3.04	2.64	2.79	2.74	3.20	4.74	2.80	3.02	2.34	2.84	2.93	3.26	3.02	3.63
MgO	0.48	0.30	0.46	0.36	0.24	0.45	0.81	1.39	0.37	0.68	0.29	0.46	0.83	0.23	0.64	0.97
MnO	0.37	0.24	0.37	0.24	0.26	0.27	0.29	0.24	0.19	0.30	0.23	0.28	0.27	0.32	0.28	0.27
CaO	1.10	0.86	0.94	0.87	0.90	0.97	1.47	3.20	1.41	1.48	0.95	1.24	1.78	0.81	1.58	2.32
Na_2O	8.11	8.38	8.25	9.62	9.55	9.05	7.07	6.23	8.54	7.26	9.31	7.87	6.28	8.44	7.40	6.60
K_2O	5.91	5.93	6.00	6.10	5.97	6.45	6.55	5.28	6.79	5.90	5.97	6.04	6.52	6.07	6.55	6.13
P_2O_5	0.05	0.07	0.08	0.05	0.06	0.04	0.12	0.47	0.09	0.12	0.04	0.08	0.11	0.05	0.12	0.26
LOI	1.7	6	1.5	1.3	1.2	1.5	1.7	3	1.2	1.8	1.6	1.5		1.8	1.7	1.9
Total	100.81	105.63	102.49	100.59	100.05	100.55	102.58	102.44	99.72	100.20	99.26	100.71	98.60	101.48	102.49	103.33
K_2O+Na_2O	14.01	14.31	14.25	15.72	15.52	15.50	13.63	11.50	15.33	13.15	15.28	13.91	12.80	14.51	13.95	12.73
CIPWnormative																
Quartz																
Plagioclase	39.37	42.25	43.15	28.95	29.92	26.68	42.4	49.04	24.34	45.73	29.75	41.84	47.01	39.28	39.63	46.9
Orthoclase	35.34	35.28	35.22	36.34	35.81	38.59	38.53	31.5	40.84	35.52	36.17	36.11	38.41	36.05	38.53	35.81
Corundum																
Nepheline	14.36	13.83	12.7	26.46	25.93	26.32	10.13	7.43	25.3	10.96	26.72	14.66	6.68	16.22	13.32	7.8
Diopside	4.48	3.35	3.52	3.44	3.59	3.95	4.09	2.87	5.6	2.77	3.98	3.46	1.42	3.27	4.28	3.07
Hyperstine																
Olivine	2.99	2.12	2.41	1.96	1.86	2.07	2.47	5.3	1.07	2.69	1.42	1.86	3.68	2.51	1.94	3.31
Acmite	1.68	1.36	1.3	1.16	1.22	1.22			1.24		1.04			1.42		
Na_2SiO_3	0.39	0.47	0.28	0.73	0.66	0.2			0.25		0.13			0.24		
Ilmenite	1.27	1.2	1.22	0.84	0.89	0.87	1.42	1.73	1.16	1.39	0.68	1.25	1.75	0.89	1.37	1.73
Magnetite							0.7	1.04		0.67		0.62	0.78		0.65	0.78
Apatite	0.12	0.16	0.19	0.12	0.14	0.09	0.28	1.09	0.21	0.28	0.09	0.19	0.25	0.12	0.28	0.6
Total	100	100.02	99.99	100	100.02	99.99	100.02	100	100.01	100.01	99.98	99.99	99.98	100	100	100

Continued Table 5.1

Sample Trace (ppm)	GUN5	GUN9	GUN17	Gun25b	GUN26b	GUN27	GUN28	GUN31	GUN35	GUN36	GUN44	GUN45	GUN47	GUN49	GUN50	GUN46
Sc	2.07	1.96	1.77	1.75	1.35	1.76	1.92	3.71	1.02	2.16	1.86	1.98	1.82	1.40	1.90	2.37
V	10.24	13.97	9.79	13.31	13.86	13.20	16.55	26.31	20.19	17.00	11.19	17.80	17.37	14.75	18.73	22.90
Cr	1.93	2.17	1.71	1.47	1.60	1.56	1.69	1.53	1.63	1.68	1.65	1.93	1.61	1.73	1.81	1.80
Co	9.56	16.75	8.89	13.09	10.27	11.72	9.45	9.76	11.34	8.04	11.86	9.71	5.95	8.43	7.58	6.08
Ni	2.52	1.68	1.05	0.85	0.74	0.92	1.32	1.38	1.15	1.35	1.22	1.23	1.12	0.77	0.88	1.31
Cu	4.58	5.15	4.92	3.80	3.87	3.95	4.91	6.73	5.33	5.74	3.45	5.48	6.42	3.86	22.31	6.08
Zn	131.15	99.45	126.96	100.25	97.55	106.09	103.98	104.41	87.02	101.81	82.96	97.26	159.82	127.68	95.56	91.95
Cs	0.44	0.99	1.05	1.12	1.41	0.67	0.36	3.13	1.18	0.38	1.42	0.65	0.40	1.80	0.66	0.51
Rb	146.55	122.06	116.35	149.65	133.25	163.96	111.58	157.03	120.80	94.27	182.07	98.62	92.67	201.74	99.21	88.95
Ba	29.80	2.00	23.97	38.37	31.52	32.71	289.32	884.25	72.79	643.19	5.18	82.93	347.13	3.61	749.18	1756.03
Sr	17.35	2.75	17.67	38.12	32.23	32.45	113.85	643.39	70.85	289.89	18.13	102.80	182.22	14.01	440.58	744.13
Th	26.36	15.28	22.21	23.87	23.92	27.41	15.10	25.90	17.99	16.82	28.21	17.43	15.09	23.86	15.87	11.34
U	6.59	4.05	5.37	5.62	5.99	6.49	3.66	5.99	4.56	4.13	7.43	4.49	3.73	6.18	3.93	3.09
Pb	14.99	11.49	12.13	11.62	12.78	13.21	8.57	14.23	11.82	8.88	11.98	9.18	8.03	15.58	8.50	6.79
Nb	296.63	201.08	369.71	308.14	344.79	337.93	226.37	175.55	213.65	279.69	266.72	318.91	293.17	290.05	272.36	205.62
Ta	20.83	31.59	25.77	20.00	21.79	20.36	21.72	7.51	13.10	19.35	16.85	22.48	22.01	17.49	19.98	13.62
Zr	888.26	778.80	1100.17	853.10	948.22	943.90	604.31	897.52	613.46	739.99	981.65	812.78	746.42	904.96	690.95	509.58
Hf	19.72	17.14	23.76	18.34	21.04	20.11	13.21	18.32	11.78	15.55	20.40	18.00	16.02	19.72	14.76	10.57
Y	54.66	35.42	49.37	31.46	29.15	36.31	47.08	30.36	29.49	40.91	23.63	37.70	40.86	58.45	43.97	39.04
La	153.69	100.60	191.23	122.53	115.75	140.29	157.40	103.73	110.60	159.14	97.25	143.51	149.42	166.07	177.26	153.08
Ce	294.99	202.24	357.15	209.19	198.30	229.04	308.58	161.20	191.64	299.13	148.70	288.98	310.26	295.43	334.07	291.98
Pr	32.28	20.62	36.89	18.28	17.59	20.26	34.63	15.42	18.17	31.29	12.04	29.14	32.09	30.32	36.18	32.49
Nd	103.36	65.00	110.64	48.19	46.59	52.64	111.32	50.02	53.61	96.26	29.61	89.28	100.29	90.40	110.43	106.56
Sm	16.06	10.14	15.06	6.32	6.12	6.84	16.10	7.56	7.40	13.28	3.62	12.20	14.10	12.82	14.89	14.86
Eu	2.13	1.27	2.93	0.96	0.91	1.01	3.39	2.26	1.49	3.23	0.57	2.40	3.21	1.61	3.26	4.66
Gd	12.43	7.88	11.12	5.05	4.88	5.48	11.70	6.20	5.83	9.67	3.09	9.08	10.21	10.51	10.64	10.71
Tb	2.16	1.37	1.87	0.92	0.90	1.01	1.91	0.97	0.98	1.60	0.57	1.53	1.71	1.87	1.77	1.70
Dy	11.37	7.32	9.72	5.29	5.11	5.80	9.39	5.06	5.17	7.89	3.39	7.75	8.44	10.37	8.62	7.94
Ho	2.19	1.40	1.85	1.09	1.08	1.22	1.72	1.02	1.04	1.52	0.77	1.50	1.56	2.07	1.62	1.41
Er	6.07	4.01	5.54	3.51	3.47	3.89	4.83	3.12	3.15	4.37	2.64	4.40	4.50	6.14	4.64	4.03
Yb	6.14	4.07	5.86	4.15	4.27	4.76	4.41	3.91	3.38	4.36	3.74	4.45	4.31	6.22	4.36	3.52
Lu	0.86	0.59	0.90	0.64	0.64	0.72	0.63	0.65	0.50	0.63	0.62	0.64	0.62	0.90	0.64	0.51

Continued--- table 5.1

Rock type	Trachyite				Rhyolite			Basalt	
Sample	GUN29	GUN23	GUN40	GUN42	GUN15	GUN19	GUN20	GUN11	GUN12
wt%									
SiO_2	63.17	65.72	68.42	68.34	71.18	70.41	74.60	55.31	50.31
TiO_2	0.73	0.80	0.56	0.57	0.79	0.34	0.18	2.71	3.18
Al_2O_3	19.96	17.02	13.28	13.19	13.40	14.08	10.73	14.35	13.79
Fe_2O_3tot	2.26	3.59	5.63	5.69	3.37	2.49	3.39	11.60	15.25
MnO	0.18	0.43	0.29	0.31	0.70	0.06	0.03	3.57	5.26
MgO	0.09	0.12	0.20	0.19	0.18	0.04	0.08	0.19	0.21
CaO	0.59	1.34	0.33	0.35	1.89	0.26	0.20	7.41	9.50
Na_2O	5.40	4.02	6.07	5.95	4.17	5.09	4.31	3.31	2.90
K_2O	6.57	6.04	5.23	5.10	3.36	5.73	5.30	1.56	0.75
P_2O_5	0.12	0.17	0.07	0.07	0.14	0.05	0.02	0.40	0.41
LOI	3.2	4.5	0.5	0.9	3.1	1	4.4	0.9	0.2
Total	102.27	103.75	100.58	100.66	102.28	99.55	103.24	101.31	101.76
K_2O+Na_2O	11.97	10.06	11.31	11.05	7.53	10.81	9.61	4.87	3.65
CIPWnormative									
Quartz	4.67	14.81	15.14	15.5	28.28	18.54	33.02	8.27	1.61
Plagioclase	48.34	39.88	39.33	39.69	43.73	41.2	26.01	47.97	46.78
Orthoclase	39.24	36.05	31.03	30.38	20.03	34.45	31.79	9.28	4.43
Corundum	3.23	1.89							
Nepheline									
Diopside			1.04	1.12	0.46	0.9	0.77	12.16	18.29
Hyperstine	2.33	4.62	7.58	7.66	4.92	2.75	4.35	13.69	18.61
Olivine									
Acmite			2.46	2.49		1.1	1.5		
Na2SiO3			2.21	1.92		0.3	2.18		
Ilmenite	1.41	1.54	1.06	1.08	1.52	0.65	0.34	5.17	6.02
Magnetite	0.49	0.78			0.74			2.54	3.31
Apatite	0.28	0.42	0.16	0.16	0.32	0.12	0.05	0.93	0.95
Total	99.99	99.99	100.01	100	100	100.01	100.01	100.01	100

Continued--- table 5.1

Rock Type	Trachyte				Rhyolite			Basalt	
Sample	GUN29	GUN23	GUN40	GUN42	GUN15	GUN19	GUN20	GUN11	GUN12
ppm									
Sc	2.57	6.59	10.41	10.45	8.02	4.70	5.23	21.14	26.77
V	13.57	16.12	4.06	3.73	10.25	1.81	1.00	225.66	394.47
Cr	1.69	2.00	3.68	2.05	1.77	1.68	1.70	1.88	26.10
Co	12.24	20.43	3.99	16.20	15.19	18.04	21.73	50.60	54.75
Ni	1.06	1.39	6.15	1.51	1.21	0.94	7.47	2.55	23.54
Cu	6.32	6.27	4.04	3.98	6.12	3.58	1.98	17.63	44.90
Zn	116.57	112.09	115.91	106.63	114.21	94.13	216.56	118.03	127.03
Cs	1.12	1.19	0.04	0.08	1.25	0.46	2.30	0.42	0.23
Rb	110.56	108.07	102.97	99.78	61.73	92.76	152.96	26.76	13.38
Ba	375.00	769.14	46.71	47.00	612.48	72.12	4.33	336.75	169.52
Sr	199.46	182.12	3.75	4.50	273.11	4.30	1.23	420.23	429.04
Th	16.51	12.65	24.75	25.37	8.12	12.78	16.49	3.23	2.24
U	3.85	3.43	4.78	4.60	2.47	2.12	4.83	1.34	0.71
Pb	9.75	10.23	20.13	17.04	8.67	5.93	20.71	4.06	2.46
Nb	273.09	90.51	180.87	189.65	54.70	99.41	117.07	21.35	26.34
Ta	22.50	5.15	10.54	99.49	3.64	5.87	6.93	1.88	37.81
Zr	913.22	593.26	1260.84	1281.63	605.51	834.49	1291.57	269.46	210.86
Hf	20.28	13.44	31.46	31.86	14.65	21.07	29.90	6.73	5.26
Y	44.43	55.80	85.12	112.62	74.53	49.26	130.56	41.58	32.09
La	100.86	77.36	125.88	144.56	56.35	75.98	89.97	25.78	19.31
Ce	196.17	151.37	290.16	294.29	125.71	151.17	186.89	59.58	45.63
Pr	19.69	18.05	32.10	36.80	16.71	17.53	23.43	8.22	6.33
Nd	60.71	66.18	113.10	131.52	70.31	60.53	89.92	36.32	28.63
Sm	9.44	12.49	22.06	25.94	16.30	10.47	20.91	8.98	7.30
Eu	2.01	2.94	3.82	4.54	4.25	0.77	0.88	2.73	2.37
Gd	8.03	11.01	18.94	22.67	15.50	9.04	20.88	8.91	7.27
Tb	1.44	1.86	3.37	4.10	2.56	1.59	3.80	1.46	1.18
Dy	8.24	10.39	18.97	24.10	14.54	9.63	23.95	8.20	6.62
Ho	1.64	1.98	3.57	4.70	2.69	1.93	4.78	1.52	1.21
Er	4.80	5.59	9.67	13.42	7.08	5.84	13.73	3.95	3.06
Yb	5.07	5.49	9.02	14.03	6.49	6.73	14.47	3.56	2.63
Lu	0.76	0.82	1.27	2.03	0.93	1.07	2.14	0.51	0.38

5.2. Major elements geo chemistry

The ignimbrite and lava samples from Guna volcanic centre have 56.74 to 74.60-wt-percentage SiO_2. In some of the samples the LOI values are high and their sum of the major oxides is > 101.50 this could be because of weathering of the samples. During the plots the major element data in all the samples are normalized to 100 % volatiles free. If the SiO_2 percentage have been used to group the units into acid >66%, intermediate 52-66% basic 45 to 52% and ultra basic <45%, the Guna volcanic products are all intermediate and acid. CIPW normative minerals calculations were performed using the norm-calculating program based on Johannsen A, 1931. In the course of CIPW, norm calculations 7 *quartz normative* (silica saturated) and 16 *nepheline nomative* (silica under saturated) rocks are encountered.

Analyses are recalculated or normalized to 100 % volatiles free. Total alkali versus silica classification after Le Bas et al., (1986), Figure 5.1 is plotted on anhydrous bases. On this plot, three samples fall in rhyolite field, four samples on trachyte field, and others in phonolite field. Trachytes have 63.17 to 68.34- while rhyolites have 71.18 to 74.60-wt-percentage SiO_2.

The phonolites have 56.74 to 61.66 wt percentage SiO_2 and 7.43 to 26.72 normative nepheline, they are rich in alkalis, poor in iron, magnesium & calcium with concentration of TiO_2 (<1%), FeO (total) (<5%), MnO (<0.5%), MgO (<1.5%), CaO (0.86-3.20), P_2O_5 (0.04-0.47%), Al_2O_3 (19.04-21.57wt %), K_2O (5.28-6.79%) & Na_2O (6.23-9.62%). They have 11.50-15.52 total alkalis.

It is well known that the major element data are significantly used in reconstruction of variation diagrams, which reveal interrelationship between elements in the data set on these bases, several variation diagrams (Harker diagrams) are constructed for major element oxides choosing SiO_2 wt% as the X-axis (differentiation index). SiO_2 is chosen as differentiation index because it has reasonably wide range of values and continuously decreases during crystal liquid fractionation. The variation diagrams for major elements with SiO_2 are indicated below in Figure 5.2 A-F.

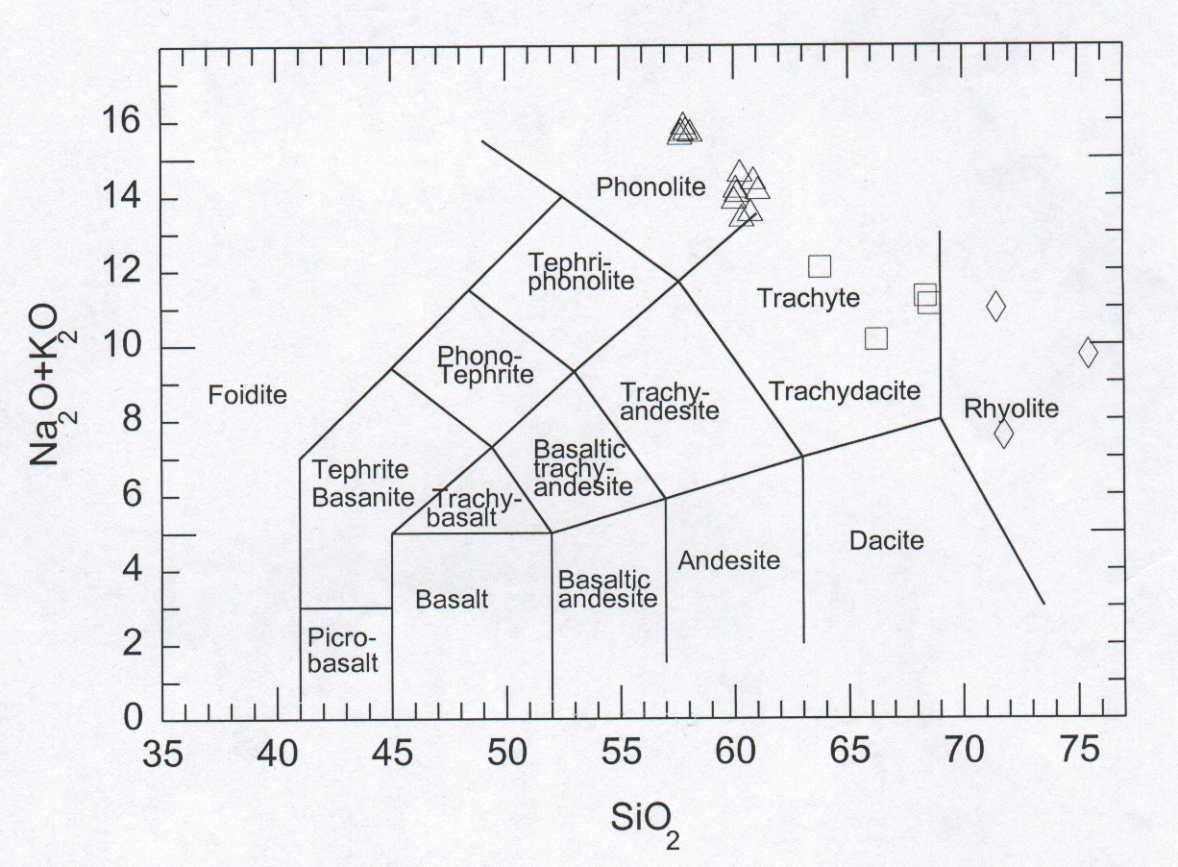

Figure 5.1: Classification of rocks from Guna rocks based on the total alkalis versus silica (TAS) diagram after Le Bas et al., 1986.

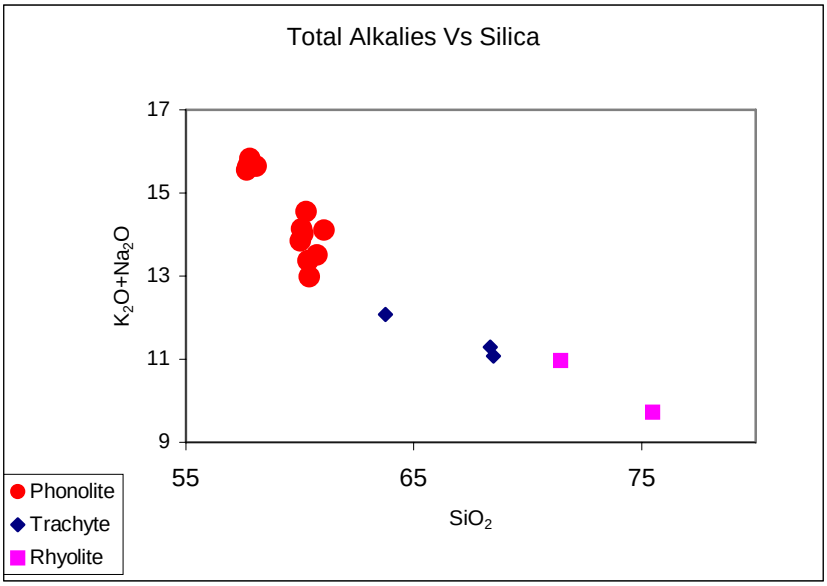

A.

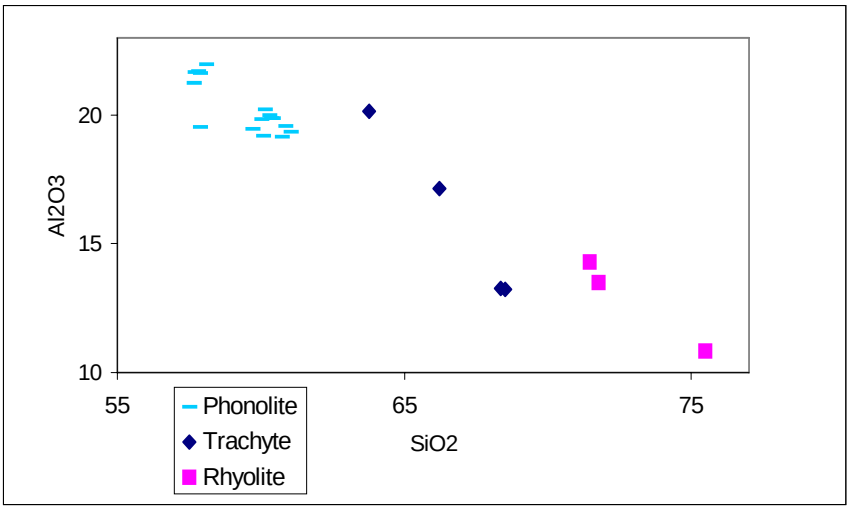
Al2O3
20
15
10
55
65
75
SiO2
Phonolite
Trachyte
Rhyolite

B

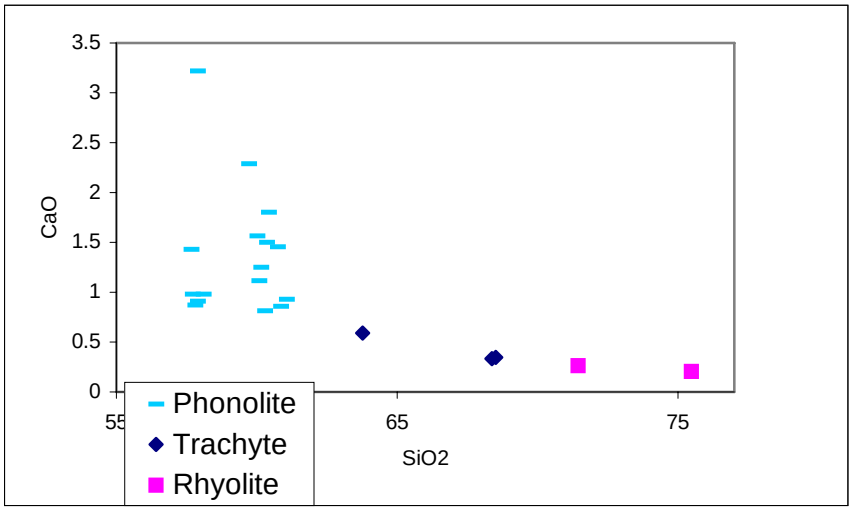
CaO
3.5
3
2.5
2
1.5
1
0.5
0
55
65
75
SiO2
Phonolite
Trachyte
Rhyolite

C

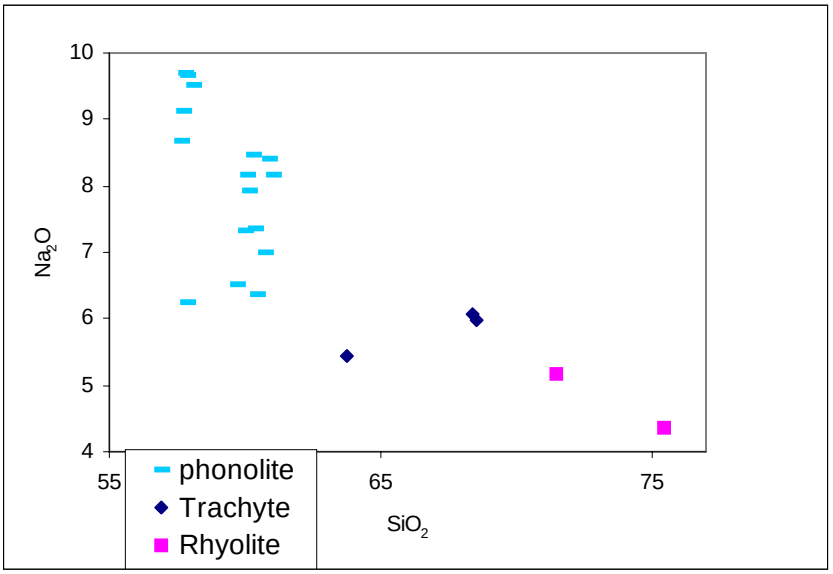
Na2O
10
9
8
7
6
5
4
55
65
75
SiO2
phonolite
Trachyte
Rhyolite

D

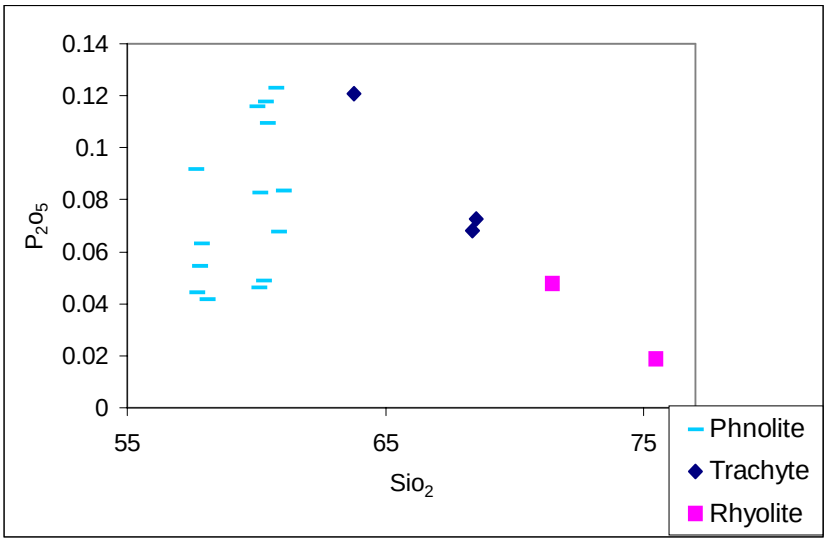

E

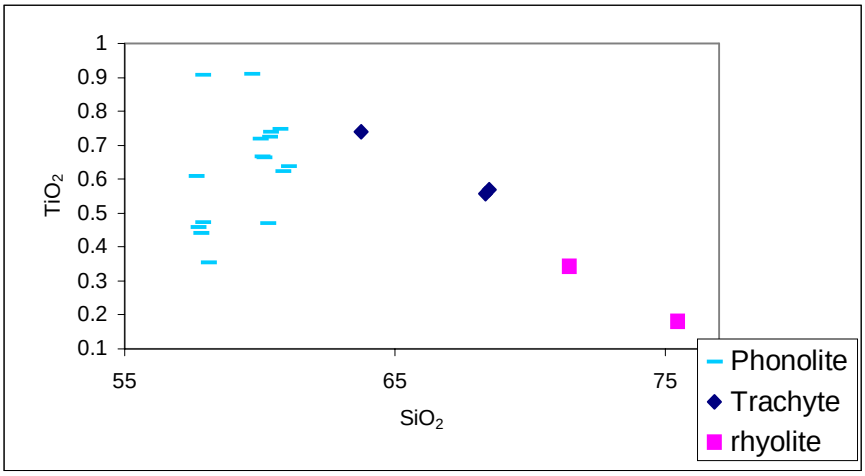

F

Figure 5.2 A-F: Variation diagrams of Major oxides against silica.

The variation of major oxides against SiO_2 is indicated in figure 5.2.A-F. The diagram shows that there is an over all decrease in total alkalis, Al_2O_3, Na_2O and CaO with increasing SiO_2. While P_2O_5 and $Ti0_2$ increase up to about 62% SiO_2 and then decrease. The over all pattern in the distribution of major elements as a function of silica indicate fractionation (separation) of feldspars, feldspathoids (nepheline, luecite and nosean), titano magnetite and apatite.

Some of the scattering observed in phonolites may be due to the porphyrithic nature of the rocks; most of them have 13 to 40 % phenocryst. Glassy natures of the rhyolite also contribute for it.

5.3. Trace elements geochemistry

Variations of trace elements also provides additional in sight in to the sources and major processes that controlled the nature of the volcanic products. The relative abundances of trace elements are used to identify the minerals that were present during melting or fractional crystallization. The Guna lavas are strongly depleted in compatible elements e.g. Ni 0.85-7.47 ppm and Cr 1.47-3.68 ppm. Both elements are < 3 ppm in phonolite flows. They are enriched in incompatible elements. Various bi variate variation diagrams i.e. trace elements vs. Sio_2 wt percentage, trace vs. trace and trace element ratios against trace are plotted. Selected trace element ratios are presented in table 5.2.

Selected trace elements plots against Sio_2 are shown in Fig 5.3 A-D. With this Rb, Sr, V, and Nb, shows a decreasing trend.

The fractionation of alkali – feldspars will lead to the removal of Rb from the liquid where Rb is accommodated therefore a decrease in Rb with increasing SiO_2 indicates feldspar fractionation.

Sr preferentially enters the plagioclase structure or other Ca bearing phases and shows a negative correlation. There for Sr fall is attributable to removal of feldspar and apatite. V similar to TiO_2 its fall is related to Fe –Ti oxide fractionation. The decreasing pattern of Nb is related to fractionation of sphene. This is coherent to observations made from petrography and major element variations

a) Trace vs Silica

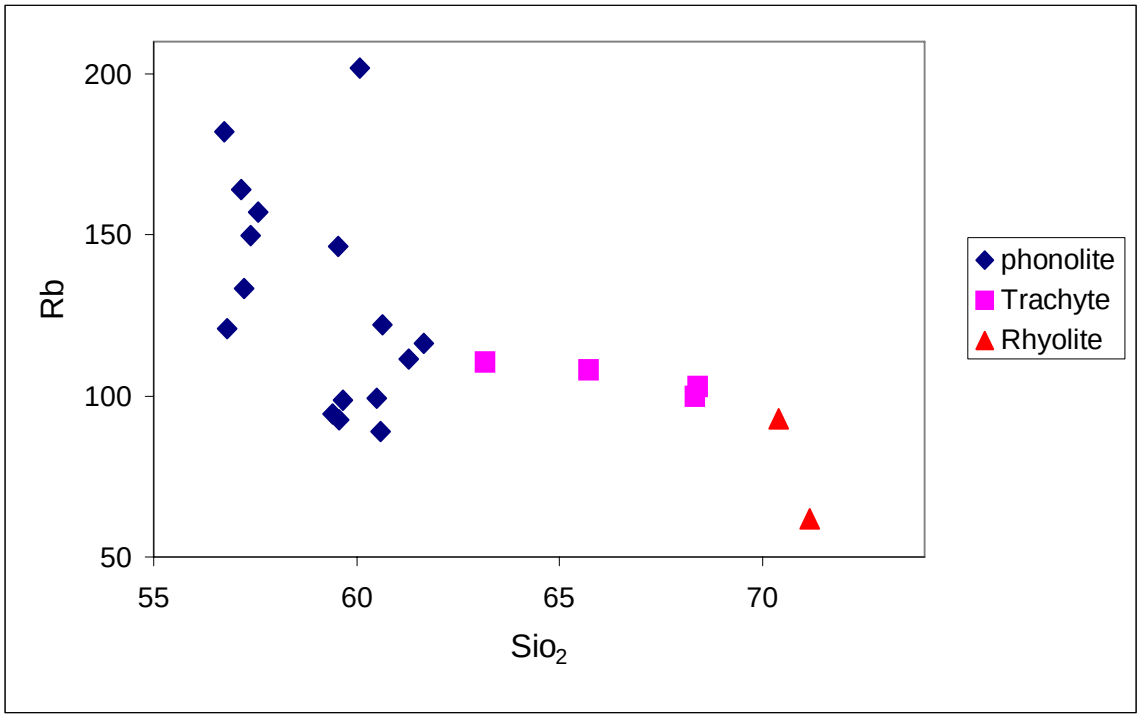

A

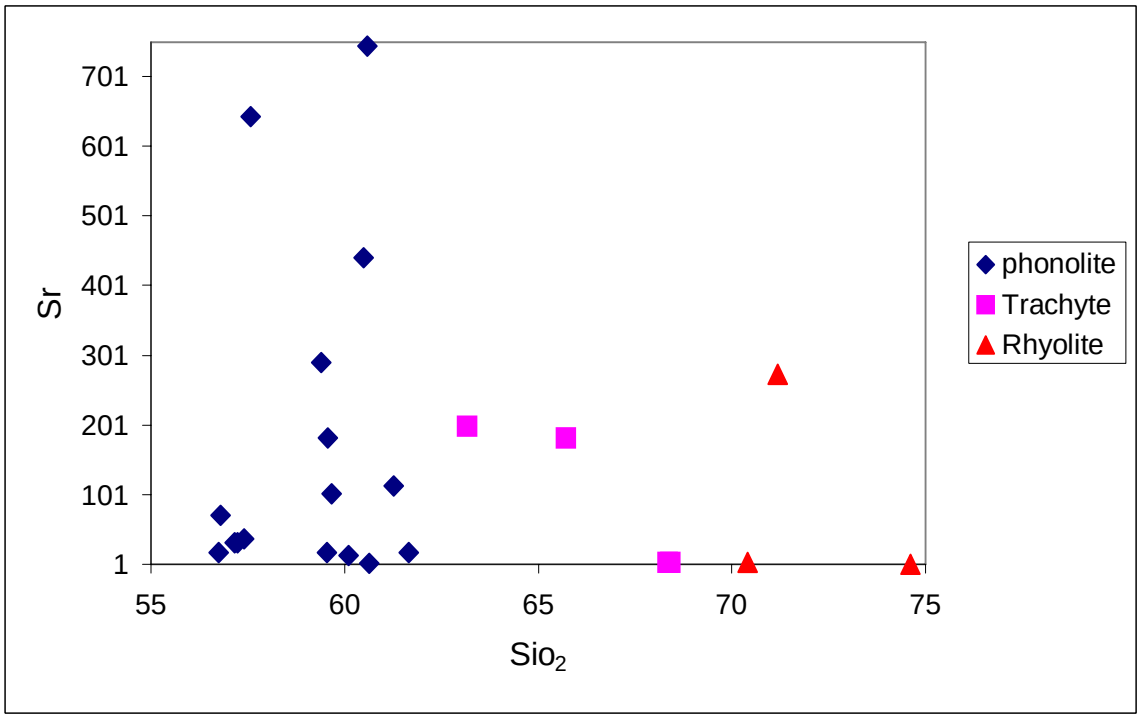

B

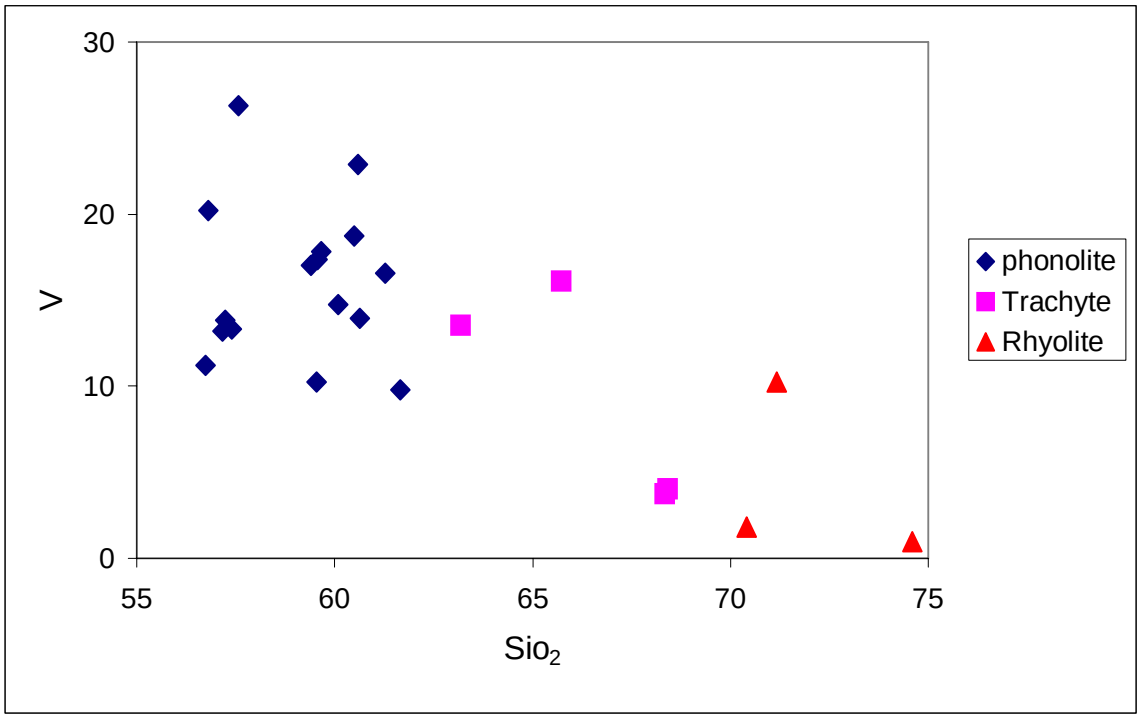

C

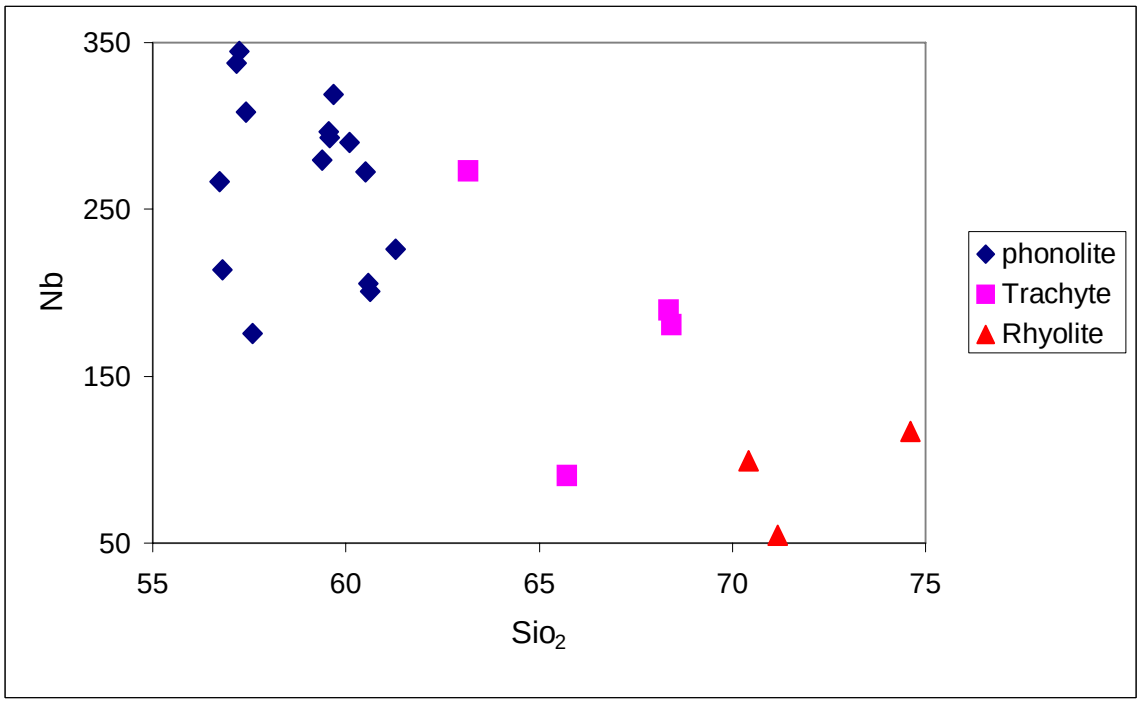

D

Figure 5.3: A-D Plot of selected trace element abundance against silica.

b) Trace vs trace

A series of lavas related by crystal fractionation will plot on a straight line on element – element scatter plots.

On trace- trace elements scatter plots Fig.5.4. A-D. Th, U and Ce versus Rb and La versus Nb show a positive linear correlation. These linear positive correlations possibly explain the fact that the two highly incompatible elements are fractionated through extended amounts of crystal fractionation. And also it may indicate that the Guna products are from the same source related by crystal fractionation.

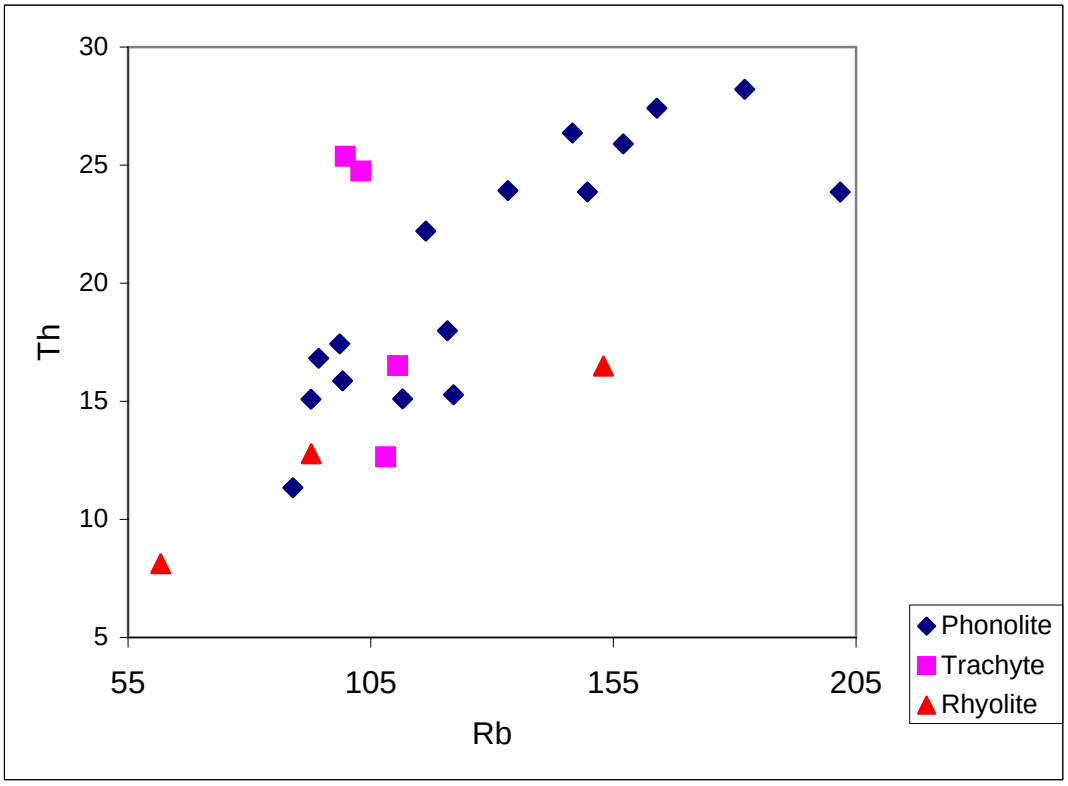

A

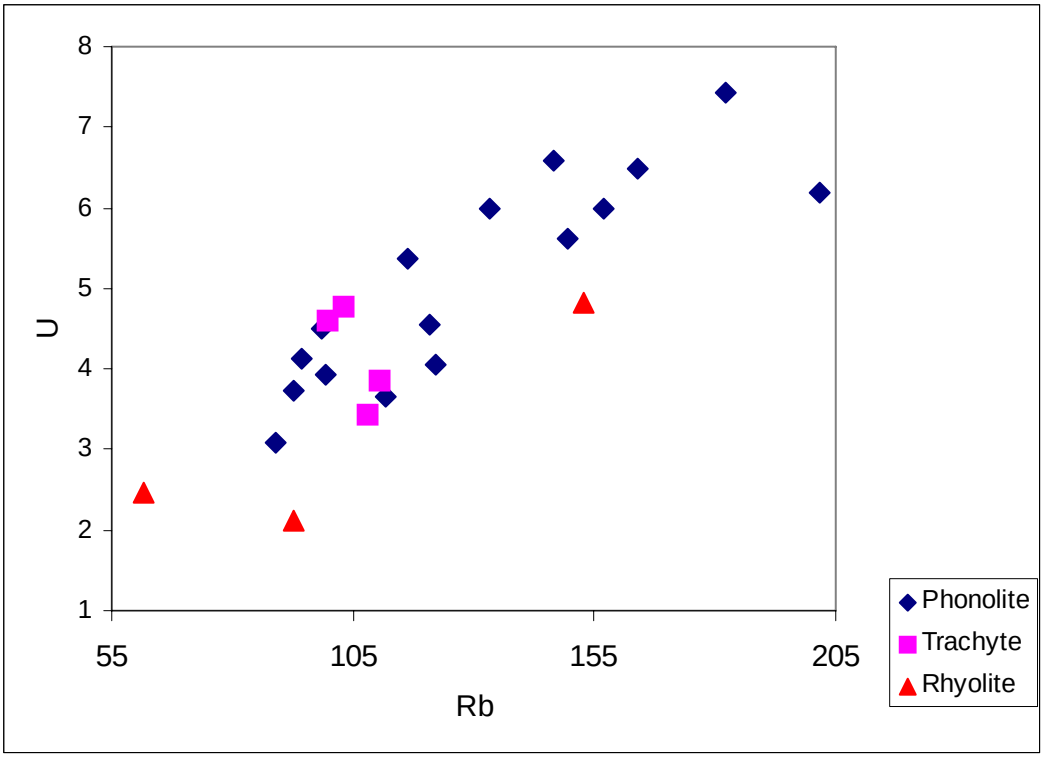
8
7
6
5
4
3
2
1
U
55
105
155
205
Rb
Phonolite
Trachyte
Rhyolite

B

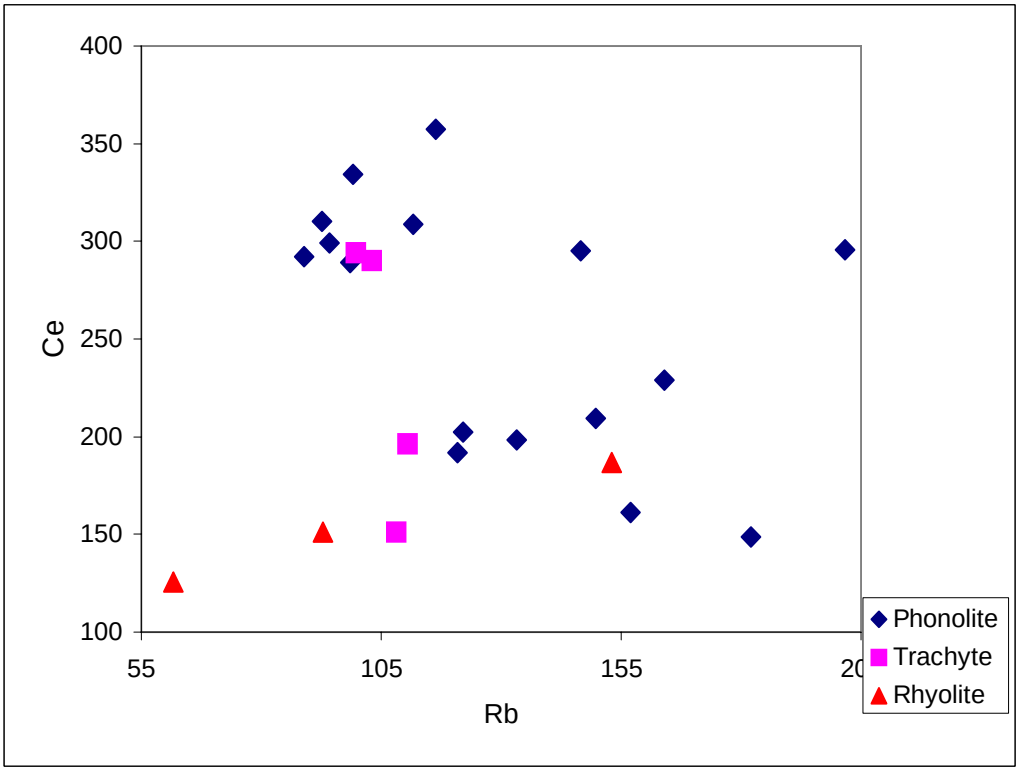
400
350
300
250
200
150
100
Ce
55
105
155
Rb
Phonolite
Trachyte
Rhyolite

C

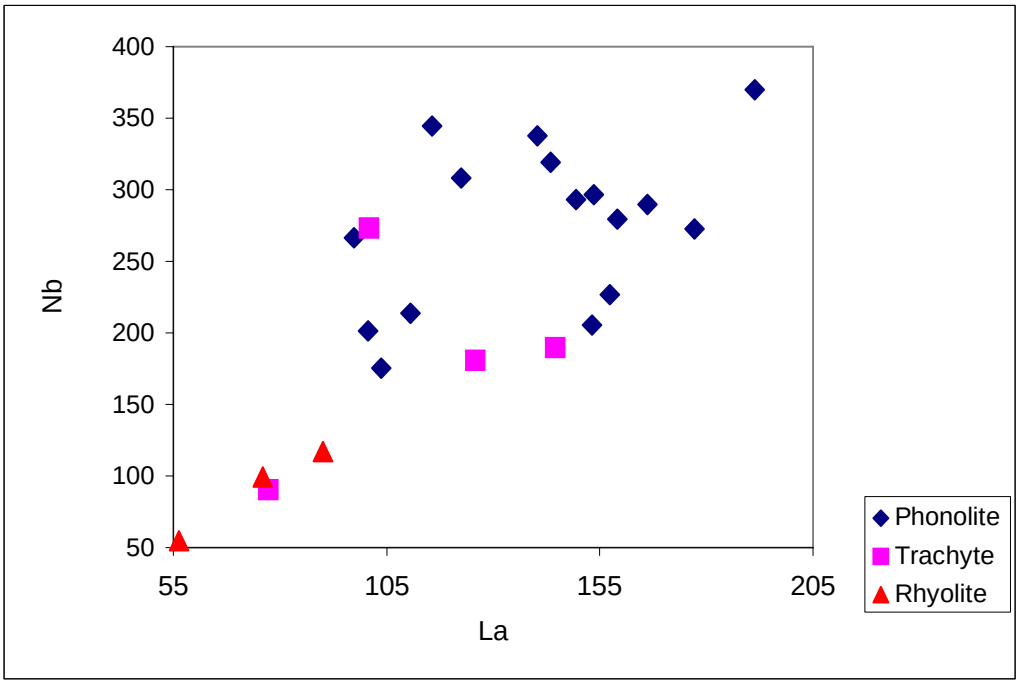

D

Figure 5.4: A-D Trace- trace variation patterns.

C) Trace ratio

Table 5.2 shows selected trace element ratios. The linear enrichments of incompatible element ratios plotted against traces albeit less diagnostic compared with element – element plots, also support that the lava series resulted from single magmatic source. The trace ratio versus trace plots of the Guna products Fig 5.5 A-C shows Zr/Dy ,Th/La and Nb/Y versus Rb show a positive linear correlation interpreted as the lavas are from same magmatic source and related by differentiation.

Rock type	phonolite															
Sample	GUN5	GUN9	GUN 17	Gun 25b	GUN 26b	GUN 27	GUN 28	GUN 31	GUN 35	GUN 36	GUN 44	GUN45	GUN47	GUN 49	GUN 50	GUN 46
Ratio																
La/Nb	0.52	0.50	0.52	0.40	0.34	0.42	0.70	0.59	0.52	0.57	0.36	0.45	0.51	0.57	0.65	0.74
Zr/Nb	2.99	3.87	2.98	2.77	2.75	2.79	2.67	5.11	2.87	2.65	3.68	2.55	2.55	3.12	2.54	2.48
Rb/Nb	0.49	0.61	0.31	0.49	0.39	0.49	0.49	0.89	0.57	0.34	0.68	0.31	0.32	0.70	0.36	0.43
Nb/Th	11.25	13.16	16.65	12.91	14.41	12.33	14.99	6.78	11.88	16.63	9.45	18.30	19.43	12.16	17.16	18.13
Zr/Dy	78.12	106.39	113.19	161.27	185.56	162.74	64.36	177.38	118.66	93.79	289.57	104.87	88.44	87.27	80.16	64.18
Th/La	0.17	0.15	0.12	0.19	0.21	0.20	0.10	0.25	0.16	0.11	0.29	0.12	0.10	0.14	0.09	0.07
Rb/Sr	8.45	44.39	6.58	3.93	4.13	5.05	0.98	0.24	1.71	0.33	10.04	0.96	0.51	14.40	0.23	0.12
Rb/Ba	4.92	61.03	4.85	3.90	4.23	5.01	0.39	0.18	1.66	0.15	35.15	1.19	0.27	55.88	0.13	0.05
Ba/Y	0.55	0.06	0.49	1.22	1.08	0.90	6.15	29.13	2.47	15.72	0.22	2.20	8.50	0.06	17.04	44.98
Nb/Y	5.43	5.68	7.49	9.79	11.83	9.31	4.81	5.78	7.24	6.84	11.29	8.46	7.17	4.96	6.19	5.27
La/Yb	48.04	49.69	60.95	50.41	46.44	48.12	69.97	41.23	56.70	68.61	39.76	64.94	71.99	47.50	76.62	82.95
La/Lu	178.71	170.51	212.48	191.45	180.86	194.85	249.84	159.58	221.20	252.60	156.85	224.23	241.00	183.91	276.9	300.1

	Trachyte				Rhyolite		
Sample	GUN29	GUN23	GUN40	GUN42	GUN15	GUN19	GUN20
Ratio							
La/Nb	0.36933	0.85471	0.69597	0.762246	1.03016	0.76431	0.7685
Zr/Nb	3.34	6.55	6.97	6.76	11.07	8.39	11.03
Rb/Nb	0.40	1.19	0.57	0.53	1.13	0.93	1.31
Nb/Th	16.5409	7.15494	7.30788	7.475365	6.73645	7.77856	7.0995
Zr/Dy	110.83	57.10	66.46	53.18	41.64	86.66	53.93
Th/La	0.16	0.16	0.20	0.18	0.14	0.17	0.18
Rb/Sr	0.55	0.59	27.46	22.17	0.23	21.57	124.36
Rb/Ba	0.29	0.14	2.20	2.12	0.10	1.29	35.33
Ba/Y	8.44024	13.7839	0.54872	0.417333	8.2179	1.46407	0.0332
Nb/Y	6.14652	1.62204	2.12488	1.683982	0.73393	2.01807	0.8967
La/Yb	38.6923	27.5719	32.1685	20.97577	19.3698	22.4621	12.916
La/Lu	132.711	94.3415	99.1181	71.21182	60.5914	71.0093	42.042

Table 5.2 Selected trace element ratios

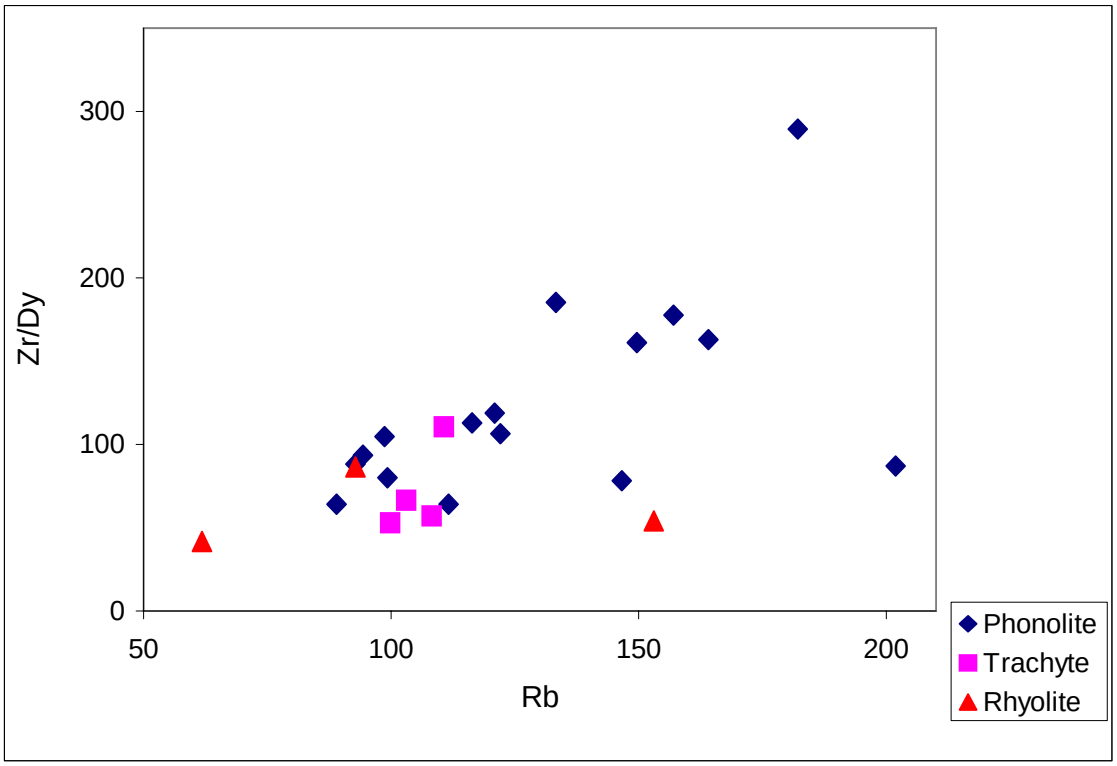
300
200
100
0
Zr/Dy
50
100
150
200
Rb
Phonolite
Trachyte
Rhyolite

A

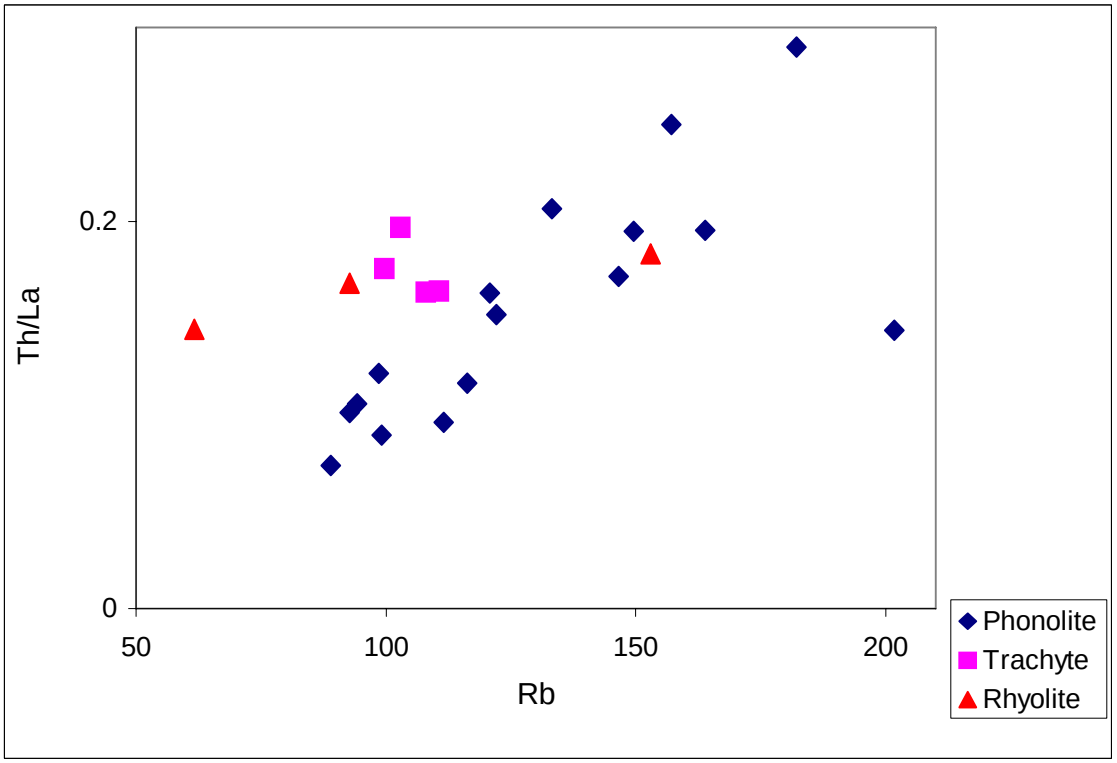
0.2
0
Th/La
50
100
150
200
Rb
Phonolite
Trachyte
Rhyolite

B

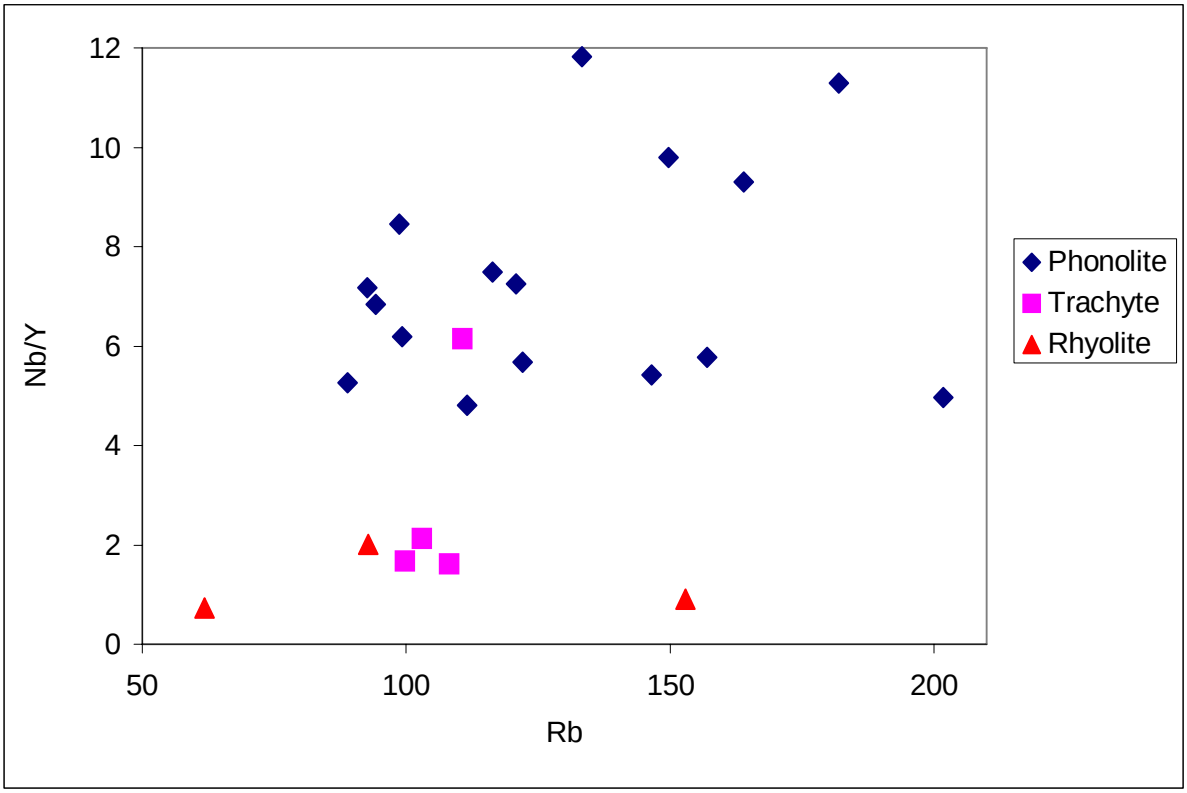

C

Figure 5.5: A-C Traces ratio versus trace variation patterns.

5.4.Rare earth elements (REE) geochemistry

Chondrite normalized rare earth element (REE) abundance patterns for representative samples are shown in Fig 5.6.A-C (normalizing values are according to Boynton 1984). Generally, the rare earth elements pattern indicates enriched light rare earth element (LREE) and almost flat heavy rare earth element (HREE) pattern. All samples show a negative Eu anomaly. The LREE enrichment increases from rhyolite through trachyte to phonolite. The trough or size of negative Eu anomaly increases from phonolite through trachyte to rhyolite.

During fractional crystallization of magma LREE increase whereas HREE, remain almost constant with these regard the increase (enrichment) of light rare earth LREE and almost constant heavy rare earth (HREE) pattern of Guna lavas indicates fractional crystallization (fractionation) of magma. The conspicuous negative Eu anomaly also displays significant fractionation of feldspars. The La/Lu ratio, which increases with on

going fractional crystallization, shows 42.00-71.00 for rhyolite, 71.2-132.71 for trachyte and 159.6-300.2 for phonolite.

Fig .5.7 displays primitive mantle normalized in compatible trace elements abundance profiles (Spider diagrams). The pattern shows strong negative anomaly or depletions in Ba, Sr, P and Ti concentrations but enrichment in K, Rb, Th, Nb and Zr. Depletions in Ba and Sr contents are due to fractionation of feldspar (sanadine and or plagioclase) and those of P and Ti suggest fractional removal of apatite and Fe-Ti oxides.

Strong depletions in the Sr, P, and Ti in the silica under saturated rocks (Phonolitc) are probably caused by fractional crystallization of some combination of plagicoclase clinopyroxene, apatite, titanite and ilmenite (Barker, 1996).

On the spider diagrams highly in compatible elements concentration increase from rhyolitie, through trachyte to phonolite and heavy rare earth elements (HREE) show a flat trend that is also indicative of fractionation of magma. Except two samples in trachyte and rhyolite all samples of phonolite, trachyte and rhyolite show a positive Nb anomaly.

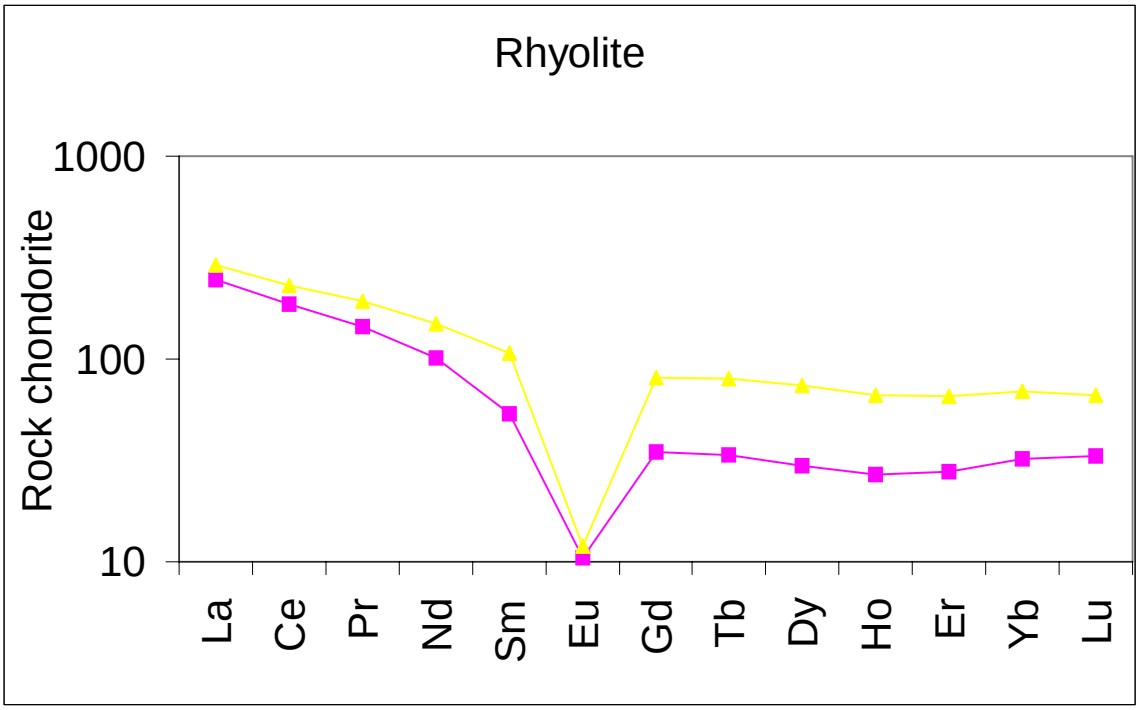

A

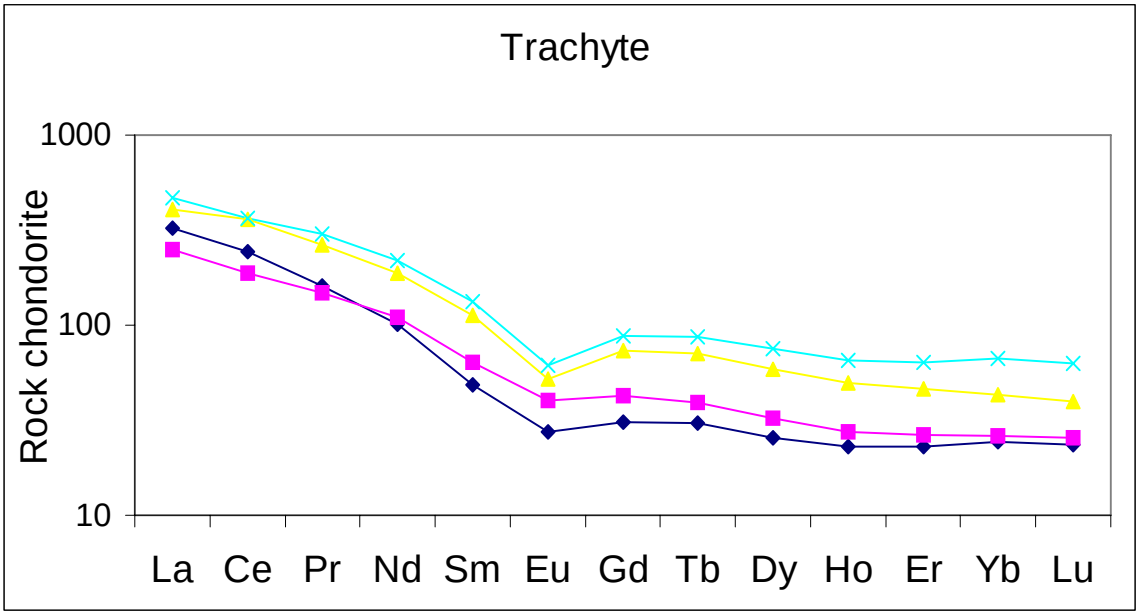

B

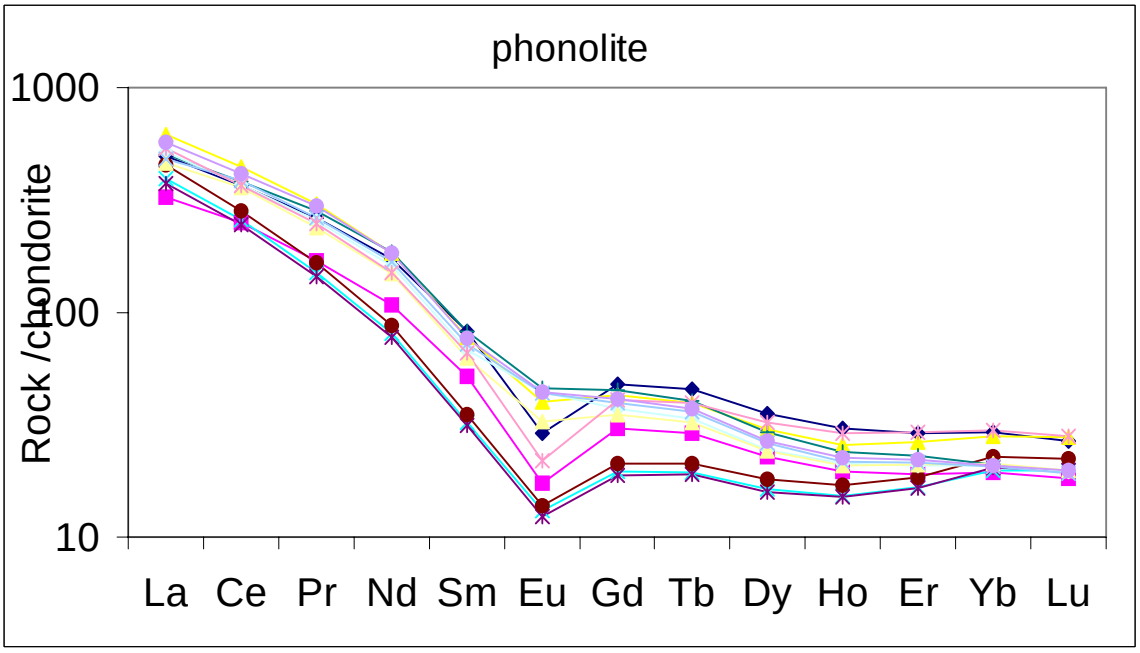

C

Figure 5.6: A-C Chondrite normalized trace element abundance pattern of Guna lavas. Normalizing values from Boynton (1984).

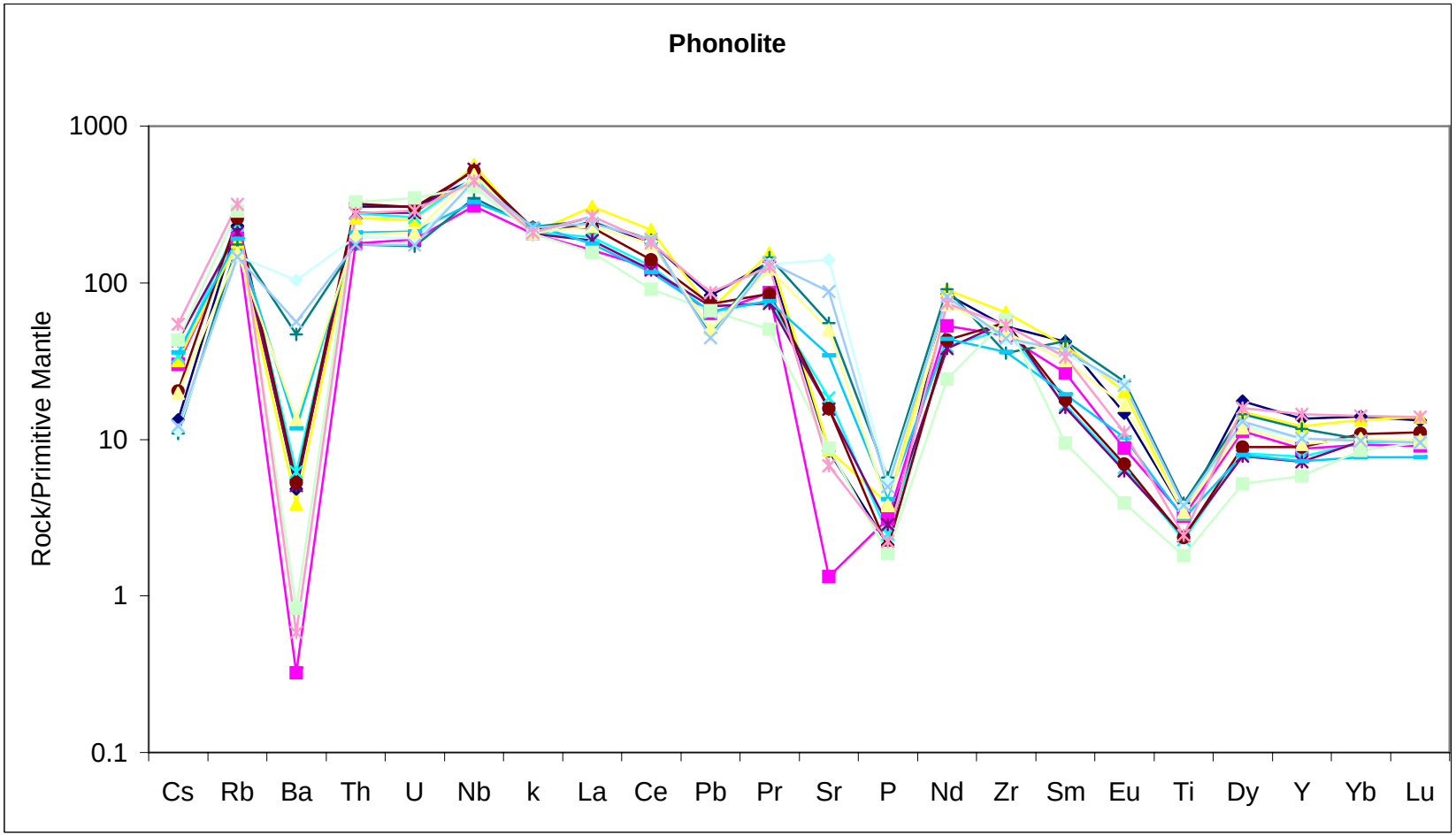

Figure 5.7: Primitive Mantle normalized abundance of selected trace elements in Guna phonolite lavas. Normalizing values and order of listing from Sun and Mac Donough (1995)

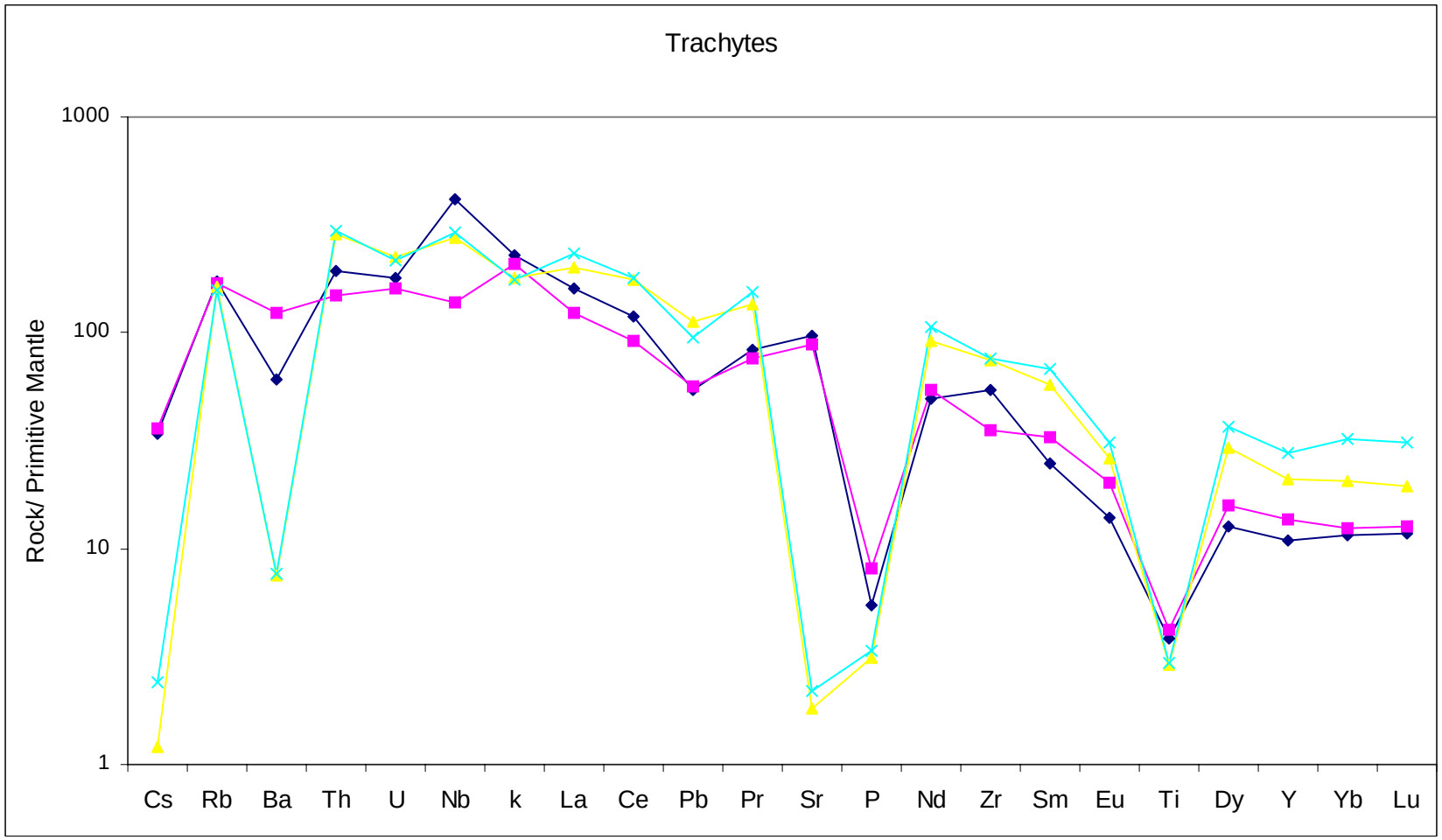

Figure 5.8: Primitive Mantle normalized abundance of selected trace elements in Guna trachyte lavas. Normalizing values and order of listing from Sun and Mac Donough (1995).

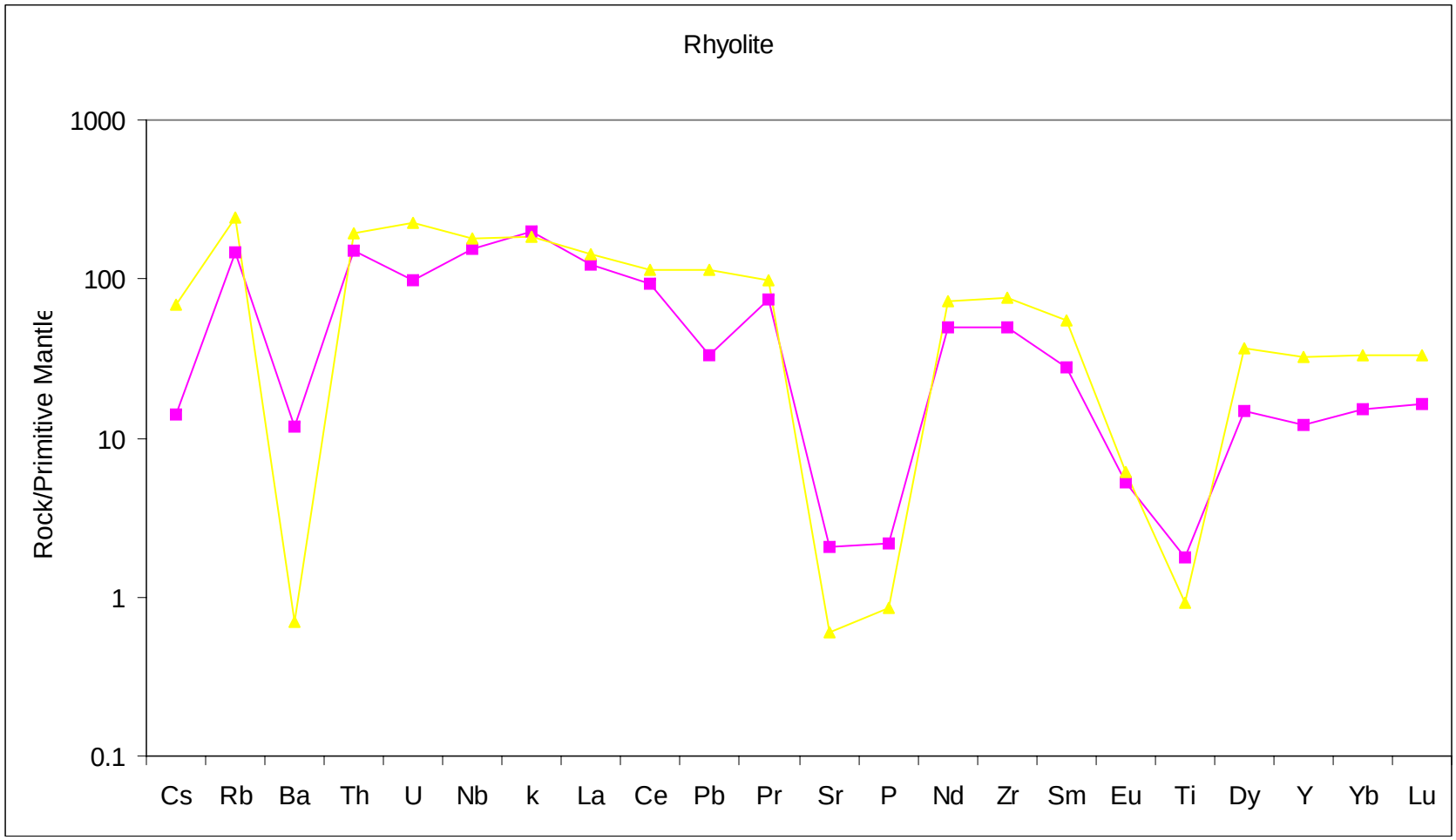

Figure 5.9: Primitive Mantle normalized abundance of selected trace elements in Guna rhyolite lavas. Normalizing values and order of listing from Sun and Mac Donough (1995).

REFERENCES

Ayalew, D., Barbey, P., Marty, B., Reisberg,L, Yirgu, G. and pik, R. 2002. Source, Genesis and timing of giant ignimbrite deposits associated with Ethiopian continental flood basalts. Geochimica et Cosmochimica Acta, 66,1429-1448.

Ayalew.D and Yirgu G. 2003, crustal contribution to the genesis of Ethiopian Plateau rhyolitic ignimbrites, basalt and rhyolite geochemical provinciality Journal of the Geological society, 160, 47-56.

Ayalew, D., Marty, B., Yirgu, G. and Pik, R. (1999). Geochemical and isotopic (Sr,Nd and Pd) characteristics of volcanic rocks from south western Ethiopia. Journal of African Earth Sciences **29** , 381-391.

Anthony R. Philpotts 1989 Petrography of igneous and metamorphic rocks Prentice Hall, Englewood Cliffs, New Jersey 167PP

Baker, D.S. 1996. Nephelinite – phonolite volcanism. In: Mitchel, R.H. (ed;), under saturated alkaline rocks: mineralogy, petrogenesis, and economic potential. The Mineralogical Association of Canada, Manitoba, **24**, pp 23-44

Abate,B, Koeberl, C, Buchanan, P.C. and Korner, W. (1998). Petrography and geochemistry of basaltic and rhyodactic rocks from lake Tana and the Gimjabet-kosober areas (north central Ethiopia). J.A far. Earth Sci. 26:119-134

Bonavia, F.F., Mohr, P., Parrot, J.F. and Tesfaye korrne (1994). The Tana basin, Ethiopia intra plateau uplift, rifting and subsidence. Tectono physics 295:351-367.

Berhe, S.M., Desta, B., Nicoletti, M. and Teferra, M. 1987. Geology, Geochronology and Geodynamic Implications of the Cenozoic Magmatic Province in W and SE Ethiopia. Journal of the Geological Society, London, **144**, 213 – 226.

Blatt, H. and Tracy, R.J. 1995 petrology: Igneous, Sedimentary and Metamorphic, 2nd ed. Freeman and Company, New York, 529p.

Brotzu, P., Ganzerli-Valentini, M.T., Morbdeili, L., Piccirillo, E.M., Stella, R. and Traversa, G. 1981 Basaltic volcanism in the Nnorthern sector of the main Ethiopian rift. Journal of Volcanology and Geothermal Research, 10, 365-382.

Brownolo, A.H. 1996. Goechemistry, 2nd ed. Prentice Hall, New Jersey, 580p.

Chorowicz. J., Collet. B., Bonavia. F.F.,Mohr. P., Parrot.J.-F., Korme.T., 1998. The Tana basin ,Ethiopia: Intra plateau uplift. Rifting and subsidence. Tectono physics 295 . 351-367.

Coulie, E., Quideleur, X., Gillot, P-Y., Courtillot, V., Lefevre, J-C. and chiesa, S. (2003). Comparative K-Ar and Ar/Ar dating of Ethiopian and Yemenite Oligocene volcanism implications for timing and duration of the Ethiopian traps. Earth and planetary science Letters 206,477-492.

Coulie, E.,(2001).Chronologie Ar/Ar et K/Ar de la dislocation du plateou ethiopien et de la dechirure continetale dans la Corne de I"Afrique depuis 30 Ma. Ph.D. thesis, University de paris Sud. Orsay.

Cox K.G., Bell, J.D. and Pankhurst, R.J. 1979. The Interpretation of Igneous Rocks. George Allen and Unwin, London, 450p.

Chernet T. 1995 Petrological, Geochemical and Geocronological Investigation of Volcanism in the Northern Main Ethiopian Rift- Southern Afar transition Region, PhD dissertation, Miami University, Oxford, Ohio.

Chazot, G. & Bertrand, H.(1993). Mantle sources and magma – continental crust interactions during early Red Sea- Aden rifting in Southern Yemen: elemental and Sr,Nd isotope evidence. Journal of Geophysical Research **98**, 1818-1835.

Davis G.R and Macdonald: 1987, Crustal Influences in the Petrogenesis of Naivasha basalt- Comendite complex: combined trace element and Sr-Nd-Pb Isotope Constrains Journal of petrology, **28**,1009-1031.

Dercq, M., Arndt,N.,Lapierre, H. and Gezahegn yirgu (2001). Les pitons trachytiques d'Ethiopiene sont pas les conduits d'alimentation des trapps.C.R.Acad. Sci. paris 332:609-615.

Deer W.A; Howie R.A.; and Zussman J., 1997, Single-chain silicates, rock-forming minerals, 2nd ed., **2A**. The Geological Society, London, 668p.

Deer W.A; Howie R.A.; and Zussman J., 1966, An Introduction to Rock Forming Minerals Longmans, England,p.528.

Davidson A. (Compiler), 1983. Reconnaissance geology and geochemistry of parts of Illubabor, Kefa,Gemu Gofa and Sidamo, Ethiopia. The Omo River Project. Ethiopian Institute of geological Surveys, Bulletin **2** . Addis Ababa.

Ebinger C.J., Yemane T. WeldeGabriel G., Aronson J. L., and Walter R.C., 1993, Late Eocene-Recent volcanism and faulting in the Southern main Ethiopian Rift , Journal of the Geological Society, London, V. 150,P.99-108.

George R, M. (1997) Thermal tectonic controls on magmatism in the Ethiopian provence. PhD. Thesis. Open University.

Gobena H, 200 Petrology ,Geochemistry and geochronology of volcanic rock suites of the Dodola area south eastern Ethiopia , PhD, Dissertation, university of Vienna.

Gichile S., 1991. Structures , Metamorphism and tectonic setting of a gneissic terrane , the Sagan- Aflata area ,southern Ethiopia. MSc thesis, University of Ottawa. Canada.

Hatch, F.H, A.K. Wells & M.K. Wells, 1972. Petrology of the igneous rocks 13th ed. George Allen & unwintd, London

Hibbard M.J Petrography to Petrogonesis Department of Geological Sciences Mackay School of mines university of Nevada, Reno, prentice Hall, Engle Wood Cliffs, New Jersey 07632.

Hall A. 1996, Igneous Petrology, 2nd ed. Longman Group, London, 551p.

Hanson, G.N. 1989. An approach to trace element modeling using a simple igneous system as an example. In: Lipin, B.R. and McKay, G.A. (eds), Geochemistry and mineralogy of rare earth elements. Reviews in Mineralogy, The Mineralogical Society of America, Washington D.C., **21**, pp79-97.

Hess, P.C. 1989. Origin of Igneous rocks. Harvard University Press, Cambridge, 336p.

Hofmann, A.W. 1979. Mantle geochemistry: the message from oceanic volcanism. Nature, **385**, 219 – 229.

Hibbard M.J Petrography to Petroganesis Department of Geological Sciences Mackay School of mines University of Nevada, Reno, plentice Hall, Engle wood Cliffs, and New Jersey 07632.

Hofmann, A.W. and White, W.M. 1982. Mantle Plumes from ancient oceanic crust. Earth and Planetary Science Letters, **57**, 421 – 436.

Hofmaan, C., Courtillot, V., Feraud, G., Rochette, P., Yirgu, G., Ketefo, E. and Pik, R. 1997.Timing of Ethiopian flood basalt event and implications for plume birth and global change. Nature, **389**, 838 – 841.

Hay.D.E.R.F. wendlandt, and E.D wendlandt (1995) The origin of Kenya rift plateau type flood phonolites Evidence from Geochemical studies for fusion of lower crust Modified by alkli basaltic magmatism. J. Geophysical Research, 100 (Bl), 411-422.

Hart W.K. Woldegabriel G., Walter R.C., and Mertzman,S.A.(1989) Basaltic volcanism in Ethiopia: Constaints on continental rifting and mantle interactions. J. Geophysical Research,**94** 7731-7748.

Irvine, T.N. and Baragar, W.R.A. 1971. A guide to the chemical classification of the common volcanic rocks. Canadian Journal of Earth Sciences, **8**, 523 – 548.

Justin visentin E., Nicolettin M., Tolomeo, L and zanettin, B. (1974). Miocene and Pliocene volcanic rocks of the Addis Ababa-Debre Berhan area (Ethiopia). Bulletin of volcanology 38, 237-253.

Kazmin, V., 1972 Geological Map of Ethiopia ,1:2,000,000 Scale ,With explanatory note (1975, 14 p, Geological Survey of Ethiopia.

Kazmin, V. Shiferaw A., Balcha T., 1978, The Ethiopian basement: Stratigraphy and possible manner of evolution, Geol. Rdsch. V.67,p.531-546.

Kazmin, V. 1979. Stratigraphy and correlation of volcanic rocky in Ethiopia. Ethiopian Institute of Geological Surveys, Note No. 106, 26p.

Kazmin V., 1987, Two types of rifting depending on the condition of extension; Tectonophysics, v. 143,p.85-92.

Kazmin V., Berhe S.M., Nicolitti M. and Petruccian C., 1980, E volution of Northern part of the Ethiopian Rift , in Geodynamic Evolution of the Afro- Arabian Rift System, Accademia Nazionale dei Lincei, Roma,v.47,p.275-291.

Kent, R. 1995. Continental and oceanic flood basalt provinces: current and future prospectives. In: Srivatava, R.K. and Chandra, R. (eds), Magmatism in relation to diverse tectonic settings. A.A. Balkema, Rotterdam, pp17 – 42.

Kieffer B., Nicholas A., Henriette L., Florenece B., Delphine. B. Arnaud P., Gezahegn Y Dereje A., Dominique W., Dougal A.J, Francine K., and Claudine M., (2004). Flood and shield Basalt from Ethiopia magmas from the African superswell Journal of petrology 45,793-834

Le Bas, M.J., Le Maitre, R.W., Streckeisen, A. and Zanettin, B. 1986. A chemical classification of volcanic rocks based on the TAS diagram. Journal of Petrology, **27**, 745 – 750.

Le Bas, M.J. and Streckeisen, A.L. 1991. The IUGS systematics of igneous rocks. Journal of the Geological Society, London, **148**, 825 – 833.

Mengesha T., Cherenet T. and Haro W., 1996, Geological map of Ethiopia, scale 1:2000,000 with an explanatory note Ethiopian Institute of Geological Survey.

Mackenzie W.S., Donaldson C.H. and Gulifird C., 1982, Atlas of Igneous rocks and their textures, Longmans, England, 148P.

Merla, G., Abbate, E., Azzaroli, A., Bruni, P., Fazzuoli, M., Sargi, M. and Tacconi, P. 1979. A geological map of Ethiopian and Somalia: Comment. Petgamon, 95p.

Merla, G., Abbate, E., Ganuti P., Sargi, M. and Tacconi, P. 1973, Geological map of Ethiopian and Somalia, 1:2,000,000 Scale, Stabilimento Poligrafico Florentino.

Mezies, M., Baker,J., Bosence D.,Dart,C., Davison,I., Hurford.A., Al-Kadasi,M., Mcklay,K.,Nicholas, G., Al-Subbary,A,& Yelland, A.(1992). The timing of magmatism , uplift and crustal extension : preliminary observation from Yemen. In: Storey, B.C., Alabaster,T.& Pankhurst, R.J.(eds) Magmatism and the Causes of Continental Break up. Geological Society, London, Special Publications 68,293-304.

Middlemost, E.A.K. 1985. Magmas and magmatic rocks: an introduction to igneous petrology. Longman Group. London, 266p.

Mohor, p. 1963. The Ethiopian Cenozoic lavas p a study of some trends: spatial, temporal and chemical. Bulletin of the Geophysical Observatory, Addis Ababa, **6**, 103 – 144.

Mohr, P. (1983b). Volcano tectonic aspect of Ethiopian evolution Balletins descentres de Rechcrches Exploration production Elf-Aquitaine 7(1), 157-189.

Mohr, P. (1967). Review of the geology of the semien mountains. Bulletin of the Geophysical observatory of Addis Ababa 10,7993

Mohr, P. 1983a. Ethiopian flood basalt province. Nature, **303**, 577 – 584.

Mohr, P. 1983c. Perspectives on the Ethiopian volcanic province. Bulletin Volcanologique, **46**, 23 – 43.

Mohr, P. A. 1971 The Geology of Ethiopia .253p Hailslassie I University,Addis A.baba

Mohr, P. and Zanettin, B. 1988. The Ethiopian flood basalt province. In: Macdougall, J.D.(ed.), Continental flood basalts. Kluwer Academic Publishers, Dordrecht, pp63 – 110.

Mc Donough,W.F.and Sun,S.S.1995. The composition of the earth. Chemical Geology **120** 223-253.

Neumann, E.-R., Wulff-Pedersen, E., Simonsen, S.L., Pearson, N.J., Mart, J. and Mitjavila, J. 1999. Evidence for fractional crystallization of periodically refilled mama chambers in Tenerife, Canary Islands. Journal of Petrology, **40**, 1089 – 1123.

Panter, K.S., Kyle, R.P. and Smellie, J.L. 1997. Petogenesis of a phonolite – tachyte succession at Mount Sidley, Marie Byrd Land, Antarctica. Journal of Petology, **39** 1225 – 1253.

Pearce, J.A. and Cann, J.R. 1973. Tectonic setting of basic volcanic rocks determined using trace elements analyses. Earth and Planetary Science Letters, **19**, 290-300.

Phillpotts, A.R. 1990. Principles of igneous and metamorphic petrology. Prentice Hall, New Jersey, 498p.

Piccirillo, E.M., Justin-Visentin, E., Zanettin, B., Joron, J.L. and Treuil, M. 1979. Geodynamic evolution from plateau to rift: major and trace element geochemistry of the central-eastern Ethiopian plateau volcanics. Neues Jahrbuch fur Geologie and Plaontologie Abhandlungen, **158**, 139 – 179.

Piccirillo A, M.R.Barberio, G.yirgu, D.Ayalew, M.Barbieri and T.W.U. (2003) relationships between mafic and Peralkaline silicic magamatism in continental rift settings: a petrological geochemical and isotopic study of the Gedemsa volcano central Ethiopia Rift. Journal of petrology 44-, 2003-2032

Pik, R., Deniel, C., Coulon, Ch., Yirgu, G., Hofmann, C. and Ayalew, D. 1998. The northwestern Ethiopian plateau flood basalts: classification and spatial distribution of magma types. Journal of Volcanology and Geothermal Research, 81, 91-111.

Pik, R., Deniel, C., coulon, C., Yirgu, G. and marty, B. (1999). Isotopic and trace element signatures of Ethiopian basalts evidence for plume lithosphereic interactions. Geochimica et Cosmochemica Acta 63, 2263 – 2279.

Rollinson, H. 1993. Using Geochemical Data: Evaluation, Presentation and Interpretation. Longman Group, London, 352p.

Rogers N.W, D James, S.P.Kelley and M.De mulder, 1998, The Generation of potasic lavas from the eastern virunga province, Rwanda, Jounal of petrology, **39**,1223-1247.

Spath, A., Le Roex, A. P. and opiyo – Akech, N. (2001). Plume lithosphere interaction and the origin of continental rift related alkaline volcanism the chyulu Hills volcanic province, southern Kenya. Jornal of petrology 42, 765-787.

Solomon Gerra, 2000, A short introduction to the geology of Ethiopia, Chronique de la Recherche minieral Na 540, 2000, 3-10

Stewart, K. and Rogers, N. (1996) Mantle Plume and Lithosphere Contributions to Basalts from Southern Ethiopia. Earth and Planetary science letters 139, 195-211.

Sorensen, H: 1986 The alkaline rocks- a review' fortschritte der mineralogie, 64,64,63-86.

Taylor, S.R. and Mclennan, S.M. 1985. The continental crust: its composition and evolution. Blackwell Scientific Publication, Oxford, 312p.

Tura, T., Deniel,C., Mazzuoli, R., 1999. Crustal controls in the genesis of Plio-Quaternay bimodal magmatism of the Main Ethiopian Rift (MER): geochemical and isotopic (Sr,Nd, Pb) evidences. Chemical Geology ,155, 201-231.

Ukstins, I.A., Renneo p.R., Wolfenden, E., Baker, J., Ayalew, D. and menzies, M. (2002). Matching conjugate volcanic rifted margins. $^{40}Ar/ Ar^{39}$ K-Ar Chrono-stratigraphy of pre-and syn rift bimodal flood volcanism in Ethiopia and Yemen. Earth and planetary Science Letters **198**, 289-306.

Wilson, M. 1989. Igneous Petrogenesis. Unwin Hyman, London, 446p.

Wright, T.L. 1974. Presentation and Interpretation of Chemical Data for Igneous Rocks. Contributions to Mineralogy and Petrology, **48**, 233-248.

Wolde, B. and Widenfalk, L (1994). Petrochemical and geochemical constraints on Cenozoic Volcanism in Ethiopia. African Geosciences Reviews 1, 475-494.

Zanettin, B., Justin-Visentin, E. and Piccirillo, E.M. 1978. Volcanic succession, tectonics and magmatology in central Ethiopia. Atti e Memorie dell' Accademia. Patavina Scienze, Lettere ed Arti, **90**, 5-19.

Zanettin, B., Justin-Visentin, E., Nicolrtti, M., and Piccirillo, E.M. 1980. Correlations among. Ethiopian volcanic formations with special references to the chronological and stratigraphical problems of the "Trap Series"' Atti dei Convegni Lincei, **47**, 231-252.

Zanettin, B., Gregnanin, A., Visentin, E., Mezzacas a, G. and piccirillo, E.M. (1976), New Chemical Analysis of the Tertiary volcanics from the Central Ethiopian plateau. Consiglio Nazionale delle Ricerche, Istituto di mineraloga petrografia padova universita di padova, PP. 1-43.

Zanettin, B. and Justin Visentin, E. (1975). Tectonical and volcano logical Evolution of the Western Afar Margin (Ethiopia). Afar depression of Ethiopia. Situttgart, schweizerbart, PP. 300-309.

Zanettin, B. and Justin Viseninoe. (1974). The volcanics of the western Afar and Ethiopia rift margins. Memoriedegli Istituti di Geologiae mineralogia deli universita di padava 31, 19.

Zanettin, B. (1992). Evolution of the Ethiopian volcanic province. Memorie Lincee xcienze Fisiche e Naturali 1, 155-181

Zanettin, B., 1993. On the evolution of the Ethiopian volcanic province. In: Abbate, E., Sagri, M., Sassi,F.P.(Eds.), Geology and Mineral Resources of the Somali and Surrounding Regions (with a geological map of Somalia 1:1500000). Ins. Agronomico Per L Oltremare, Firenze, pp. 279-310.

Appendix A

Petrographic descriptions of thin sections

No	Sample No.	Rock name	Hand specimen description	Microscopic description of phases, texture…
1	GUN-11	Basalt	Dark gray to black and very fine grained	Trachytic texture. Composed of 43% lath plagioclase, 30%pyroxene (augite), 17% opaque and 10% volcanic glass (brown). Micro phenocrysts of euhedral- subhedral pyroxene and opaque are seen over the fluidal ground mass.
2	GUN-12	Olivine basalt	Dark gray to black and very fine grained	Inter granular and flow textured. Composed of 40% plagioclase, 35% pyroxene (augite), 15% opaque, 4% olivine and 6% volcanic glass (green). They also show sub parallel orientation (pilotaxitic texture). Some micro phenocrysts of plagioclase are seen in the groundmass.
3	GUN-18	Olivine Basalt	Dark gray to black and very fine grained	Flow texture. Composed of 40% plagioclase, 32%pyroxene (augite), 15% opaque, 12% olivine and 1% devitrified volcanic glass. Some flat tabular plagioclase, large crystals of olivine & pyroxene is seen as phenocrysts.
4	GUN-13	Rhyolite	Black, colored and glassy	Hypocrystalline and vitrophyric texture with 15 % phenocrysts. The phenocrysts are 7% euhedral to subhedral, sanadine, 5% plagioclase, 2% clinopyroxene (augite) and 1% opaque The ground mass is 85% volcanic glass and some microlithic plagioclase. Empty voids and some fractures filled by Fe –oxide are visible.
5	GUN-14	Rhyolite	Brownish gray, very fine grained & with flow banding	Vitrophyric texture with 13% phenocrysts, of 4% euhedral- subhedral sanadine, 6% Plagioclase, 2% opaque and 1% quartz. 87% groundmass is made of volcanic glass plagioclase, opaque sanidine and quartz. Some microphenocrysts of opaque, quartz and pyroxene are also visible. Volcanic glass shows flow banding and devetrification to calcite and biotite.
6	GUN-15	Glassy Rhyolite	Black, colored glassy	Hypocrystalline, vitrophyric texture with euhedral to subhedral phenocrysts of 7 % sanadine, 3% plagioclase, 3% clino pyroxene and 2% opaque (Fe-oxide). Some plagioclase phenocrysts show zoning. Groundmass is composed of 85 % volcanic glass, some microlithic plagioclase and very fine pyroxene.
7	GUN-38	Rhyolite	Light gray and very fine grained.	Micro porphyrthic textured with 22% micro phenocrysts that are 10% euhedral Plagioclase, 4 % sanidine, 3% quartz, 4% opaque and 1% calcite. The groundmass that is 78 % composed of microcrystalline aggregate of feldspars (crystallite materials). Some plagioclase phenocrysts show zoning.
8	GUN-19	Rhyolite	Light gray and very fine grained	Porphyritic texture with 12% phenocryst consisting of 6% euhedral sanadine, 3% quartz, 1% apatite, 1% plagioclase and trace amount of opaque. The 88% ground mass is made of volcanic glass and microlithic lath sanidine, quartz and opaque. Interstial glass with devetrification to mica & green hornblede are also seen between microlithic k-feldspars (sanidine).

Appendix A continued

9	GUN-20	Perlite	Dark-gray to black colored & glassy	Perlithic and vitrophyric texture. Phenocrysts of 20% euhedral to subhedral sanadine, trace (<1%) opaque and calcite are set in an 80% volcanic glass ground mass. It shows a perlitic texture (numerous curving cracks).
10	GUN-21	Lithic tuff	Gray colored and coarse grained	Equigranular textured. Composed of 50% rock fragment, 20% sanidine, 15%quartz and 15% volcanic glass. The rock fragments are andesitic, pumice, basalt and rhyolte .
11	GUN-22	Welded tuff /Ignimbrite/	Gray colored and coarse grained	Vitrophyric texture with 22% phenocrysts, 25% rock fragments and 53% glassy ground mass. The phenocrysts are7% euhedral to subhedral plagioclase, 3% quartz, 15% alkali –feldspar (sanidine) and trace of opaque. The rock fragments are of andesite, basalt, Pumice and rhyolite. The glass shards are slightly flattened and welded. Some devitrification of volcanic glass to chalcedony is visible.
12	GUN-23	Welded tuff / Ignimbrite	Dark gray with white spots in color and coarse grained	Vitrophyric texture with 20% phenocrysts, 25% rock fragments and 55% glassy ground mass. The pheocrysts are10% euhedral to subhedral plagioclase, 5% quartz, 5% alkali –feldspar (sanidine), trace of opaque and calcite. The rock fragments are of andesite, basalt, Pumice and rhyolite. The glass shards are slightly flattened and welded.
13	GUN-8b	Lithic tuff	Reddish – brown to gray colored	Vitrophyric textures, 50% glassy groundmass, 25% phenocryst and 25% rock fragments. The rock fragments are of andesite, pumice and rhyolite. The phenocrysts are 10% euhedral to subhedral plagioclase, 10% sanadine and 5% quartz.
14	GUN-40	Trachyte	Light gray colored and very fine grained	Porphyritic texture with 15% phenocryst and 85% ground mass. The phenocrysts are 9% euhedral alkali-feldspar (sanidine), 4%hornblende 1%plagioclase and 1% opaque. The ground mass is composed of alkali feldspar (sanidine), Ppyroxene (augite), hornblende, calcite and biotite. It has trachytic texture defined by parallel to sub parallel orientation of microlithic alkali –feldspar (sanidine).
15	GUN-42	Trachyte	Light gray colored and very fine grained.	Porphyritic, 15% phenocrysts with euhedral to subhedral crystals of 10% alkali feldspar (sanidine), 2% plagioclase, 3% hornblende, traces of pyroxene and opaque. Microphenocrysts of alkali-feldspar and hornblende are also seen. 85% ground mass is trachytic textured and composed of microlithic alkali –feldspar (sanidine), Pyroxene, hornblende and opaque
16	GUN-29	Trachyte	Gray colored	Porphytritic texture with 30% phenocryst and 70% ground mass. The phenocrysts are 7% k-feldspar (sanadine), 20% orthoclase, 2% opaque and 1% sphene. The ground mass is mainly composed of k-feldspar (sanadine), orthoclase, pyroxene and volcanic glass. The ground mass also shows flow texture.

Appendix A continued

17	GUN-27	Phonolite	Greenish gray to gray colored, greasy luster highly porphyrhitic	Porphyritic texture with 20% phenocrysts set in 80% ground mass. The phenocrysts are 7% tabular and euhedral k-felspar (mainly sanadine), 5% euhedral -anhedral nepheline, 5% euhedral- subhedral nosean. Some micro phenocrysts of clino pyroxene, sphene and opaque are also seen .The ground mass is composed of lath alkali feldspar, nepheline, pyroxene, opaque and some sphenes. Microlitic k-feldspar shows sub parallel alignment. Some clino pyroxene shows zoning.
18	GUN-17	Phonolite	Greenish gray colored, poorly porphyrhitic	Micro porphyritic texture with about 5% micro phenocrysts consisting of 2% euhedral to subhedral nosean, and 3% opaque. The ground mass is composed of 74% k-feldspar (sanadine), 10% leucite, 7% pyroxene, 4% opaque, <1% nepheline and nosean.
19	GUN-5	Phonolite	Greenish tint colored, with flow foliation, poorly porphyrithic	Trachytic texture, microlitic k-feldspar and pyroxene show parallel alignment. It is composed of about 84% k-feldspar 12% pyroxene (aegirine), 4% nepheline and <1% opaque.
20	GUN-9	Phonolite	Greenish tint colored	Porphyritic and trachytic textured with 22% phenocrysts and 78% groundmass. The phenocrysts are 10% euhedral - tabular alkali feldspar (sanadine), 4% subhedral nepheline, 3% anhedral pyroxene, 2% euhedral - subhedral nosean, 2% subhedral opaque and 1% euhedral sphene. The ground mass is composed of alkali feldspar, nepheline, nosean, pyroxene and opaque. It has trachytic texture defined by parallel alignment of k-feldspars. Some phenocrysts of k-feldspars show glomerophorphyritc texture.
21	GUN-25b	Phonolite	Greenish gray-to-gray colored, greasy luster	Porphyritic textured with about 30% phenocrysts and 70% ground mass. The phenocrysts are 15% euhedral - subhedral k-feldspar (sanadine), 10% nepheline, 3% nosean and 2% pyroxene. The ground mass is mainly composed of pyroxene, alkali feldspars, nepheline, nosean, sphene and opaque.
22	GUN-31	Phonolite	Greenish gray-to-gray colored, greasy luster.	Porphyritic and trachytic texture with about 40% phenocryst and 60% ground mass. The phenocrysts are 10% lucite, 6% alkalifeldspar, 6% nepheline, 5%, nosean, 9% brown hornblende and 24% biotite. The ground mass is made of pheocryst minerals plus sphene, pyroxene, opaque and apatite.
23	GUN-32	Phonolite	Greenish gray-to-gray colored, greasy luster.	Porphyritic texture with 15% phenocryst consisting of 6% euhedral - subhedral k-feldspar, 5% nosean, 2% lucite, 2% pyroxene and <1% opaque. Microphenocrysts of sphene and pyroxene are also seen. The ground mass (85%) is composed of alkali-feldspar, pyroxene and some nosean, nepheline, opaque, calcite and sphene.
24	GUN-47	Phonolite	Greenish gray-to-gray colored, greasy luster	Porphyritic and trachytic texture, 20% phenocryst and 80% ground mass. The phenocrysts are 9% k-feldspar (sanadine), 5% nosean, 3% nepheline, 2% leucite and 1% pyroxene. Some pyroxenes are also seen as micro phenocrysts.The ground mass

				is mainly composed of k-feldspar, Pyroxene, some nosean, nepheline and opaque.

Appendix A continued

25	GUN-28	Phonolite	Greenish gray-to-gray colored, greasy luster	Porphyritic and trachytic texture, 22% phenocryst and 78% ground mass. The phenocrysts are 7% k-feldspar, 5% nepeline, 4% nosean, 3% pyroxene and 3% opaque. The ground mass is mainly of lath k-feldspar (sanadine), pyroxenes, nepheline, some nosean and opaque.
26	GUN-36	Phonolite	Greenish gray-to-gray colored, greasy luster	Porphyrithic texture with 19% phenocryst and 81% ground mass. The phenocrysts are 6% k-feldspar (sanadine), 5% nepheline, 5% nosean, 2% Pyroxene and1% opaque. Pyroxene is visible also as micro phenocrysts. The ground mass is composed as of the phenocrysts assemblage.
27	GUN-44	Phonolite	Greenish gray-to-gray colored, greasy luster	Porphyritic texture. 15% phenocryst and 85% ground mass. The phenocrysts are 7% k-feldspar (sanadine), 4% nepheline, 2% pyroxene, 2% leucite, <1% opaque and sphene. The ground mass is mainly made of k-feldspar (sanadine), volcanic glass and pyroxenes, with some nepheline and opaque.
28	GUN-45	Phonolite	Greenish gray-to-gray colored, greasy luster.	Porphyritic and trachytic texture. 27% phenocryst and 73% ground mass. The phenocrysts are 8% k-feldspar, 7% nosean, 4% nepheline, 4% opaque and 3% sphene. The ground mass is made of hair like k-feldspar, pyroxene, some volcanic glass and calcite.
29	GUN-49	Phonolite	Greenish gray-to-gray colored, greasy luster.	Trachytic texture, very few (<1%) phenocrysts of k- feldspar (sanadine), sphene, with a ground mass made of 70% k-feldspar (sanadine), 15% pyroxene and 15% volcanic glass.
30	GUN-26b	Phonolite	Greenish gray-to-gray colored, greasy luster.	Porphyritic texture, with 16% phenocrysts, 10% alkali feldspar (sanadine), 3% nepheline, 2% nosean and 1% pyroxenes. The ground mass (84%) is mainly composed of lath alkali feldspar, green pyroxene (aegrine) and some nepheline, noscan, sphene and opaque. sphene, pyroxene and opaque are also seen as microphenocrysts.
31	GUN-46	Phonolite	Greenish gray to gray colored, greasy luster.	Porphyritic and trachytic texture. Phenocrysts (17%) are composed of 7% alkali feldspar (sanadine), 5% leucite, 3% pyroxene, 2% nosean and traces of opaque, sphene and biotite. The ground mass is made of mainly alkali feldspar (sanadine), and pyroxene with some amount of leucite, nosean and calcite. Some nosean shows alteration to zeolite.
32	GUN-50	Phonolite	Greenish gray-to-gray colored, greasy luster	Porphyritic texture with 19% phenocrysts and 81% ground mass. The phenocrysts are 7% alkali feldspar, 5% nepheline, 3% leuite 1% pyroxene and <1% opaque, and 3% nosean. Phenocrysts of alkali feldspar (sanadine), shows cluster or glomeroporphyritic
33	GUN-35	Phonolite	Greenish gray-to-gray colored, greasy luster	Porphyritic textured with 17% phenocryst and 3% ground mass. The phenocrysts are 7% alkalifeldspar (sanadine), 5% nosean, 3% nepheline and 2% Pyroxene. Traces of biotite and sphene are seen also as microphenocrysts. The ground mass is mainly

				composed of lathe alkalifeldspar (sanadine), few Pyroxene, opaque, nosean and nepheline. Lath alkalifeldspar (sanadine), shows sub parallel alignments.

Appendix A continued

34	GUN-33	Phonolite	Greenish gray-to-gray colored, greasy luster	Porphyritic texture, with 35% phenocrysts and 65%ground mass. The ground mass has a trachythic texture. The phenocrysts are 20% sanadine, 4% nepheline 10% lucite and 1% pyroxene. Some sphene, Pyroxene and opaque are also seen as microphenocrysts. The ground mass consists of lath sanadine, pyroxene, nepheline, nosean, opaque and calcite.
35	GUN-30	Phonolite	Greenish gray-to-gray colored, greasy luster	Porhyritihic texture with 20% phenocryst and 80% ground mass. The phenocrysts are 2% nepheline, 13% sanadine, 2% leucite, 1% Pyroxene and 2% Plagioclase. Microphenocrysts of biotite and opaque are also seen. The ground mass is trachythic textured and composed of sanadine, pyroxene, plagioclase opaque, nepheline, leucite, biotite and calcite.
36	GUN-48	Phonolite	Greenish gray-to-gray colored, greasy luster	Microlithic textured very few (<1%) phenocrysts of nepheline and leucte. Microphenocrysts are sanadine, nepheline and leucite. Groundmass is microlithic with parallel orientation (flow texture). It is composed of 62% alkali feldspar, 30% alkali pyroxene, 5% nepheline, 3% leucite and trace amount of calcite and opaque.
37	GUN-25A	Phonolite	Greenish gray-to-gray colored, greasy luster.	Porphyritihic texture, 23% phenocryst and 77% ground mass. The phenocrysts are 10% sanadine, 7% nosean, 5% nepheline and 1% Pyroxene. sphene, opaque and pyroxenes are also visible as microphenocrysts. The ground mass is composed of alkali feldspar pyroxene, some nepheline and opaque.

Appendix B list of samples collected from Gun massif

No.	Sample No.	Altitude	Coordinates (UTM)	Rock type	Remark
1	GUN-5	3100	1297811N-424643E	Phonolite	
2	GUN-6	3052	1297104N-424094E	pyroclastic	
3	GUN-7	3000	1294250N-423598E	Welded ash	
4	GUN-8a	3020	1294202N-423675E	pyroclastic	
5	GUN-8b	"	"		
6	GUN-9	3003	1289025N-421755E	Phonolite	
7	GUN-10	2498	1254819N-417136E	Basalt	
8	GUN-11	2512	125840N-417066E	Bsalt	
9	GUN-12	2546	1259433N-417008E	Basalt	
10	GUN-13	2690	1263222N-414511E	Rhyolite	glassy
11	GUN-14	2741	1264242N-414398E	Rhyolite	Layered lava
12	GUN-15	2853	126833N-414028E	Rhyolite	glassy
13	GUN-16	2854	1268549N-413904E	Pyroclastic	
14	GUN-17	2941	1205054N-413521E	Phonolite	
15	GUN-18	2439	1284902N-397723E	Basalt	
16	GUN-19	2445	1285511N-398403E	Rhyolite	dome
17	GUN-20	2657	1293387N-396384E	Rhyolite	glassy
18	GUN-21	2664	1293721N-396686E	pyroclastic	
19	GUN-22	2700	1293873N-396768E	Ignimbrite	
20	GUN-23	2692	1293867N-396752E	Ignimbrite	Trachyte
21	GUN-24	"	"	Pumice clasts	
22	GUN-25a	2910	1304710N-410221E	Phonolite	
23	GUN-25b	2980	1304563N-410513E	Phonolite	
24	GUN-26a	3050	130465N-410559E	Phonolite	
25	GUN-26b	3050	130359N-410593E	Phonolite	
26	GUN-27	2900	1304914N-409962E	Phonolite	
27	GUN-28	3350	1301186N-411715E	Phonolite	
28	GUN-29	3429	1299182N-411930E	Trachyte	
29	GUN-30	3442	1296869N-412387E	Phonolite	
30	GUN-31	3521	1296758N-412868E	Phonolite	
31	GUN-32	3100	1299050N-410132E	Phonolite	
32	GUN-33	3073	1299612N-409743E	Phonolite	
33	GUN-34	3063	1300201N-409233E	pyroclastic	
34	GUN-35	3100	130557N-417056E	Phonolite	dome
35	GUN-36	3154	1303386N-419908E	Phonolite	
36	GUN-37	3066	1295466N-424133E	Ash	
37	GUN-38	2889	1291057N-422337E	Rhyolite	Layerd lava
38	GUN-39	3040	1271598N-414396E	Rhyolite	Layerd lava

39	GUN-40	3100	1274442N-414391E	Trachyte	
40	GUN-41b	3156	1276274N-413341E	Rhyolite	
41	GUN-42	3182	1276772N-413593E	Trachyte	
42	GUN-43	3226	1283949N-415213E	pyroclastic	
43	GUN-44	3500	1285176N-416416E	Phonolite	
44	GUN-45	3800	1291327N-417352E	Phonolite	
45	GUN-46	3700	1290627N-417633E	Trachyte?	
46	GUN-47	3600	12897810N-418168E	Phonolite	
47	GUN-48	3500	128829N-418549E	Phonolite	
48	GUN-49	3200	1286850N-418825E	Phonolite	
49	GUN-50	3232	1298538N-421236E	Phonolite	
50	GUN-51	3199	1297913N-423274E	Phonolite	
51	GUN-52	3234	1298318N-421187E	Phonolite	
52	GUN-53	2700	1315361N-405335E	Ignimbrite	

Appendix C

Procedure for calculations of a chemical formula from a mineral analysis

1. The mineral analysis is listed in Wt % of oxides
2. Molecular (mol.) Proportion of oxides is calculated by dividing the wt% of oxides to the molecular weight of each oxides
3. Atomic proportion of oxygen from each mol. Proportion is derived by multiplying it by the number of oxygen atom in the oxide concerned (e.g. 2 for SiO_2)
4. The sum of the atomic proportions (T) is obtained by adding the values in step 3
5. Divide the number of oxygen bases (e.g. 8, 24, ---) to the sum of atomic proportions (T)
6. Multiply the values in step 3 by the values in step 5 for each oxides
7. The number of cations associated with the oxygen is obtained by multiplying the values in step 6 by the proportion of oxygen in molecules of oxides. e.g for $Si0_2$ there is one silicon for 2 oxygen's there for the step 6 values are multiplied by 2, for Al 2O3 ,by 2/3 ,for divalent ions step 6 value will be kept the same
8. Proportions of mineral species (eg An, Ab, Or) is obtained by dividing the number of cations, Values in step 7 e.g. for An dived Ca by the sum Ca +Na +K and then multiply by 100